W.A.S.P.Abeysiriwardhana

ACTIVE VIBRATION SUPPRESSION WITH DISTURBANCE FORCE ESTIMATION

Wickaramaarachchi Abeysiriwardhana Shanaka Prageeth Abeysiriwardhana

(148031V)

University of Moratuwa, Sri Lanka.
Electronic Theses & Dissertations
www.lib.mrt.ac.lk

Degree of Master of Science

Department of Electrical Engineering

University of Moratuwa

Sri Lanka

September 2015

M.Sc

2015

ACTIVE VIBRATION SUPPRESSION WITH DISTURBANCE FORCE ESTIMATION

Wickaramaarachchi Abeysiriwardhana Shanaka Prageeth Abeysiriwardhana

(148031V)

University of Moratuwa, Sri Lanka.
Electronic Theses & Dissertations
www.lib.mrt.ac.lk

Thesis submitted in partial fulfillment of the requirements for the degree Master of Science

Department of Electrical Engineering

University of Moratuwa

Sri Lanka

September 2015

DECLARATION

I declare that this is my own work and this thesis does not incorporate without acknowledgement any material previously submitted for a Degree or Diploma in any other University or institute of higher learning and to the best of my knowledge and belief it does not contain any material previously published or written by another person except where the acknowledgement is made in the text.

Also, I hereby grant to University of Moratuwa the non-exclusive right to reproduce and distribute my thesis/dissertation, in whole or in part in print, electronic or other medium. I retain the right to use this content in whole or part in future works (such as articles or books).

Signature: Date:

University of Moratuwa, Sri Lanka.
Electronic Theses & Dissertations
www.lib.mrt.ac.lk

Wickramaarachchi Abeysiriwardhana Shanaka Prageeth Abeysiriwardhana

The above candidate has carried out research for Masters Dissertation under my supervision. I endorse the declaration by the candidate.

Dr. A.M.Harsha S.Abeykoon Date:

ACKNOWLEDGEMENT

This thesis is a partial requirement for the completion of Master of Science degree in University of Moratuwa. This text is a compilation of research work that has been carried out at the Control and Robotics Laboratory, Electrical Engineering Department, Faculty of Engineering, University of Moratuwa, Sri Lanka. This research was supported by University of Moratuwa Senate Research Grant no: SRC/ Cap/14/14.

This research was performed under the supervision of **Dr. A.M.Harsha S. Abeykoon**. I would like to show him my gratitude for his continuous guidance and support to fulfill this task.

Many thanks and gratitude to **Professor Sudath Rohan Munasinghe**, **Dr. W. D. Asanka S. Rodrigo** Faculty of Engineering, University of Moratuwa. As the review panel, their valuable comments, encouragements and discussions in the progress review meetings helped me to achieved this task

I deeply thank Mr. Viraj Muthugala and R.M.M. Ruwanthika, Postgraduate students, Electrical Engineering Department, Faculty of Engineering, University of Moratuwa.

All members of Electrical Engineering Department, University of Moratuwa are also gratefully acknowledged. They constantly helped me during my research activity.

I would like to express my sincere gratitude to all those who have assisted me in my life specially my parents. Last but not least, I should thank Dr.A.M.Harsha S.Abeykoon for his guidance.

Finally, I would like to thank everybody who was important to the successful realization of thesis, as well as expressing my apology that I could not mention personally one by one.

University of Moratuwa, Sri Lanka.
Electronic Theses & Dissertations
www.lib.mrt.ac.lk

Wickramaarachchi Abeysiriwardhana Shanaka Prageeth Abeysiriwardhana
University of Moratuwa
September 2015

ABSTRACT

Vibration is a basic phenomenon that has attracted control engineering's attention for many decades. Vibration rejection in control systems is implemented with passive, semi active and active vibration suppression systems. These methods commonly use multiple redundant sensors. Multiple sensor usage and complex control has implemented the cost of operation and complexity. Minimal sensor usage to provide vibration suppression within the commonly used acceleration or deflection observation could be used to reduce the complexity and cost of the system. This dissertation proposes a novel methods which uses either the acceleration or motor deflection measurement based disturbance force observers for vibration observations and to suppress the vibrations with active vibration suppression. The proposed system is capable of estimating the disturbances and compensate disturbances using the only a acceleration or suspension deflection sensory data. Proposed system still could work as a traditional vibration suppression system in case of a failure to active system. Active force to be injected is calculated based on the disturbance forces acting on the sprung mass. A novel method is proposed for spring and damper parameter measurement with electromagnetic actuators which enhance the overall system performance. A Quarter car model is used to illustrate the adaptability, robustness, and the vibration suppression capabilities of the system. Performance of the active vibration suppressor and disturbance observer is measured using system simulations and practical results. Simulation and practical system responses provide evidence of robust vibration suppression capabilities of the proposed method under different conditions.

University of Moratuwa, Sri Lanka.
Electronic Theses & Dissertations
www.lib.mrt.ac.lk

Keywords:
Active Suspension, Active Vibration Suppression, Disturbance Observer, Reaction Force Observer, Disturbance Rejection.

Table of Contents

University of Moratuwa, Sri Lanka.
Electronic Theses & Dissertations
www.lib.mrt.ac.lk

University of Moratuwa, Sri Lanka.
Electronic Theses & Dissertations
www.lib.mrt.ac.lk

University of Moratuwa, Sri Lanka.
Electronic Theses & Dissertations
www.lib.mrt.ac.lk

List of Figures

University of Moratuwa, Sri Lanka.
Electronic Theses & Dissertations
www.lib.mrt.ac.lk

University of Moratuwa, Sri Lanka.
Electronic Theses & Dissertations
www.lib.mrt.ac.lk

TABLE OF TABLES

LIST OF ABBREVIATIONS

Abbreviation	Description
DOB	Disturbance Observer
RFOB	Reaction Force Observer
DOF	Degree of Freedom
BLDC	Brushless Direct Current
SPI	Serial Peripheral Interface
QEI	Quadrature Encoder Interface
ppr	pulses per revolution
FPGA	Field Programmable Gate Array

University of Moratuwa, Sri Lanka.
Electronic Theses & Dissertations
www.lib.mrt.ac.lk

Chapter 1

1 INTRODUCTION

1.1 Background

Vibration is a phenomena that occur in real world systems including robotics, motion control and automobile systems. Vibration causes to loss pf energy, damage to the components, and discomfort to the humans. Engineers and scientists have designed systems to overcome the problem of vibrations in real world systems with vibration suppression systems. Mainly these problems arise in motion control and automobile technologies.

Automobile suspension systems are developed to overcome these problems starting from the development of first shock-absorber by a French cyclist in 1898 [1] that was used in a bicycle. These automobile vibration suppression systems are developed to provide better vehicle control, passenger comfort and better ride quality in automobiles. Humans feel dizziness and sea sickness for vibrations in ranges of 0.5 Hz to 1Hz and 18 to 20Hz [2]. Automobile Suspension systems connected in between vehicle body and tires suppressing vibration transfer from the road surface to vehicular body through tires and suspension system. Suspension system reduces vehicle body movement reducing roll and pitch of the body and providing better ride quality to passengers. Passive suspension systems, semi active suspension systems, and active suspension systems were designed to reduce vehicle vibrations, and to improve vehicle handling in automobiles [3].

University of Moratuwa, Sri Lanka.
Electronic Theses & Dissertations
www.lib.mrt.ac.lk

Vibration suppressions are also used in mechanical systems including motion control systems, that has been developed with resonance ratio control and used to suppress the vibrations of two mass resonant system and three mass resonant systems, where reaction torque occurred in the motor actuator shaft is used to suppress the vibrations without using any position sensors [4]. In addition disturbance observers and reaction torque observers [5-11] has been used to suppress the effects of external interventions and vibrations on the motion control systems.

The active vibration suppression systems has been evolved in last few decades with increasing number of sensors and actuators [12-15]. These systems are complex in control and relay on multiple sensing mechanisms [16]. This research focuses on applicability of observable motor characteristic observation mechanisms that can be used to minimize the cost and complexity of

the vibration suppression system with the ability of providing adequate active vibration suppression with a single available sensor under failures to the multiple sensors. In addition the proposed methods focus on active vibration suppression techniques that can be used to where simplified design and implementation cost is a main consideration.

1.2 Vibration

Vibration can be defined as a mechanical oscillation about a fixed point [17]. Vibrations in a mechanical or control system creates discomfort to operators, instability in controllers, mechanical damage, energy wastage and noises. Vibrations can be classified in to different type free vibrations, damped vibrations and force vibrations [18]. Free vibration can be expressed as the natural movement of a system. Damped vibration can be explained using an example of one degree of freedom pendulum motion or an oscillation of a mass around a spring damper system, where the vibrating movement will get damped out and become stable. A force exerted on a system similar to an earthquake or road defect can be categorized in to forced vibrations. Force vibrations occur due to the effects of external environment and or forced movements of objects. A vehicle body or a motion control system will get disturbed by these kinds of vibrations. As an example vehicle passengers will experience discomfort and the vehicle body or sprung mass will start to move under these conditions. In addition unstable working platforms and discomfort in work environment could be a cause of vibration. In motion control systems the controller will fail to keep the desired level of output due to the effects of vibrations and vibration suppression systems will provide some compensation in these systems to improve the performance, precision and withstand capabilities for these kinds of vibrations [19].

University of Moratuwa, Sri Lanka.
Electronic Theses & Dissertations
www.lib.mrt.ac.lk

1.3 Vibration suppression and measurement

In conventional vibration suppression systems spring damper elements are commonly used for vibration suppression. The spring damper based suspension elements are developed in last decades and mainly used in automobile vibration suppression systems. The spring damper suspension system has been categorized to three different areas with the development of these systems. Passive suspension systems only use passive elements to suppress vibrations, the conventional passive system is mainly built using springs and dampers [20]. The inability to change its properties in different conditions cause passive suspension systems to produce uneven

vibration suppression capabilities in different conditions. Semi active suspension system can achieve controllability by changing suspension system properties. Semi active suspension systems do not introduce energy in to the suspension system, but dissipate or absorb vibration energy from the system by changing the properties [21]. Active vibration suppression systems were developed to overcome problems faced in passive and semi active suspension systems. Active suspension systems consists of active elements such as motors and hydraulic pumps. The active elements has the ability to absorb and add energy to suspension system, and to change suspension system properties accordingly to provide robust vibration suppression performance under different conditions.

Semi active suspension systems provide better vibration suppression than passive suspension systems [22], theoretically active suspension systems are far more superior than passive and semi active systems [23]. But semi active suspension systems are commercially used due to cost effectiveness. Variable dampers are commonly used in semi active suspension system with the ability to change damping constant under different conditions [24]. Mechanical orifice or smart fluids are used to control the fluid properties in variable dampers [25]. Active suspension systems contain hydraulic or electromagnetic actuators [26]. Hydraulic actuators use higher power than electromagnetic suspension systems. Electromagnetic active suspension systems have faster responses than hydraulic systems and can regenerate energy to reduce power consumption of the system [27]. Usually multiple high cost sensors are is used as an input in vehicle active vibration suppression system controllers [28]. Internal motor parameter sensation to observe the disturbances provide a less costly and simpler solution for active vibration suppressors.

University of Moratuwa, Sri Lanka.
Electronic Theses & Dissertations
www.lib.mrt.ac.lk

Disturbance observers (DOB) [29, 30] and reaction force observers (RFOB) [31, 32] has been used in motion control as disturbance rejecters to reduce the effects of external forces with the use of disturbance estimation mechanisms. These observers use internal parameters and provide good performance for external loads including low frequency vibrations. The disturbance estimation with accurate parameter estimation have the ability to provide a high performance in vibration suppression without the direct force sensors [33]. The disturbance observer provide higher bandwidth in disturbance measurement as the torque sensors have a lower bandwidth

comparison to a DOB. DOB and Reaction Force Observer (RFOB) are mainly developed for motor position and velocity controllers where the effects of external disturbance is quickly compensated by the DOB disturbance force nullify effect. Motors are mounted on the motor forcer and the disturbance is provided to motor shaft. A vibration suppression system with passive vibration suppression capabilities should contains a movable forcer and movable shaft that is different from the conventional motion controller arrangement. DOB based disturbance sensing vibration suppression can therefore be modified and developed to an active vibration suppression system.

1.4 Objectives and Contribution

A novel concept to provide active vibration suppression using either the sprung mass acceleration or motor deflection has been researched in this dissertation. Conventional vibration suppression system uses multiple sensors to generate vibration suppression capabilities. These complex sensor based control greatly increase the cost and complexity of the vibration suppression system. Thereby reduce the applicability of system where design cost and complexity is an issue. But the minimal observed parameter usage in applications has been considered due to advantages of high bandwidth, less cost, applicability in new application areas such as platform stabilization and that controller's capability to provide vibration suppression even when only a single sensory data is available in a multiple sensor system. This research look in to the ability to estimate and suppress vibrations using either the sprung mass acceleration or suspension deflection. The proposed method nullify the effects of vibrations by virtually disconnecting the system from the external environment for dynamic forces while a passive suspension system withstand the steady state weights. And the research analyses the parameter effects on the internal estimation and the method to measurement of parameters to minimize the system errors. Proposed Controller estimate the disturbance force acting on the sprung mass of the two degree of system spring damper system using estimated spring dampers deflection forces and use that information to suppress the effects of vibrations. The researched controller is developed with the ability use with minimum number of sensors to prevent the effects of environmental uncertainties and sensor failures. The applicability of the control method is measured using a 2 Degrees of Freedom Quarter car model as the proposed method tries to nullify the effects of vibration forces by single direction disturbance force transfer estimation.

University of Moratuwa, Sri Lanka.
Electronic Theses & Dissertations
www.lib.mrt.ac.lk

1.5 Thesis Content

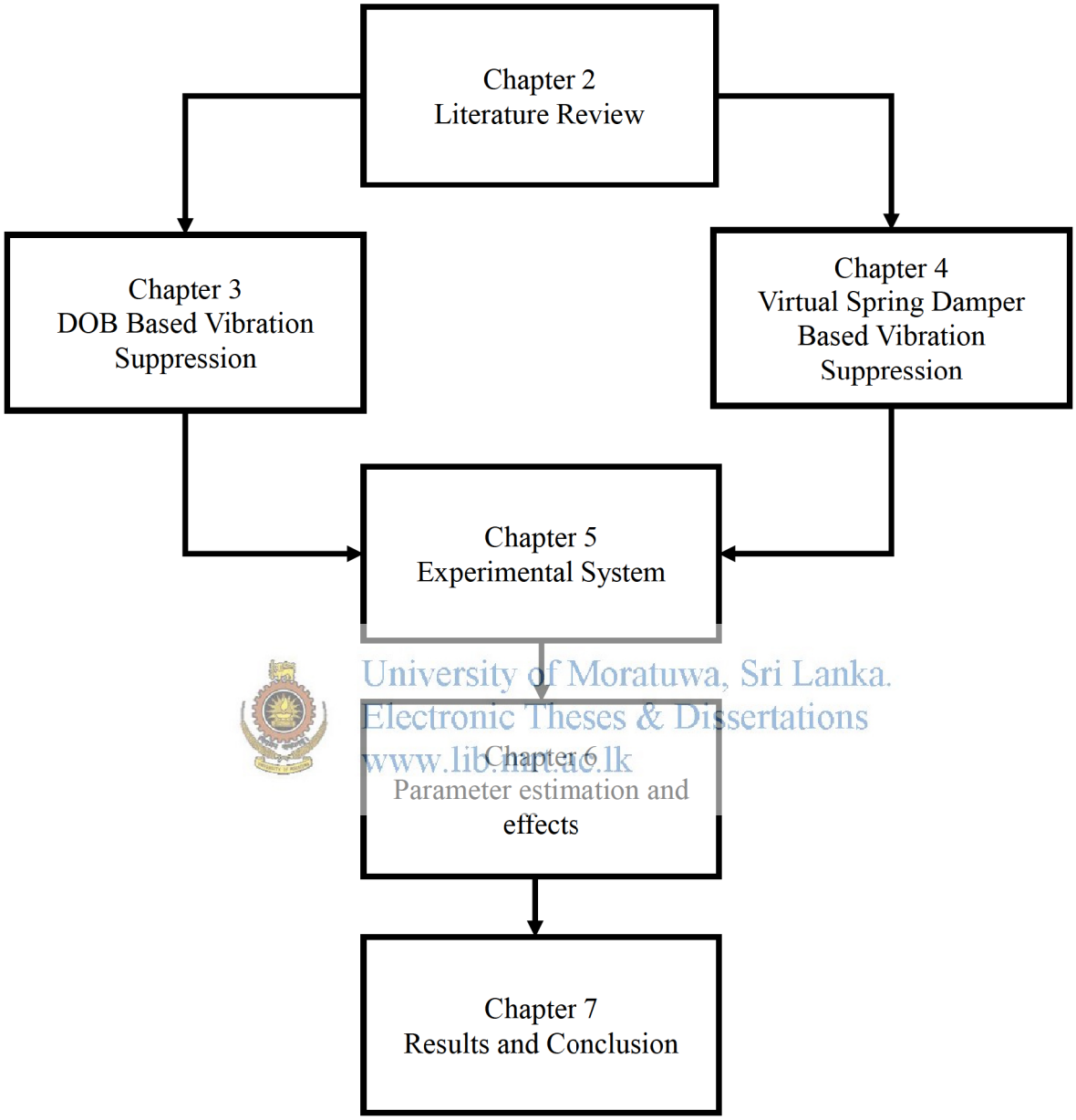

University of Moratuwa, Sri Lanka.
Electronic Theses & Dissertations
www.lib.mrt.ac.lk

Chapter 2: Literature Review.

This chapter looks in to the available methods in vibration suppression including controllers, actuators and sensing mechanisms. In addition basic suspension equations for quarter car model is analyzed in the chapter.

Chapter 3: Disturbance Observer.

Mathematical analysis on disturbance observer design for linear motor system has been realized in the chapter. In addition a disturbance force nullifying vibration suppression system has been designed with disturbance observers. The proposed controller tested for simulated performance and experimental performance and it is included in this chapter 7.

Chapter 4: Virtual Spring Damper Vibration Suppression.

This chapter analyses the performance and mathematical characteristics of the virtual spring damper based vibration suppressor. Simulation and Experimental results are illustrated to conclude the effects of the proposed control model are given in chapter 7.

Chapter 5: Experimental System

Experimental system hardware design and software design methodology is discussed in this chapter.

Chapter 6: Parameter Estimation and Effects

The internal sensing controller parameter estimation method has been discussed in this chapter. The parameter estimation results are given in the results. And the chapter discusses the effects of the parameters on controller measurements.

University of Moratuwa, Sri Lanka.
Electronic Theses & Dissertations
www.lib.mrt.ac.lk

Chapter 7: Results and Conclusion

This chapter is devoted to results and concluding remarks.

Chapter 2

2 LITERATURE REVIEW

2.1 Introduction to Vibration Suppression

Humans are trying to improve the living conditions and their life styles to more luxurious life styles using electrical and mechanical control systems. In addition industrial systems are trying to improve the performance and efficiencies using complex control systems. Vibration is one of the topics that is related to both of those fields due to the effects it have on humans and machines. According to medical literature, vibrations at certain frequencies and accelerations can harm humans [34, 35]. Furthermore vibrations play a key role in reliability issues of electrical and mechanical systems. As an example Li-ion batteries in vehicles may suffer from damages occur due to vibrations [36]. External disturbances and vibrations play a key role in other systems like precision motor control systems, where a sudden external disturbances may cause vibrations in the controller output [37].

University of Moratuwa, Sri Lanka.
Electronic Theses & Dissertations
www.lib.mrt.ac.lk

Modern control systems include vibration suppression systems to prevent the above draw backs. Various techniques have been developed to reduce the effects of vibrations in control systems and to prevent the effects to human beings. This includes suppression mechanisms and preventive mechanisms such as limiting the exposure to vibrations [38]. One of the most popular vibration suppression systems include the passive vibration suspension systems used in vehicles [39]. With the improvements of the control systems these passive systems have been developed as semi active suspension systems. Semi active suspension systems have been commercially used and provide good quality vibration suppression as compared to passive suspension system. Active suspension systems were developed in recent years and commercially used only in high end vehicles and systems due to cost and complexity of the systems. Vibration suppression systems design and its complexity varies on the required level of performance. A modern luxury vehicle may requires a comfortable ride while a sport vehicle needs good grip. An industrial vibration suppression systems try to reduce the effects of vibration on electrical mechanical components. These requirements therefore varies with the need of the designers, controllers and implementation strategies. The reasons to design an active vibration suppression

system has been discussed in this chapter that provide the criteria for selecting active vibration suppression with minimal sensor usage.

2.2 Passive Vibration Suppression

Conventional passive vibration suppression systems contain passive elements of spring and dampers. And the mounting methods of these systems varies with the system. As an example spring damper based conventional vehicular suspension systems includes solid axial system [40], double wishbone system [41], and Macpherson strut [42] system. These systems are developed with different spring damper arrangements and are used to minimize the effects of vibrations and in some cases used to increase vehicle control. Passive vibration suppression systems have static properties therefore unable to change the suspension system performance according to environmental variations. Spring and damper coefficients of passive suspension systems are constant for all disturbance levels therefore it would provide different performance levels for different frequencies and system parameter variations. This is one of the main drawbacks of the passive suspension systems. Vehicular passive suspension systems are normally connected in between the vehicle axel and body where the disturbance force acting on the vehicle axel is absorbed by the spring damper combination thus reducing the effects of road disturbances experienced by the passengers. Similarly passive vibration suppressors are applied to applications such as machine vibration suppression where unidirectional vibrations are suppressed with materials with spring damper properties. A conventional passive suspension element is shown in Figure.2.1. The semi active vibration suppression systems were later developed to overcome the drawbacks of these systems but passive suspension systems are still used in many commercial applications including vehicles and miniature in hard disk vibration

University of Moratuwa, Sri Lanka.
Electronic Theses & Dissertations
www.lib.mrt.ac.lk

Figure 2.1: Conventional Passive Suspension [43]

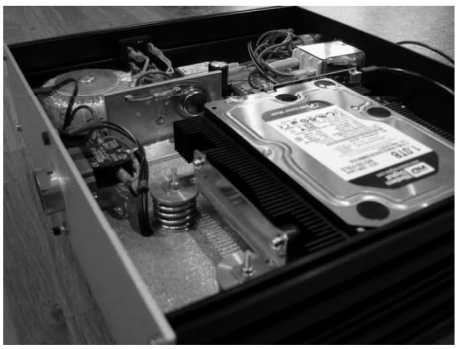

Figure 2.2: Read Head Vibration Suppression [44]

suppression system shown in Figure 2.2. And one of the reasons for using the passive suspension systems in these applications is the issues of cost, miniature size, sensor placement and complexity. Therefore a high performance active suspension system with simplistic design have the applicability in these applications.

2.3 Semi Active Vibration Suppression

Semi Active vibration suppression systems were developed with the ability to change the vibration suppression system properties according to a controller signal. As an example vehicular semi active suspension systems commonly use variable damping elements. Damping coefficient variations will produce the required effects under different conditions. Semi active suspension systems commonly used magneto rheological [45,46], electro rheological fluids [47] or variable geometry dampers. Magneto rheological or electro rheological fluids contains synthetic hydrocarbon oil containing subminiature magnetic particles and a coil inside the damper that creates a magnetic field by applying a voltage; which has the capability of supplying a real-time dissipation of energy. The drawback of these kinds of systems is that, the system can't provide an active force to reduce the response time. Theoretically active suspension systems have superior performance than the semi-active systems. But due to ability to integrate to conventional vehicles, less cost and complexity semi active systems are commercially available for vehicles.

University of Moratuwa, Sri Lanka.
Electronic Theses & Dissertations
www.lib.mrt.ac.lk

Semi active and active vibration suppression systems uses skyhook damping, fuzzy control, and sliding mode control techniques [49-54]. These systems use single or multiple sensors to change the suspension properties to increase suspension performance. Skyhook damping is one of the

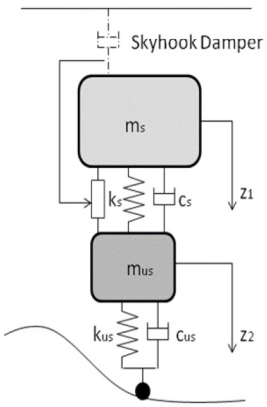

Figure 2.3: Sky hook damper model [55]

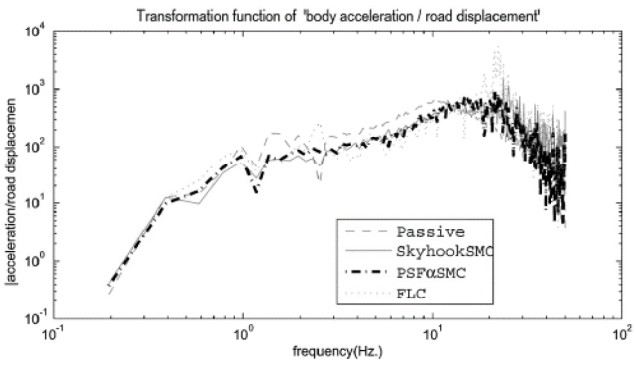

Figure 2.4: Semi active suspension system performance [56]

famous semi active and active control method that applies a hypothetical damper in between reference point (a ground reference) and sprung mass as shown in Figure 2.3. And sprung mass velocity should be sensed in this system to provide suspension performance. This is commonly done by integrating the accelerometer readings which is prone to errors. These systems improves the suspension performance but the improvement is limited due to the semi active nature as shown in Figure 2.4 taken from [56]. According to Figure 2.4 sprung mass acceleration is reduced compared to passive suspension system but the performance improvement can be further improved with active vibration suppression techniques with the expense of energy. And the measuring the sprung mass velocity with respect to a solid reference point is difficult due to the problems in accelerometer value integrations and environmental effects on accelerometers. Active vibration suppression technique with direct acceleration measurement or suspension deflection measurement can provide solutions to the problems associate with these systems.

2.4 Active Vibration Suppression

Active vibration suppression system uses actuators in the vibration suppression system to inject energy in to the suspension system to improve the system performance. These systems are commonly consume more energy than semi active systems. But the performance improvements are significant as compared to semi active systems as shown in Figure 2.5 [57], where the sprung mass acceleration is completely reduce with the active system. Active vibration suppression systems use electromagnetic or hydraulic actuators to insert energy in to the suspension system. These actuators will introduce active suspension force in to the system and actuator insertion has been done in multiple ways including series arrangement in Figure 2.6, Parallel arrangement Figure 2.7 and parallel regenerative models. And the actuator failure in these arrangement can lead to safety problems because these system forces are normally withstand by the active controller. In addition to these methods variable geometry suspension systems are developed in [58] but this system also have safety problems due to the arrangement as shown in Figure 2.9. Variable geometry suspension systems use geometrical variants in suspension to change system properties. Therefore to address these problems parallel actuator arrangement with a conventional passive spring damper system to withstand in actuator failure has proposed in this

University of Moratuwa, Sri Lanka.
Electronic Theses & Dissertations
www.lib.mrt.ac.lk

research.

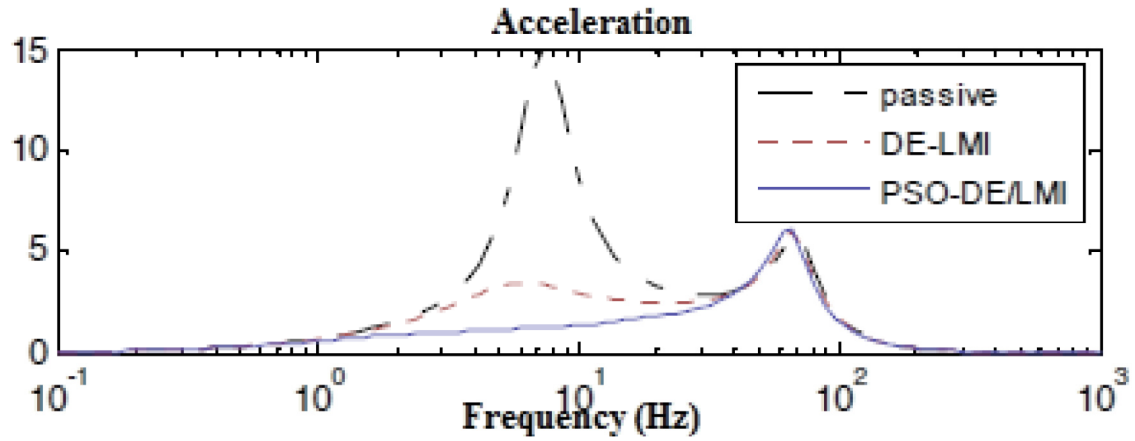

Figure 2.5: Multi Objective Active Vibration Suppression System Performance [57]

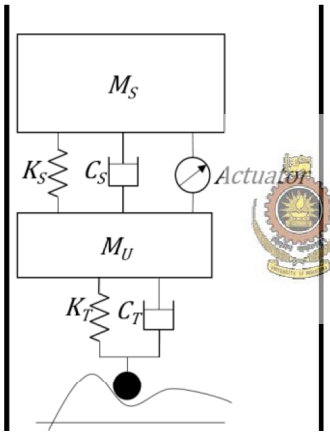

University of Moratuwa, Sri Lanka.
Electronic Theses & Dissertations
www.lib.mrt.ac.lk

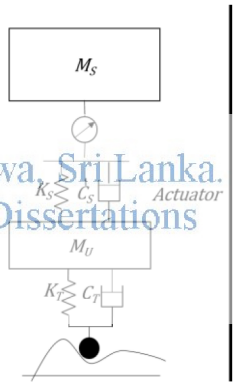

Figure 2.6: Parallel Actuator Arrangement

Figure 2.7: Series Actuator Arrangement

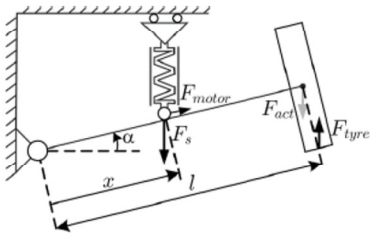

Figure 2.8: Variable Geometry Suspension [58]

2.5 Actuators and Sensors

The main component of the pure active suspension system is the actuator. Mainly two types of actuators are currently used in pure active suspension systems; hydraulic actuators and electromagnetic actuators. Hydraulic actuators are slower due to high inertia present in the fluid, valves and pistons. They tend to be very non-linear as dry friction is present in significant magnitudes. Maintenance requirement is also high in hydraulic actuated systems. Therefore electromagnetic actuators are widely used in many research areas as they have sufficient bandwidth having small system time constant, easy use and low maintenance. Electromagnetic actuators also have the capability of storing energy when they are working in the generator mode. Though hydraulic actuated systems are cost effective; the efficiency and the reliability of the suspension system can be improved by using electromagnetic actuators to provide active force into the system. Applicability of electromagnetic actuators as passive suspension systems has been analyzed and the performances are given in [59, 60] But these researches doesn't provide new active vibration suppression techniques; the electromagnetic actuator band widths and performances have been analyzed as shown in Figure 2.9. The results indicate that electromagnetic actuators have the capability to deliver the required force densities and provide high speed responses that required by active suspension systems. Therefore the proposed disturbance estimation based vibration suppression technique can be used to develop active vibration suppressor with these types of linear actuators.

University of Moratuwa, Sri Lanka.
Electronic Theses & Dissertations
www.lib.mrt.ac.lk

Active vibration sensors and observable variables are analyzed in [61]. They have been analyzed the effects of 12 observable variables as shown in Figure 2.10. Effects of using combinations of these sensors has been analyzed extensively with mathematical analysis in above paper. The

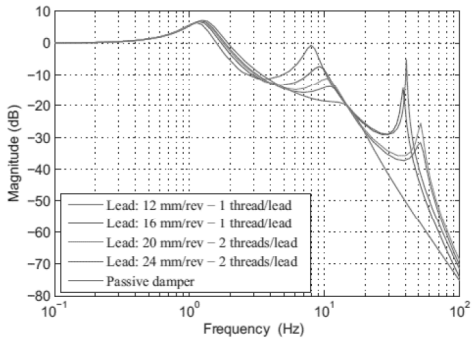

Figure 2.9: Electromagnetic Actuator Performance [59]

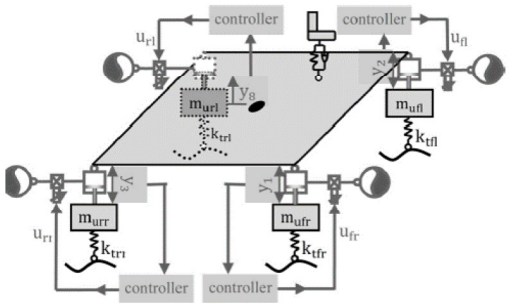

Figure 2.10: Observable Suspension Parameters [61]

results suggest that measuring deflections of three suspension elements and one axel acceleration measurement is the most stable arrangement for an active suspension system. Therefore suspension deflection and sprung mass acceleration is one of the most stable sensors that will be available in vehicular active suspension system. Therefore these sensor usage could increase the applicability of proposed system even for vehicles. Furthermore most suspension control strategies should use acceleration measurement to measure deflection and deflection speeds of sprung mass and unsprung mass. This is prone to problems in high frequency measurements due to the integration of acceleration to calculate the above variables. In addition accelerometers are prone to cause errors and problems in such calculations due to environmental effects [62]. The sensing of suspension deflection is not prone to delays and errors due to the internal measurability of the variable using optical or magnetic high precision motor encoders. Also the direct accelerometer reading can be used for sufficiently large bandwidth for disturbance calculations. The sensor delay reduction method are analyzed in [63, 64] but the applicability and usage of multiple sensors cause cost issues and still the system is prone to problems due to sensor failures. A robust suspension control method with minimal sensor usage will answer these problems and can work with only a single acceleration or deflection sensor under failures to multiple sensors. Furthermore this provides realm of new applications where using accelerometers to measure deflection and complex control capabilities are limited due to bandwidth requirements, size and application cost.

University of Moratuwa, Sri Lanka.
Electronic Theses & Dissertations
www.lib.mrt.ac.lk

2.6 Quarter Car Model

The proposed model has the ability to virtually disconnect the interested system by environment with the use of disturbance estimation. Disturbance transfer to interested system is measured in single direction therefore a commonly used 2 degrees of freedom (DOF) Quarter car model is proposed to measure the performance of the system. Quarter car model is commonly used in active vibration suppression researches to analyses the controller performance. Quarter car model is a 2 degrees of freedom vertical vibrating system as shown in Figure 2.11. This suspension system contains two controlled and uncontrolled vibration suppression elements. The top elements contains a sprung mass and a passive suspension system and the bottom contains an unsprung mass, passive suspension element and a surface contact point. The vibrations in the

contact point will travel through the bottom and top passive suspension system to the sprung mass.

The researched system use a parallel linear actuator with the conventional passive suspension system. This would prevent the system from causing safety problems in actuator failures as it would introduce the passive suspension element to the system. In addition linear actuators were selected considering the fast responses and linearity of the motor.

The system model consists of two masses M_S and M_U which are respectively known as sprung mass and unsprung mass. The system model is illustrated in fig. 2.12.

M_S : Sprung mass (kg)
M_U : Unsprung mass (kg)
K_S : Suspension system spring coefficient (N/m)
K_T : Tyre spring coefficient (N/m)
C_S : Suspension system damping coefficient (Ns/m)
C_T : Tyre damping coefficient (Ns/m)
F : Active force (N)
X_R : Displacement of road surface (m)
X_U : Displacement of unsprung mass (m)
X_S : Displacement of sprung mass (m)

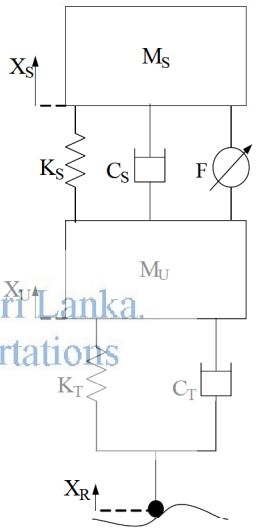

Figure 2.11: Quarter Car Model

University of Moratuwa, Sri Lanka.
Electronic Theses & Dissertations
www.lib.mrt.ac.lk

Assumptions

For modeling purposes it is assumed that all the above coefficients of the system and its masses do not vary with environmental factors and linear. In addition, it is assumed that the suspension system acts as an ideal model that only has the capability to move vertically. Therefore the system performance will be measured for vibration transfer through the elements in a single direction.

Newton's equation for sprung mass can be written as,

$$M_S\ddot{X}_S = -K_S(X_S - X_U) - C_S\left(\dot{X}_S - \dot{X}_U\right) + F \qquad (2.1)$$

Newton's equation for unsprung mass can be written as,

$$M_U \ddot{X}_U = K_S(X_S - X_U) + C_S(\dot{X}_S - \dot{X}_U) - K_T(X_U - X_R) - C_T(\dot{X}_U - \dot{X}_R) - F \quad (2.2)$$

2.6.1.1 Passive suspension system model

To derive passive suspension system equations we can assume the active force to be zero.

Using the Laplace domain function of (2.1) and (2.2), the passive suspension system transfer function can be written as,

$$X_S(s) = \frac{[C_T s + K_T][C_S s + K_S]}{\left[\begin{array}{c} M_S M_U s^4 + [M_S(C_S + C_T) + M_U C_S]s^3 + \\ [M_S(K_T + K_S) + M_U K_S + C_S C_T]s^2 \\ + [K_S C_T + K_T C_S]S + K_T K_S \end{array}\right]} X_R(s) \quad (2.3)$$

Passive suspension system frequency response to a disturbance profile can be measured using the above equation (2.3).

2.6.1.2 Active suspension system model

The active force F provided by the control system is used to model the active suspension system.

Following state variables are chosen to create a state space model of active suspension system.

University of Moratuwa, Sri Lanka.
Electronic Theses & Dissertations
www.lib.mrt.ac.lk

x_1: Relative displacement between sprung mass and unsprung mass

x_2: Velocity of sprung mass

x_3: Relative displacement between unsprung mass and road

x_4: Velocity of unsprung mass

Y : System output

F : Active force

$$x_1 = X_S - X_U \quad (2.4)$$

$$\dot{x_2} = \dot{X}_S \quad (2.5)$$

$$x_3 = X_U - X_R \quad (2.6)$$

$$\dot{x_4} = \dot{X_U} \quad (2.7)$$

$$Y = [\ddot{X}_S] = \dot{x_2} \quad (2.8)$$

Following equations are obtained by using the (2.1),(2.2),(2.4),(2.5),(2.6),(2.7) and (2.8).

$$\dot{x_1} = \dot{X_S} - \dot{X_U} = x_2 - x_4 \tag{2.9}$$

$$\dot{x_2} = \frac{-K_S(x_1) - Cs(x_2 - x_4) + F}{M_S} \tag{2.10}$$

$$\dot{x_3} = \dot{X_U} - \dot{X_R} = x_4 - \dot{X_R} \tag{2.11}$$

$$\dot{x_4} = \frac{K_S(x_1) + C_S(x_2 - x_4) + K_T(x_3) + C_T(x_4 - \dot{X_R}) - F}{M_U} \tag{2.12}$$

The system state space can be written using equations (2.9), (2.10), (2.11) and (2.12)

$$\begin{bmatrix} \dot{x_1} \\ \dot{x_2} \\ \dot{x_3} \\ \dot{x_4} \end{bmatrix} = \begin{bmatrix} 0 & 1 & 0 & -1 \\ -\frac{K_S}{M_S} & \frac{-C_S}{M_S} & 0 & \frac{C_S}{M_S} \\ 0 & 0 & 0 & 1 \\ \frac{K_S}{M_U} & \frac{C_S}{M_U} & \frac{K_T}{M_U} & \frac{C_S - C_T}{M_U} \end{bmatrix} \begin{bmatrix} x_1 \\ x_2 \\ x_3 \\ x_4 \end{bmatrix} + \begin{bmatrix} 1 \\ \frac{1}{M_S} \\ 0 \\ \frac{-1}{M_U} \end{bmatrix} F + \begin{bmatrix} 0 \\ 0 \\ -1 \\ \frac{C_T}{M_U} \end{bmatrix} \dot{X}_R \tag{2.13}$$

$$[Y] = \begin{bmatrix} \frac{-K_S}{M_S} & \frac{-C_S}{M_S} & 0 & \frac{C_S}{M_S} \end{bmatrix} \begin{bmatrix} x_1 \\ x_2 \\ x_3 \\ x_4 \end{bmatrix} + \begin{bmatrix} \frac{1}{M_S} \end{bmatrix} F \tag{2.14}$$

University of Moratuwa, Sri Lanka.
Electronic Theses & Dissertations
www.lib.mrt.ac.lk

The system performance can be measured using sprung mass deflection vs contact point displacement transfer function or sprung mass acceleration vs road surface displacement frequency response as in equation (2.15) and (2.16),

$$\frac{\ddot{X}_S}{X_R} = \frac{[C_T s + K_T][C_n s + K_n]s^2}{\left[\begin{matrix} M_S M_U s^4 + [M_S(C_n + C_T) + M_U C_n]s^3 + \\ [M_S(K_T + K_n) + M_U K_S + C_n C_T]s^2 \\ + [K_n C_T + K_T C_n]S + K_T K_n \end{matrix}\right]} \tag{2.15}$$

$$\frac{X_S}{X_R} = \frac{[C_T s + K_T][C_n s + K_n]}{\left[\begin{matrix} M_S M_U s^4 + [M_S(C_n + C_T) + M_U C_n]s^3 + \\ [M_S(K_T + K_S) + M_U K_S + C_n C_T]s^2 \\ + [K_n C_T + K_T C_n]S + K_T K_n \end{matrix}\right]} \tag{2.16}$$

Where K_n, C_n are the effective spring damper coefficients with the active controller.

Chapter 3

3 DISTURBANCE OBSERVER BASED CONTROL

3.1 Linear Motor Model

The DC motor is the simplest machine which converts electrical energy to the mechanical energy. Rotary DC motors are commonly used in widely used in numerous control applications, including robot manipulators, disk drive, machine tools and servo actuators etc. DC motor is very popular especially in precise motion control applications, as the modeling is much simple than all the other motors [65] [66]. Linear DC motor or Linear Brushless DC motor (BLDC) motor is a DC motor that can deliver linear forces and motion and similar to Rotary DC motors in characteristics. A DC linear motor contains a motor shaft and a motor forcer as shown in Figure 3.1. Motor forcer similar to the stator of a DC rotary motor and the shaft acts as the rotor. The linear BLDC motor shaft contains a permanent magnet core that acts with the motor forcer/

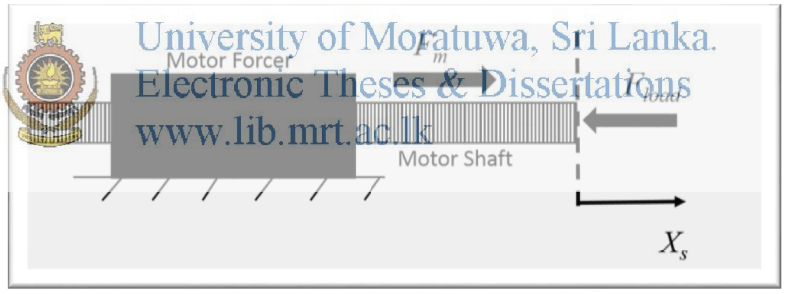

University of Moratuwa, Sri Lanka.
Electronic Theses & Dissertations
www.lib.mrt.ac.lk

Figure 3.1: Linear Motor Design

stator coil magnetic field to produce linear motion.

Figure 3.2 shows the Electrical Model of a forcer mounted BLDC linear motor where R_a and L_a represents the forcer resistance and inductance respectively.

Applying Kirchhoff's voltage law the DC motor model (3.1) can be obtained.

$$V_a = L_a \frac{dI_a}{dt} + R_a I_a + E_b \tag{3.1}$$

Where E_b is the back emf.

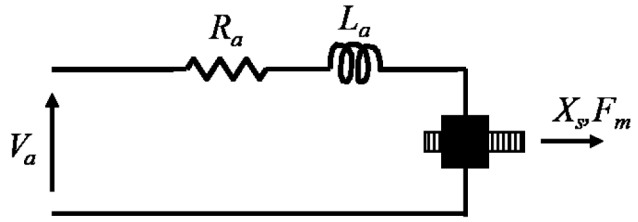

Figure 3.2: Linear Motor Electrical Model

$$E_b = K_e v(s) \tag{3.2}$$

Where K_e is the back emf constant and v is the shaft speed, then

$$V_a = L_a \frac{dI_a}{dt} + R_a I_a + K_e v(s) \tag{3.3}$$

If the total mechanical output given by the motor is F_m

$$I_a = \frac{F_m}{K_t} \tag{3.4}$$

Where k_t is the force constant of the motor.

University of Moratuwa, Sri Lanka.
Electronic Theses & Dissertations
www.lib.mrt.ac.lk

Applying (3.3) in (3.4) gives (3.5),

$$V_a = L_a \frac{d(F_m / K_t)}{dt} + R_a \frac{F_m}{K_t} + K_e v(s) \tag{3.5}$$

Motor force F_m can be written as follows,

$$F_m = M \frac{dv}{dt} + Bv + F_l + F_f \tag{3.6}$$

Where,

M- Motor Shaft Mass

B-Viscous friction Coefficient

F_l– Load Force

F_f- Static Friction

Speed of the motor can be calculated as

$$v(s) = \frac{F(s) - \left[F_l(s) + F_f(s)\right]}{Ms + B} \tag{3.7}$$

3.2 Disturbance Force Measurement

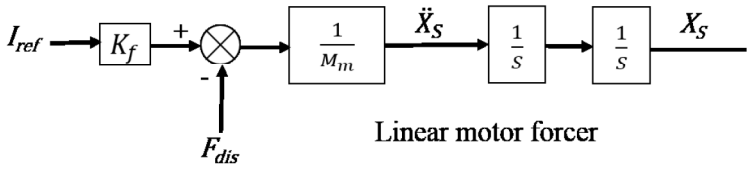

Figure 3.3: Simplified Model of a Linear Motor

Figure 3.3 shows a simplified diagram of BLDC motor model with a current controller. I_{ref} is the current command determined by the DC motor motion controller where K_f is the force constant. For illustration we will consider I_{ref} and I_a to be equal. The variation of the force constant due to the BLDC motor commutation creates motor force pulsation. F_m is the generated motor force obtained by the product of I_{ref} with K_f. F_m is the disturbance force exerted on the system by environment.

University of Moratuwa, Sri Lanka.
Electronic Theses & Dissertations
www.lib.mrt.ac.lk

The load force F_{load} includes the interactive force that act on the motor shaft as the motor forcer is considered to be mounted. The friction has the components of both the static friction and the viscosity. F_s is the static friction force and β is the viscosity coefficient. The disturbance force is defined to have all the above components. From the above discussion the disturbance force is defined as equation 3.8 using equations (3.4), (3.6) and (3.7).

$$F_{dob} = -M_n vs + K_{fn} I_{ref} \tag{3.8}$$

Where,

I_{ref} - Motor Current

M_n - Nominal Motor mass

K_{fn} -Nominal Force constant

v - velocity

S - Laplace operator

The disturbance force is directly calculated from the velocity of the motor and the real motor current.

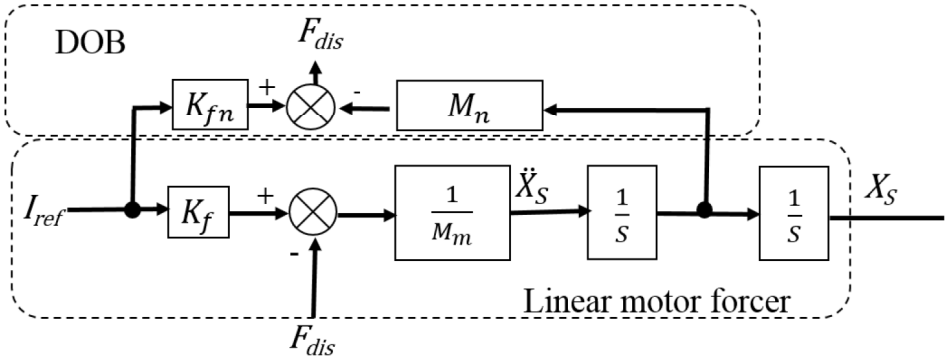

Figure 3.4: Disturbance observer model

It is difficult to realize Figure 3.4 directly, due to high frequency noises in current sensors and velocity calculations a low pass filter should be introduced in disturbance force calculation as shown in Figure 3.5. The modeled system uses a first order Butterworth filter with a cut off frequency of 100Hz.

University of Moratuwa, Sri Lanka.
Electronic Theses & Dissertations
www.lib.mrt.ac.lk

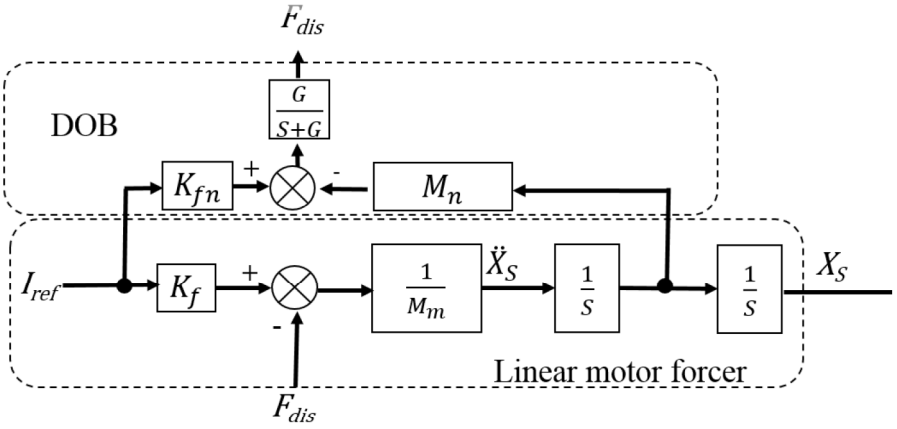

Figure 3.5: Modified DOB Estimation

Where g is the filter constant, from Figure 3.5. The estimated disturbance force is represented in (3.9).

$$\hat{F}_{dis} = \frac{g}{s+g} F_{dob} \tag{3.9}$$

In (3.9) the disturbance force is estimated through a first order lag with a time constant g, for the precise and accurate measurement, it is preferable to choose g as large as possible.

The feedback of the estimated disturbance force will have an ability to suppress the disturbance effects of the motor.

The disturbance observer calculates and estimates the reaction forces and torques as quickly as possible [67] [68]. By having the disturbance feedback, it could compensate for the unknown disturbance acting on the system.

3.3 Free moving Linear Motor Model

Even though the conventional linear motor model suggests the movement of motor shaft with a mounted motor forcer the active vibration suppression model linear motor is connected in between sprung mass and unsprung mass with the possibility of relative movement and without the possibility of motor velocity measurement. The Newton's equations for motor forcer can be written as (3.10) using Figure 3.6,

University of Moratuwa, Sri Lanka.
Electronic Theses & Dissertations
www.lib.mrt.ac.lk

$$F_m = M_f X_f s^2 + F_{forcer} \tag{3.10}$$

Where

M_f - Motor forcer weight

X_f - Motor forcer position

F_{forcer} - Total external force acting on the motor forcer

Using (3.10) we can come up with (3.11) for motor forcer using the same techniques used in conventional DOB calculations.

$$F_{forcer} = F_{load,forcer} + v\beta + F_s \tag{3.11}$$

Where

$F_{load,forcer}$ - Load force on the motor forcer

The disturbance force on the motor forcer can be calculated using similar equations as for motor shaft,

$$F_{dis} = -M_f X_f s^2 + K_f I_{ref} \quad (3.12)$$

The measured disturbance can be written as (3.14)

$$F_{dis} = -M_{fn} X_f s^2 + K_{fn} I_{ref} \quad (3.13)$$

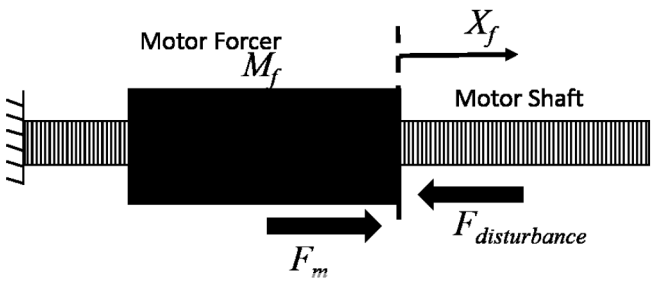

University of Moratuwa, Sri Lanka.

Figure 3.6: Linear Motor with a Moving Forcer

Electronic Theses & Dissertations
www.lib.mrt.ac.lk

3.4 Application of DOB in Active Suspension

The active suspension system is actuated by a BLDC linear motor which connected in between the sprung mass and the unsprung mass as shown in Figure 3.7. The Newtown's equations for motor forcer can be written as (3.14) form equilibrium position. And the friction effects can be neglected because BLDC motors disconnected forcer and shaft arrangement.

The effects of gravity is taken by the initial deflections of spring damper and therefore F_{load} will contain only the effects of dynamic vibrations,

$$(M_f + M_s) X_s s^2 = K_s(X_s - X_u) + C_s(X_s - X_u) + F_\alpha + F_m \quad (3.14)$$

Where

F_α is the non-linear effects of the spring damper system

Using equation (3.13) and (3.14) we can calculate the disturbance acting on the sprung mass is,

$$F_{dis} = K_s(X_s - X_u) + C_s(X_s - X_u) + F_\alpha \quad (3.15)$$

This disturbance can be estimated using a new disturbance observer model shown in Figure. 3.8.

$$\widehat{F_{dis}} = (-(M_n)X_s s^2 + K_{fn} I_{ref}) \frac{g}{s+g} \quad (3.16)$$

Where

M_n - Nominal mass of motor forcer and sprung mass

This disturbance force measurement will estimate the external disturbances acting on sprung mass with the use of direct accelerometer readings. The external disturbances acting on sprung mass is occur due to vibrations travel through passive suspension system to the sprung mass. The accelerations of the system can be minimized negating the effects of disturbance forces. A force controller with PID feedback loop is developed for this purpose. The PID controller will compensate the effects of non-linearity and delays. The total control loop is shown in Figure 3.9.

The DOB based controller will calculate the disturbance forces exerted on the system by passive

University of Moratuwa, Sri Lanka.
Electronic Theses & Dissertations
www.lib.mrt.ac.lk

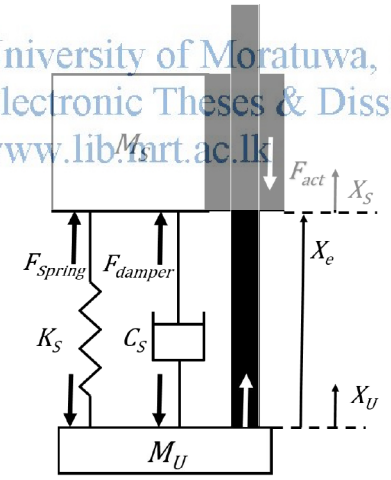

Figure 3.7: Active Suspension System Forces

vibrating elements. The controller will try to negate the effects of these vibrations using a PID based force control loop where the reference is equal to a value of zero. This controller will try to minimize the effects of disturbances and will keep the total force acting on the sprung closer to zero.

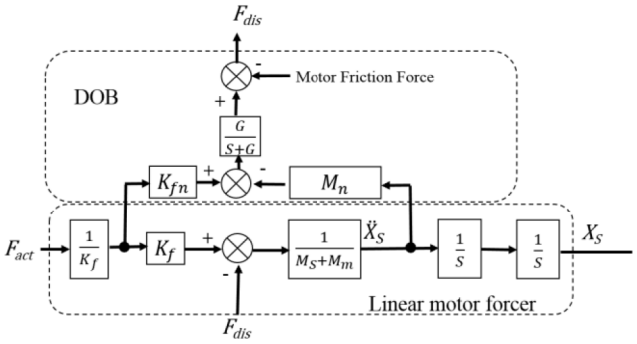

Figure 3.8: Active Vibration Measurement DOB/RFOB

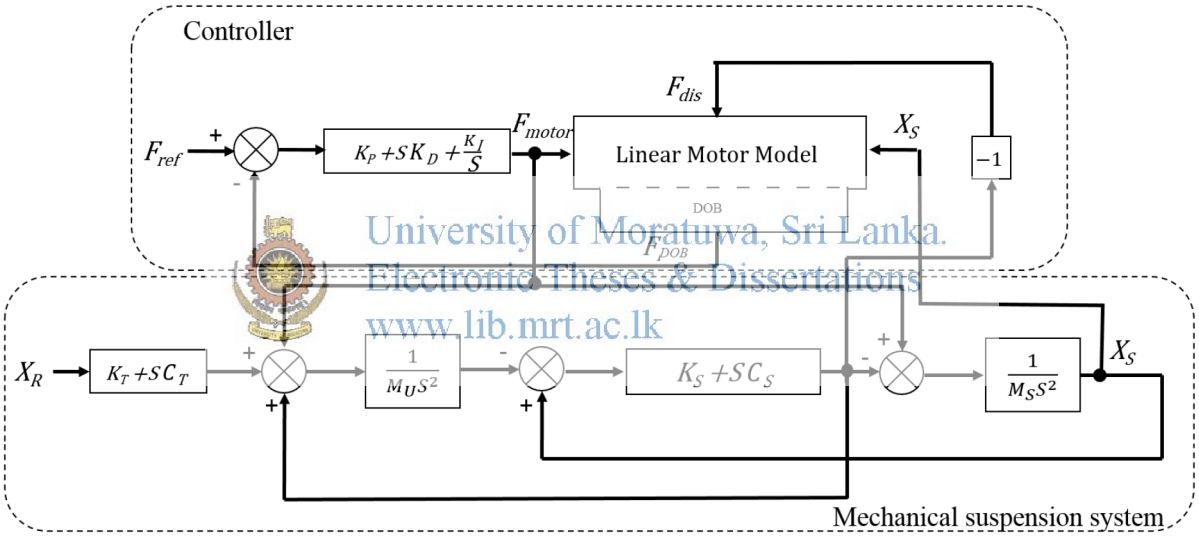

University of Moratuwa, Sri Lanka.
Electronic Theses & Dissertations
www.lib.mrt.ac.lk

Figure 3.9: Active Vibration Suppression System Model

3.5 Proposed Disturbance Force Based Vibration Suppressor Performance

3.5.1 Simulation Results

The active vibration suppression system is modeled and simulated in Matlab Simulink simulation environment. Considering a quarter car system shown in Figure 2.6. The controller block diagram that is used in the simulation is shown in Figure 3.9. Table 3.1 shows the simulation parameters that were used in the active vibration suppression model.

Table 3.1: Simulation Parameters

Symbol	Parameter value
M_S	300kg
M_U	60kg
K_S	16000 N/m
K_T	190000 N/m
C_S	1000 N/m^2
C_T	0 N/m^2
K_f	47 N/A
K_{fn}	47 N/A
M_m	1.1kg
M_{sn}	300kg
M_{mn}	1.1kg
K_P	0.99
K_I	0
K_D	0.0000002
G_{gis}	100

University of Moratuwa, Sri Lanka.
Electronic Theses & Dissertations
www.lib.mrt.ac.lk

The modeled suspension system's frequency response without the active controller is shown in Figure 3.10. The active suspension system provides superior vibration suppression properties than in the passive suspension system throughout the human sensitive frequency range. The

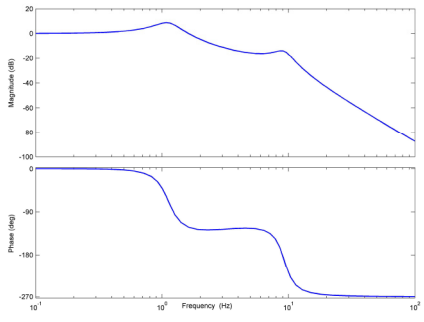

Figure 3.10: Passive Suspension Response

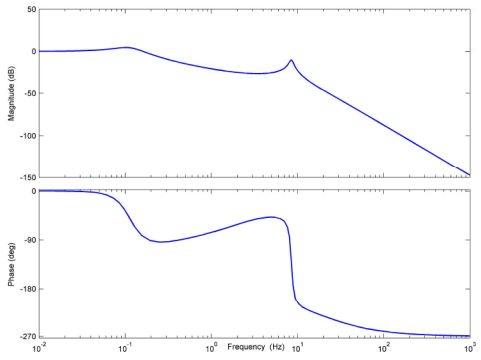

Figure 3.11: Active Suspension Response

Figure 3.11 shows the active suspension system's frequency response diagram providing evidence to the robust vibration suppression capabilities of novel proposed controller even at

lower frequencies. The suspension system provides vibration suppression of -5dB even at 0.1Hz. The vibration suppression capabilities of the system improves at higher frequencies.

The active vibration suppression system's pole zero diagram is shown in Figure 3.12. There are nine poles and eight zeros in negative side of the imaginary axis of pole zero diagram. The system shows stability for given parameter values. The Figure 3.11 frequency response diagram and Figure 3.12 pole zero diagram diagrams shows applicability of the proposed vibration suppression system. At 20Hz phase cross over the 180 degrees but the gain at this point is below 1. Therefore the system is stable at this frequency. And the poles and zeros are in 100Hz or higher frequency range doesn't affect the interested low frequency bandwidth.

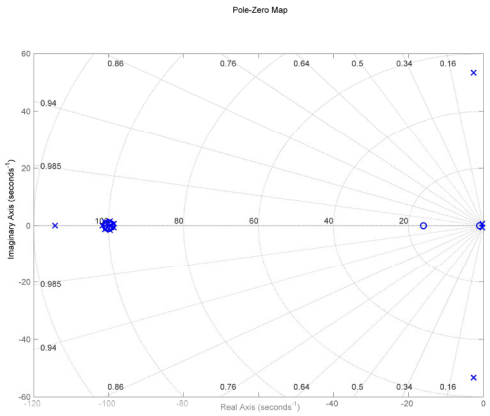

Figure 3.12: Pole Zero Diagram of Active Suspension System

University of Moratuwa, Sri Lanka.
Electronic Theses & Dissertations
www.lib.mrt.ac.lk

The system DOB filter gain value depends upon the sampling frequency of controller. The active suspension system performance therefore varies with the system controller speed and the suspension system frequency for different gain values shown in Figure 3.13. The Figure 3.13 shows the system vibration suppression performance improvement for higher gain values.

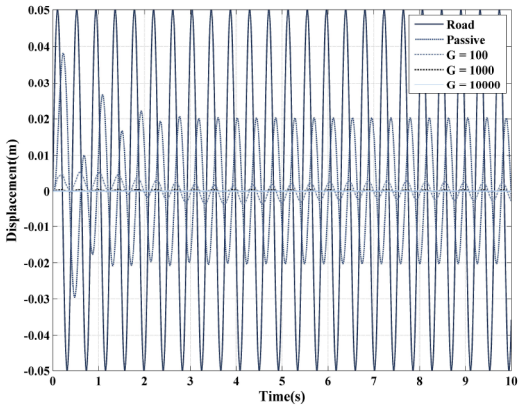

Figure 3.13: System Response for Filter Gains

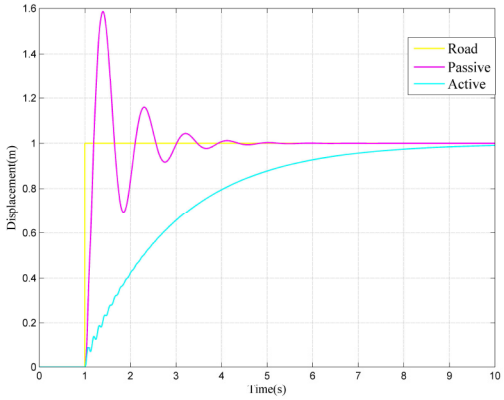

Figure 3.14: Step Response of the System

Figure 3.14 shows the step response of the active suspension system and passive suspension system. Active suspension system has small vibrations caused by the sample filtration of DOB/RFOB, but provide better system response for step inputs than the passive suspension system. The passive system performance can be improved with damping coefficient variations but the active performance is superior for sinusoidal vibrations.

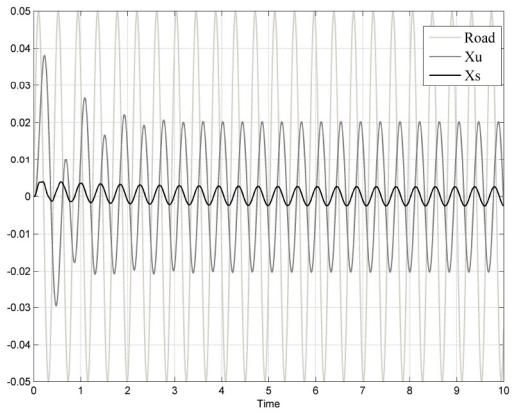

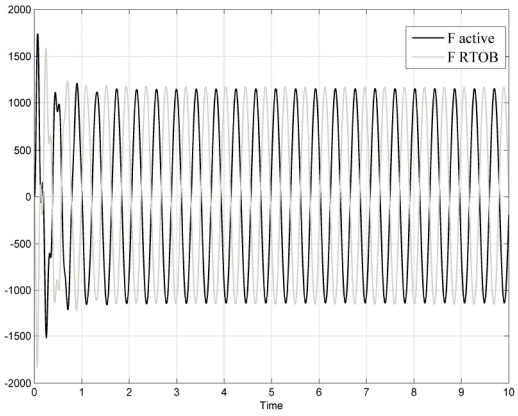

Figure 3.15: System Response for Sinusoidal Vibration **Figure 3.16: Disturbance and RFOB forces**

University of Moratuwa, Sri Lanka.
Electronic Theses & Dissertations
www.lib.mrt.ac.lk

The system sprung mass vibration for sinusoidal disturbance is shown Figure 3.15. Figure 3.16 shows the active suspension motor force. The system provides good vibration suppression for sinusoidal vibrations and active suspension system motor force is around 800N in 5cm deflection level. These output shows that the system can provide a superior vibration suppression for

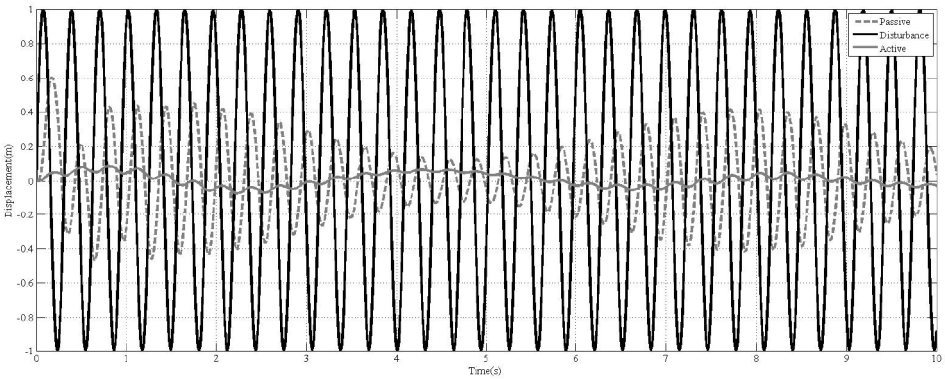

Figure 3.17: System Response for a sinusoidal sprung mass weight variation with disturbance

vibrations with the use of electromagnetic actuators. And actuator saturation may limit the performance of the proposed system therefore motor should select to prevent the saturation conditions.

The proposed system performance was further simulated for variations to the sprung mass weight. A sinusoidal sprung mass variation and a ramp sprung mass variation was tested with a sinusoidal disturbance and a complex disturbance to analyze the controller performance. Figure 3.17 shows the superior performance of the vibration suppressor under a sinusoidal disturbance with a sinusoidal variation of weight under a different frequency. Proposed controller also analyzed for a furrier series based vibration under an increasing sprung mass weight and the proposed system provide a more stable platform compared to the passive system as shown in Figure 3.18.

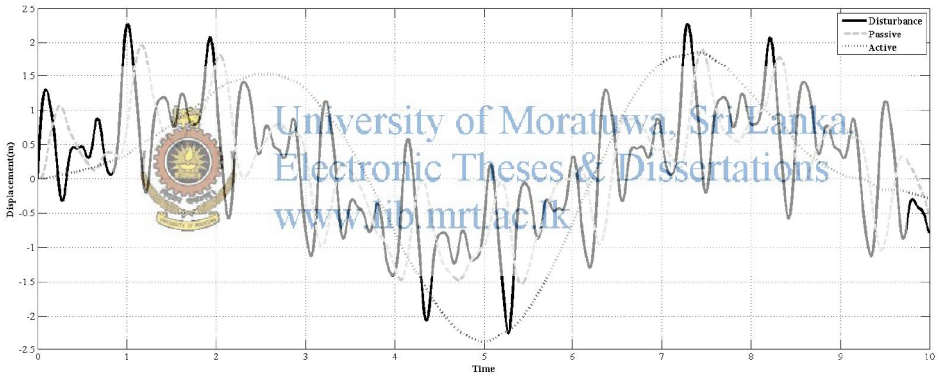

University of Moratuwa, Sri Lanka.
Electronic Theses & Dissertations
www.lib.mrt.ac.lk

Figure 3.18: System Response for a complex sinusoidal disturbance

Experimental results of the system performance is described in section 7.1 in chapter 7.

Chapter 4

4 VIRTUAL SPRING DAMPER VIBRATION SUPPRESOR

4.1 Virtual Spring Damper Motor Model

The DOB based active vibration suppression system have drawbacks due to the effects of sensor noises. And accelerometers are prone to external environmental variations. Therefore a suspension deflection based disturbance measurement scheme was developed for the active vibration suppression system. The disturbance acting on the sprung mass or motor forcer is exerted by the passive elements in the suspension model can be derived as,

$$(M_f + M_s)X_s s^2 = K_s(X_s - X_u) + C_s(X_s - X_u) + F_\alpha + K_f I_{ref} \quad (4.1)$$

$$F_{dis} = K_s(X_s - X_u) + C_s(X_s - X_u) + F_\alpha \quad (4.2)$$

Therefore the disturbance force acting on the sprung mass can be approximated using the linear equation (4.3)

University of Moratuwa, Sri Lanka.
Electronic Theses & Dissertations
www.lib.mrt.ac.lk

$$F_{dis} = K_{sn}(X_s - X_u) + C_{sn}(\dot{X}_s - \dot{X}_u) \quad (4.3)$$

Where

K_{sn} is nominal spring coefficient

C_{sn} is nominal damping coefficient

However this linear measurement doesn't contain the effects of non-linearity. The non-linear effects can be approximated in to the observable variables as in (4.4),

$$F_\alpha = f_{1(X_s - X_u)} + f_{2(\dot{X}_s - \dot{X}_u)} + f_{3(\ddot{X}_s - \dot{\ddot{X}}_u)} + \cdots. \quad (4.4)$$

The only sensor used in the controller is the motor deflection and it can derived to (4.5),

$$X_e = (X_s - X_u) \quad (4.5)$$

Where

X_e is the motor deflection

4.2 Disturbance Force Measurement

The disturbance force acting on the sprung mass can be measured using equation (4.3) where it is assumed that the system is linear. But to minimize the errors some of the nonlinearities can be reduced with estimation of nonlinear functions with respect to deflection.

$$\hat{F}_{\alpha} = f_{1(X_s - X_u)} + f_{2(\dot{X}_s - \dot{X}_u)} \tag{4.5}$$

The motor deflection and deflection speed is observed by linear encoders and they are less prone to environmental effects and have high speeds and high bandwidths due to digital signal processing techniques,

Using (4.1), (4.3) and (4.5) we can come with the equation for disturbances acting on sprung mass using only deflection observations,

$$\hat{F}_{dis} = K_{sn}(X_s - X_u) + C_{sn}(\dot{X}_s - \dot{X}_u) + f_{1(X_s - X_u)} + f_{2(\dot{X}_s - \dot{X}_u)} \tag{4.6}$$

The nonlinear effects can be added to the controller by the use of look up tables and the equation can be simplified using nonlinear spring damper coefficients of $K_{sn(xe)}$ and $C_{sn(xe)}$.

University of Moratuwa, Sri Lanka.
Electronic Theses & Dissertations
www.lib.mrt.ac.lk

$$\hat{F}_{dis} = K_{sn(X_e)}(X_s - X_u) + C_{sn(\dot{X}_e)}(\dot{X}_s - \dot{X}_u) \tag{4.7}$$

The spring damper based disturbance measurement scheme includes one velocity calculation. Even though theoretically it is not necessary to have a filter, a low pass filter should added in high speed digital computing as shown in Figure 4.1. But this filter constant can be sufficiently large in range of 1 kHz giving this measurement a wider bandwidth.

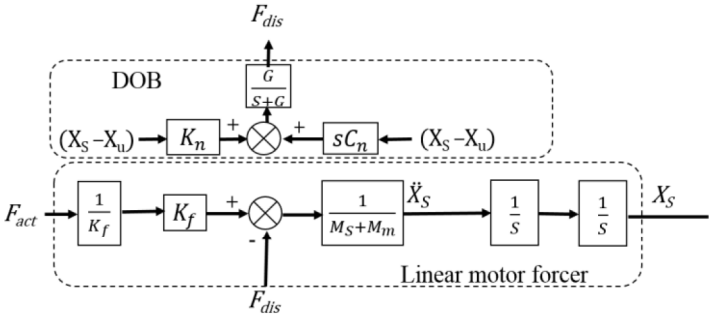

Figure 4.1: Spring Damper Based Disturbance Observer

4.3 Virtual Spring Damper Controller

The spring damper based disturbance calculation can be used to reduce the effects of disturbances on sprung mass. A feedback force controller can be used to negate the effects of passive spring damper system disturbances. The force reference of the feedback controller can be used to negate the effects of vibrations or else can be used to create virtual spring damper coefficients as in equation (4.8).

$$F_{ref} = K_v(X_s - X_u) + C_v(\dot{X}_s - \dot{X}_u) \tag{4.8}$$

Where

K_v is the virtual spring constant

C_v is the virtual damping constant

A PID controller is introduced in the controller to minimize the effects of nonlinearities and delays. The controller model is shown in Figure 4.2. Where the spring damper based disturbance observer is used to measure the disturbance and a feedback force controller is trying to minimize the effects of vibrations. The system transfer function between sprung mass and unsprung mass Newton's equations can be derived as (4.9) (4.10).

University of Moratuwa, Sri Lanka.
Electronic Theses & Dissertations
www.lib.mrt.ac.lk

$$M_S\ddot{X}_S = (K_n - K_S)(X_S - X_U) + (C_n - C_S)(\dot{X}_S - \dot{X}_U) \tag{4.9}$$

$$M_u\ddot{X}_u = -(K_n - K_S)(X_S - X_U) - (C_n - C_S)(\dot{X}_S - \dot{X}_U) + K_t(X_u - X_r) + C_t(\dot{X}_u - \dot{X}_r) \tag{4.10}$$

Using equation 4.9 and 4.10 we can derived the transfer function in between road surface and sprung mass as 4.11 for zero K_v and C_v coefficients,

$$\frac{X_S}{X_R} = \frac{[C_T s + K_T]\left[(C_S(1-\frac{G}{s+G}))s + K_S(1-\frac{G}{s+G})\right]}{\begin{bmatrix} M_S M_U s^4 + \left[M_S\left(C_S(1-\frac{G}{s+G}) + C_T\right) + M_U(C_S(1-\frac{G}{s+G}))\right]s^3 + \\ \left[M_S\left(K_T + K_S(1-\frac{G}{s+G})\right) + M_U(K_S(1-\frac{G}{s+G})) + (C_S(1-\frac{G}{s+G}))C_T\right]s^2 \\ + \left[(K_S(1-\frac{G}{s+G}))C_T + K_T(C_S(1-\frac{G}{s+G}))\right]S + K_T(K_S(1-\frac{G}{s+G})) \end{bmatrix}} \tag{4.11}$$

The virtual spring damper based disturbance observation and control system has higher bandwidth than the DOB based system due to the removal of accelerometer and current sensor

noises in the disturbance measurement. In addition the system can be easily controlled to provide different spring damper effects with only internal sensor measurements.

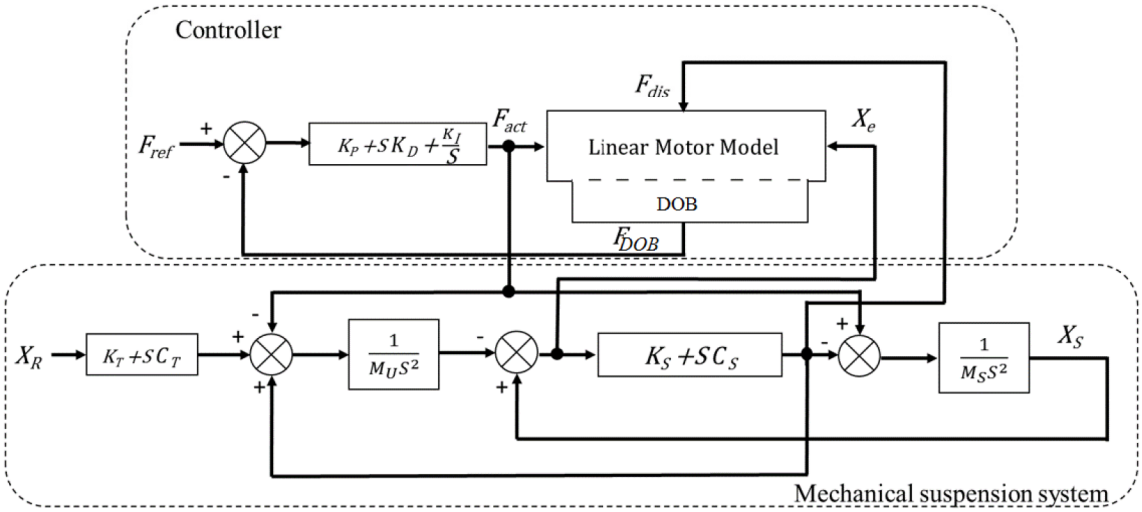

Figure 4.2: Virtual Spring Damper Controller

University of Moratuwa, Sri Lanka.
Electronic Theses & Dissertations
www.lib.mrt.ac.lk

4.4 Proposed Virtual Spring Damper Vibration Suppression Performance

4.4.1 Simulation Results

Table 4.1: System Parameters

Symbol	Simulated system values
M_S	300kg
M_U	60kg
K_S	16000 N/m
K_T	190000 N/m
C_S	1000 N/m2
C_T	0 N/m2
K_f	47 N/A
K_{fn}	47 N/A
M_m	1.1kg
M_{sn}	301.1kg
K_P	0.99
K_I	0 0.001
K_D	0.0000002
G_{gis}	100

Table 4.1 shows the list of simulation parameters used in the quarter car model simulation. Matlab Simulink is used for modelling. The System was modeled and simulated with parameters considering an actual quarter car model and the hardware design was built considering the quarter car parameter ratios. The modeled system frequency response is simulated under different conditions to measure the vibration suppression ability at different frequencies. Bode plot diagram for the passive suspension is shown in Figure 4.3. The system vibration suppression capabilities for active vibration suppression controller is shown in Figure 4.4. The simulation results shows the superior vibration suppression capabilities of the novel disturbance observer based system. The passive and active systems show lack of vibration suppression capabilities for low frequencies but the active system's disturbance rejection bandwidth is much higher than the passive system. The active suspension system's vibration suppression starts at a lower frequency. At higher frequencies both systems shows high level vibration suppression.

The system stability is further illustrated using a pole zero diagram in Figure 4.5. The pole zero diagram shows that the poles and zeros are in the negative side of the imaginary axis and there are no poles on the imaginary axis that cause oscillations. Therefore the simulation results shows the stability and superior vibration suppression capabilities of the system in the quarter car model. The system shows similar results for step, ramp and sinusoidal inputs compared to the DOB based model.

University of Moratuwa, Sri Lanka.
Electronic Theses & Dissertations
www.lib.mrt.ac.lk

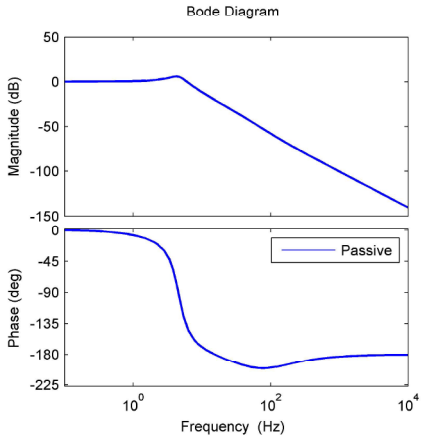

Figure 4.3: Passive Suspension Frequency Response

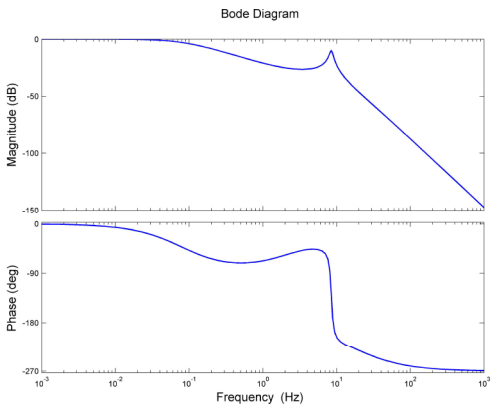

Figure 4.4: Active Suspension Frequency Response

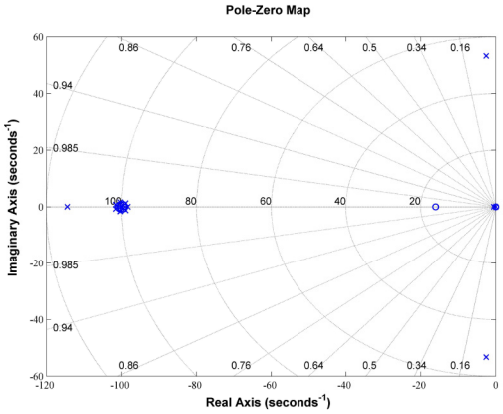

Figure 4.5: Active Suspension System Pole Zero Diagram

The proposed system was simulated for quarter car parameters given in [56], [57], [59]. The simulation results suggest the high quality performance of the proposed vibration suppression system compared to them. The Figure 4.6, 4.7, 4.8, 4.9, 4.10, 4.11 Compare the simulated results with the frequency response results of the literature. The similar frequency points are marked using A,B and C characters for ease of identification. The proposed controller provide higher acceleration reduction and deflection reduction compared to the available methods. The simulation was done in linearized model therefore the results may contain small variations. Experimental results of system are shown in section 7.2 in chapter 7.

University of Moratuwa, Sri Lanka
Electronic Theses & Dissertations
www.lib.mrt.ac.lk

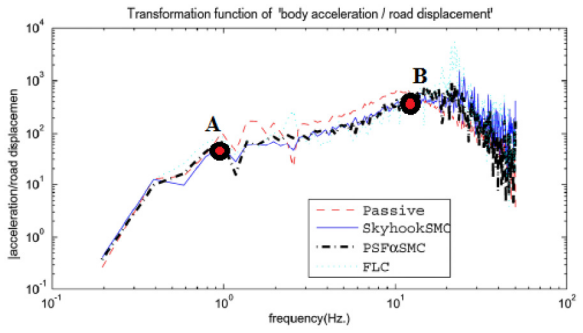

Figure 4.6 : Fuzzy, SMC frequency response [56]

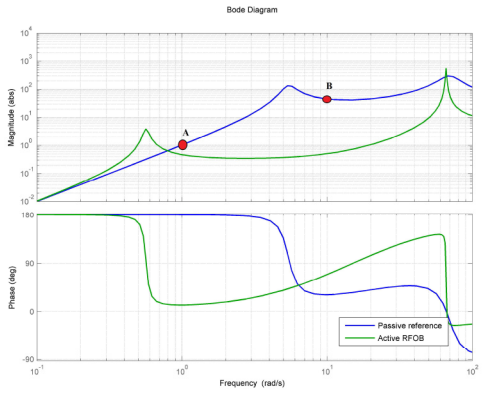

Figure 4.7: Proposed system frequency response

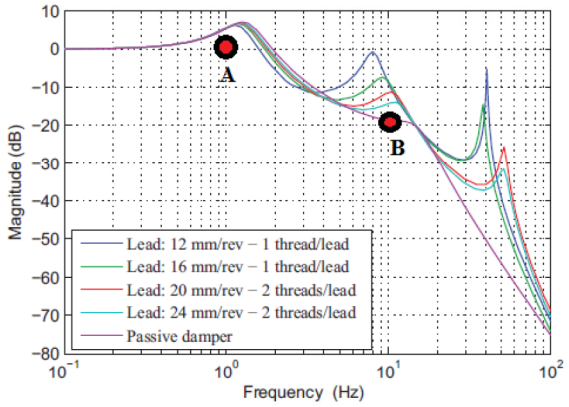

Figure 4.8: Lead Screw system frequency response

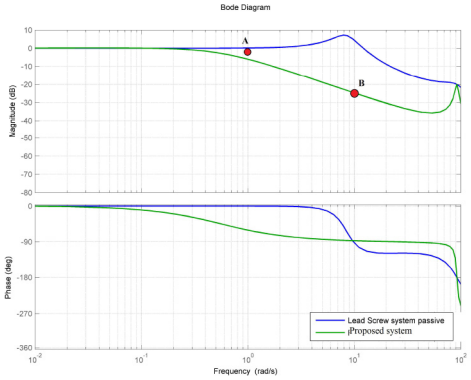

Figure 4.9: Proposed system frequency response

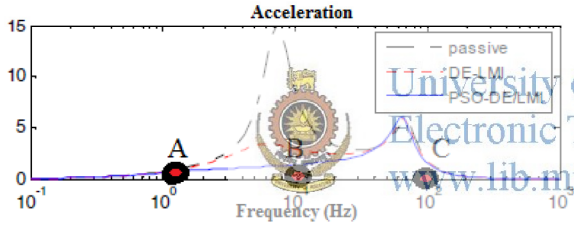

Figure 4.10: Multi objective suspension performance

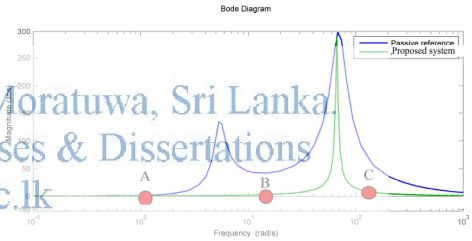

Figure 4.11: Proposed system performance

University of Moratuwa, Sri Lanka.
Electronic Theses & Dissertations
www.lib.mrt.ac.lk

Chapter 5

5 PARAMETER ESTIMATION AND EFFECTS

5.1 Passive Spring Damper System Model

Passive quarter car model can be used to analyze the parameter effects of active suspension system. The suspension system spring damper models can be used to calculate the amount of force that is exerted by the suspension system on active suspension actuator and the sprung mass. The effects of these parameters on suspension system should be analyze in actuator selection to prevent suspension performance degrading and issues with actuator saturation. The passive suspension system mainly installed in the systems to suspended the sprung mass weight without introducing that static energy to the active vibration suppression system actuator. The active vibration suppression controller try to minimize the accelerations and deflections of sprung mass by negating the effects of passive vibration suppression system. In simple term the passive system takes the static loads of sprung mass and the controller virtually disconnect the passive suspension system for dynamic loads as shown in Figure 5.1.

University of Moratuwa, Sri Lanka.
Electronic Theses & Dissertations
www.lib.mrt.ac.lk

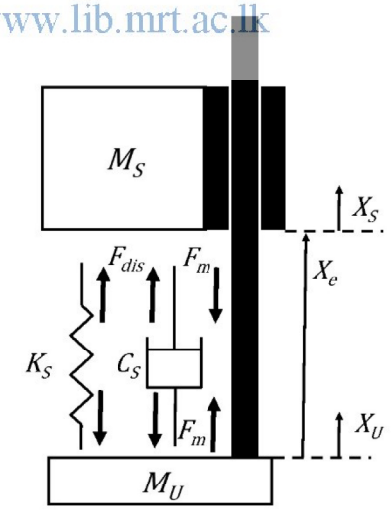

Figure 5.1: Illustration of Suspension System under Dynamic Loads

Considering the ideal conditions the active vibration suppression system Newton's equations for static weights and dynamic forces can be written as (5.1) and (5.2),

$$(M_s + M_f)g = K_s X_{e,initial} \quad (5.1)$$

$$(M_s + M_f)X_s s^2 = (K_s - (K_{sn} - K_v))(X_s - X_u) + (C_s - (C_{sn} - C_v))(\dot{X}_s - \dot{X}_u) \quad (5.2)$$

Where

g is the acceleration coefficient of gravity

$X_{e,initial}$ is the initial deflection of suspension

The motor force can be derived from (5.2) as,

$$F_m = (K_{sn} - K_v)(X_s - X_u) + (C_{sn} - C_v)(\dot{X}_s - \dot{X}_u) \quad (5.3)$$

And K_v and C_v should be set to zero to fully nullify and virtually disconnect the sprung mass from the environment performance. Therefore the actuator force depends on the passive suspension system spring damper coefficients and the virtual spring damper coefficients. The weight of suspension on spring removes the need of the actuator to constantly supply energy to the actuator to handle the weight. In design the saturation effects can be modeled using the linearized transfer functions of the system in different spring damper effects.

University of Moratuwa, Sri Lanka.
Electronic Theses & Dissertations
www.lib.mrt.ac.lk

5.2 Spring Damper Parameter Estimation

The researched controller is working on internal sensing mechanisms therefore parameter estimation is necessary for precise accurate vibration measurement and suppression. An electromagnetic actuator is used in the controller therefore electromagnetic actuator based parameter measurement was carried out with the use of lookup tables to include the vibration suppression system nonlinear effects.

The vibration suppression system sensors can be used to measure these parameters; the system includes a suspension deflection measurement encoder and additionally includes an accelerometer. The measurement criteria of the parameters with the use of both sensors and with only the use of deflection measurement is proposed in this section. The disturbance force measurement is done with the use of estimated parameters in equation (5.4) and (5.5),

$$\hat{F}_{dis} = K_{sn(X_e)}(X_s - X_u) + C_{sn(\dot{X}_e)}(\dot{X}_s - \dot{X}_u) \quad (5.4)$$

$$\widehat{F_{dis}} = (-(M_n)X_s s^2 - K_{fn} I_{ref}) \frac{g}{s+g} \quad (5.6)$$

The disturbance force estimation includes the following variable estimations,

K_{sn} is the estimated spring constant

C_{sn} is the estimated damping constant

M_n is the estimated nominal sprung mass (includes forcer weight)

K_{tn} is the estimated motor force constant

The motor force constant used in the estimation is taken directly from the motor specification.

The spring damper coefficients and the mass can be measured in stable conditions using position and velocity control loops as shown in fig. 5.2.

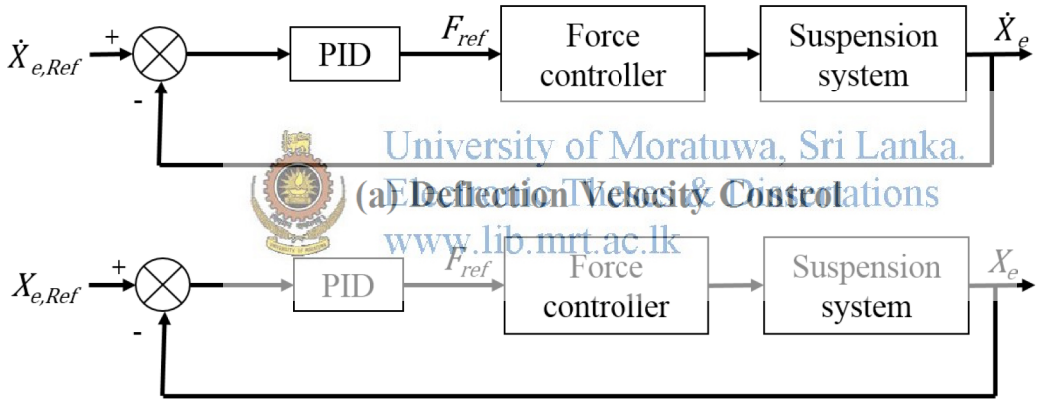

University of Moratuwa, Sri Lanka.
Electronic Theses & Dissertations
www.lib.mrt.ac.lk

Figure 5.2: Velocity and Position Control Loops

Mass of sprung mass and motor forcer can be measured by (5.7) under stable conditions,

$\dot{X}_e$ =0, $\ddot{X}_e$=0, $\dot{X}_s$ =0 and $\ddot{X}_s$=0

$$M_n = \frac{K_{sn}(X_{e,inital})}{g} \quad (5.7)$$

Spring and damper constants with the effects of non-linearity can be measured using (5.8) and (5.9),

When $\dot{X}_e$ =0, $\ddot{X}_e$=0 and $\ddot{X}_s$=0

$$K_{sn(X_e)} = \frac{F_m}{X_e} \tag{5.8}$$

When $\ddot{X}_e$=0 and $\ddot{X}_s$=0

$$C_{sn(\dot{X}_e)} = \frac{F_m - K_{sn(X_e)} X_e}{\dot{X}_e} \tag{5.9}$$

This parameter measurement should be done under stable conditions because the system only uses the deflection in the measurements.

But if the system contains any accelerometers we can observe the sprung mass acceleration and the system can adaptively update the parameters.

When $\dot{X}_e$ =0, $\ddot{X}_e$=0 and $\ddot{X}_s$=0

$$K_{sn(X_e)} = K_{sn(X_e)} + \Delta \frac{F_m}{X_e} \tag{5.10}$$

University of Moratuwa, Sri Lanka.
Electronic Theses & Dissertations
www.lib.mrt.ac.lk

When $\ddot{X}_e$=0 and $\ddot{X}_s$=0

$$C_{sn(\dot{X}_e)} = C_{sn(\dot{X}_e)} + \Delta \frac{F_m - K_{sn(X_e)} X_e}{\dot{X}_e} \tag{5.11}$$

Where

Δ is the adaptive adjustment ratio of the controller

5.3 Effects of Parameters on Measurement and Control

The controller measurements is mainly depends on the performance of internal parameters. The active suspension system performance also depends on the measurements performance. Therefore it is necessary to observe the effects of parameters. The effects can be evaluated by considering a linearized suspension model.

The actual and measured disturbances can be derived as (5.12) and (5.13)

$$\hat{F}_{dis} = K_{sn}(X_s - X_u) + C_{sn}(\dot{X}_s - \dot{X}_u) \tag{5.12}$$

$$F_{dis} = K_s(X_s - X_u) + C_s(\dot{X}_s - \dot{X}_u) \tag{5.13}$$

And the measurement and actual performance variations can be observed by the transfer function (5.14) between the actual and measured disturbance. Where the ideal function gain should be one,

$$\frac{\hat{F}_{dis}}{F_{dis}} = \frac{K_{sn}+C_{sn}s}{K_s+C_s s} \qquad (5.14)$$

The effects of parameter variations is explained in results section.

5.4 Results

Spring and damping constants of the suspension system was analyzed using the encoder reading according to 5.3 and 5.4. And the sprung mass was measured to have a weight of 11.02kg. The spring damper coefficient measurements are shown in Figure 5.3 and 5.4. The results shows the non-linearity exist in the spring and damping coefficient. And due to the some of these effects are non-repeatable therefore the average value is taken for the experimental disturbance measurements.

University of Moratuwa, Sri Lanka.
Electronic Theses & Dissertations
www.lib.mrt.ac.lk

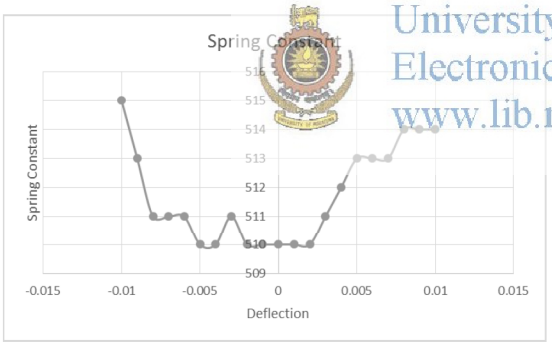

Figure 5.3: Spring coefficient variation with deflection

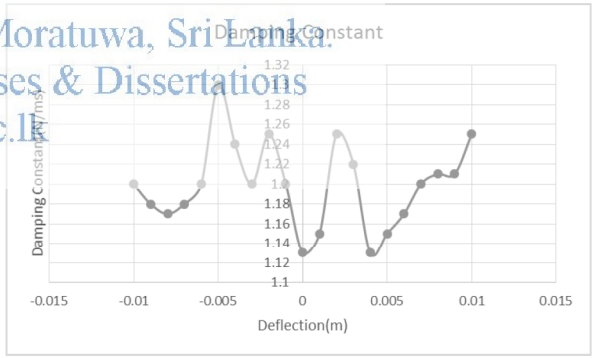

Figure 5.4: damping coefficient variation with deflection

The parameter effects on the vibration measurement was simulated using matlab linearized models. Figure 5.5, 5.6, 5.7, 5.8 shows the effects of parameter errors on the estimation of disturbance. And the system spring constant estimation greatly influence the lower frequency disturbance estimation while the damping constant affect the higher frequency range. The passive suspension resonance frequency will differentiate the spring coefficient and damping coefficient affecting areas. Therefore in design passive suspension elements should select according to the linear quality of the physical spring or dampers.

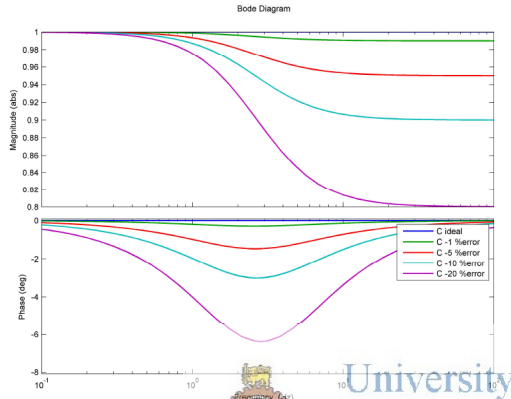

Figure 5.5: Measurement with negative Cs error

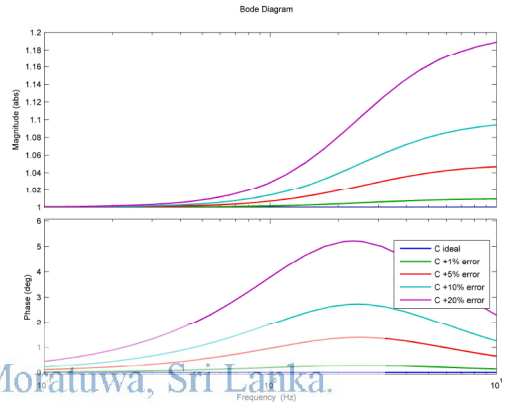

Figure 5.6: Measurement with positive Cs error

University of Moratuwa, Sri Lanka.
Electronic Theses & Dissertations
www.lib.mrt.ac.lk

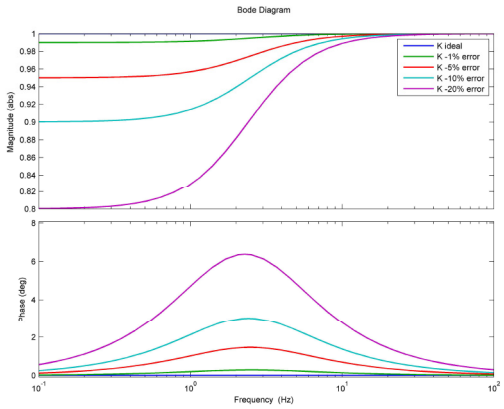

Figure 5.7: Measurement with negative Ks error

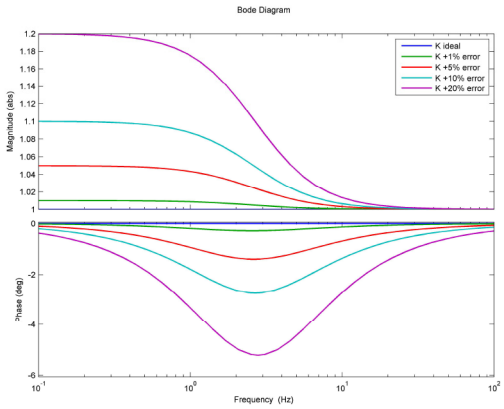

Figure 5.8: Measurement with positive Ks error

5.5 Conclusion

The system saturation analysis and parameter estimation should be properly done to increase the performance of the proposed system. A linear motor was selected to estimate the parameters considering the liner characteristics between force and current in a BLDC linear motor. The system passive vibration suppression spring dampers should be high quality linear elements. The prototype was build considering the cost and economic value. Therefore the experimental system spring dampers coefficient are nonlinear. But the conventional passive suspension elements have a linear characteristics therefore a conventional passive element would work well with the proposed controller.

University of Moratuwa, Sri Lanka.
Electronic Theses & Dissertations
www.lib.mrt.ac.lk

Chapter 6

6 EXPERIMENTAL SYSTEM

6.1 System Design

6.1.1 Electrical

6.1.1.1 Basic Electrical Hardware interconnections

The electrical system consists of ten basic electrical hardware systems. A Field programmable gate array (FPGA) development platform is used as the main controller of the system considering the high sapling frequency required to handle the high precision encoder digital input output singnals. A MBED microcontroller is used to control the rotary motor and to take measurements. Linear motor is used as the main actuator of the system and a linear motor driver is used to drive the main actuator. A rotary motor coupled with a rotary encoder is used to produce random road profile into the system. An accelerometer is used for measure the displacement of the sprung mass of the system and it is physically connected to the sprung mass of the structure. Overall hardware interconnection of the system can be shown in the Figure 6.1.

University of Moratuwa, Sri Lanka.
Electronic Theses & Dissertations
www.lib.mrt.ac.lk

6.1.1.1.1 Linear Motor

Linear motor is acting as the main component of the system. There are few types of linear actuators are available in the world. Hydraulic actuators, Pneumatic actuators, Screw type linear actuators, Linear shaft motors, etc. Reasons for selecting linear shaft are as follows,

- Capable for high thrust
- Fully non-contact operation between forcer and shaft
- Available in various stroke lengths
- High precision (0.07nm)
- High speed drive (greater than 10 m/s) with acceleration up to 20 G
- Low speed drive (8μm/s)
- Virtually no speed fluctuations
- Durable construction, capable of operation even underwater or in a vacuum

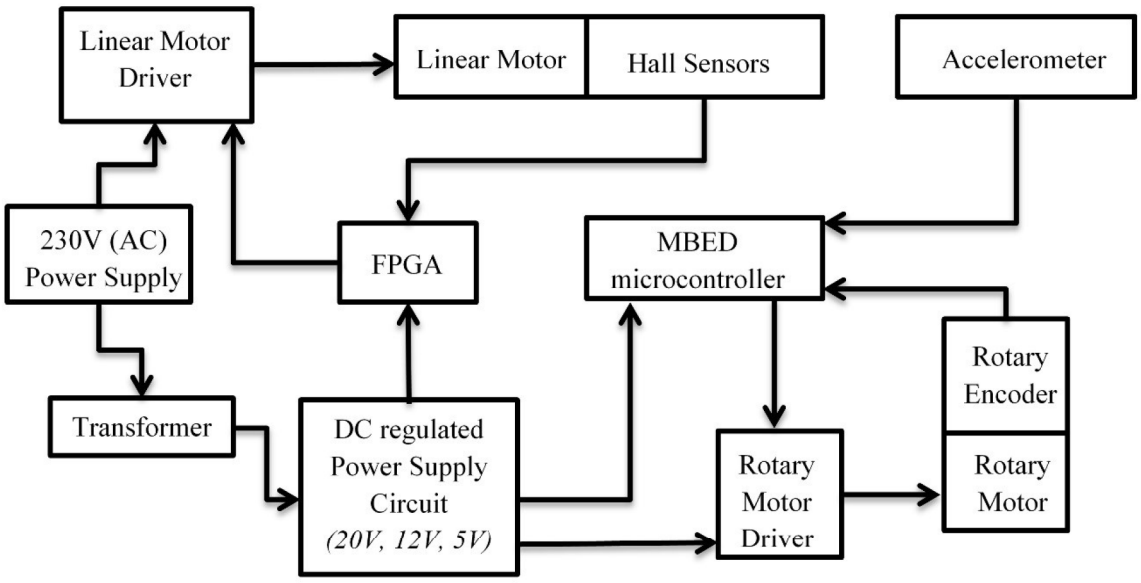

Figure 6.1: Overall hardware interconnection

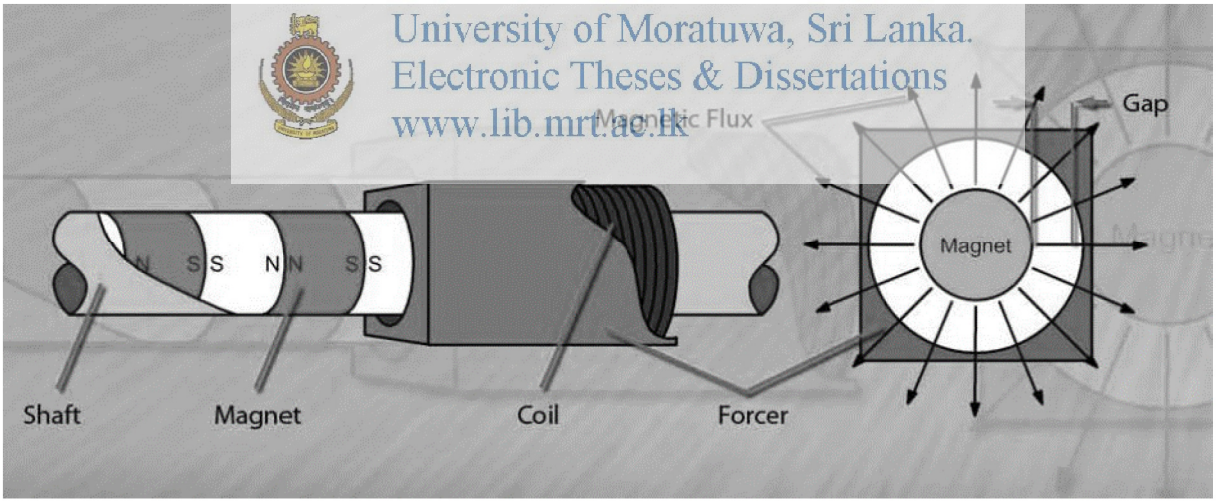

University of Moratuwa, Sri Lanka.
Electronic Theses & Dissertations
www.lib.mrt.ac.lk

Figure 6.2: Forcer and shaft assembly of linear motor [69]

Basic Structure of linear shaft motor can be shown in Figure 6.2,

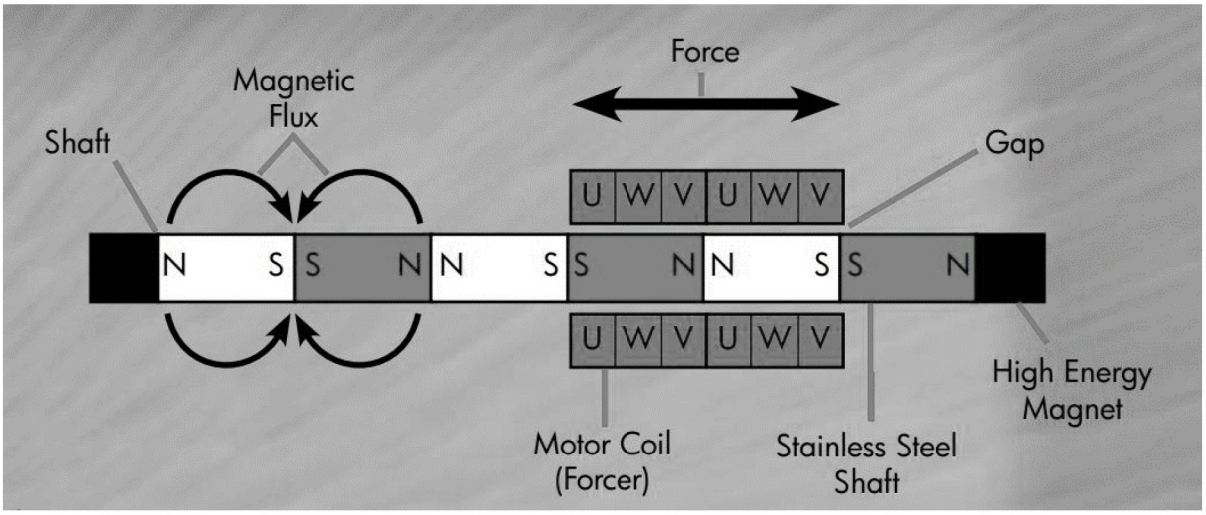

Figure 6.3: Structure of linear shaft motor [70]

The magnetic structure of the Shaft is built in such a manner that there is no space between each magnet and is fully supported within itself. The magnetic structure is then inserted into a protective stainless steel tube. This is a process which is protected by numerous patents throughout the world. This patented process used in the Linear Shaft Motor produces a very strong magnetic field which is twice that of other linear motors [63].

University of Moratuwa, Sri Lanka.
Electronic Theses & Dissertations
www.lib.mrt.ac.lk

The coils of the Linear Shaft Motor are of a cylindrical design, providing a number of key advantages over other linear motors.

- The cylindrical design of the coil assembly is very stiff without external stiffening materials (i.e. iron used by platen style linear motors).
- The coils surrounding the magnets allow for the optimal use of all the magnetic flux. This makes the air gap non-critical. As long as the forcer does not come in contact with the shaft there is no variation in the linear force.
- The magnetic flux cuts motor windings at right angles for maximum efficiency.
- All sides of the coil are positioned to allow for maximum dissipation of heat.
- The more efficient Linear Shaft Motor requires less power in a more compact design and produces a comparable force to that of a similarly-sized traditional linear motor.

According to active suspension system design, around 200mm stroke length and around 60N continuous force were required. Considering about the requirement S250T Nippon pulse linear shaft motor with hall sensors was selected. Electrical specs for equipment are included in the appendix.

6.1.1.1.2 Rotary Motor

19V, 2A geared rotary DC motor is used for the rotate cam profile. This rotary motor is driven from rotary motor driver. According to the requirement, speed and the position of DC motor can be changed.

6.1.1.1.3 Rotary Motor Driver

A rotary dc motor driver is used to control rotary motor. Driver is directly connected to the Mbed microcontroller. Mbed microcontroller produces PWM signals to run motor driver.

6.1.1.1.4 Rotary Encoder

600ppr rotary encoder is used for take the measurements of rotary motor. Rotary encode is directly connected to the Mbed microcontroller. Depending on the values of the encoder, Mbed microcontroller produced PWM values to drive rotary motor.

University of Moratuwa, Sri Lanka.
Electronic Theses & Dissertations
www.lib.mrt.ac.lk

6.1.2 Mechanical

6.1.2.1 Linear Guides

Two special guide sets are used to keep linear motor air gap constant. Mainly two pars are available of linear guide called block and rail. Block moves on top of the tail as usual. Dimensions for the block and rail are change according to the design. Maximum deflection for the designed system is nearly 200mm. Then 220mm length rail was selected. Therefore according to our design SHS20V1SS+ 220L (HRC20MN-B1-V0N-220-20-20) two units were selected. Figure of these mechanical equipment are shown in the appendix.

Weight of block	: 218 g
Weight of rail	: 2280 g/m
Length of rail	: 220 mm
length of block	: 69 mm

Two linear guides are used by either sides of motor forcer to keep linear motor air gap constant. Shaft is mounted on top of the linear guide block.

6.1.2.2 Linear Bearings

Linear bearing provides ability to move object in linear way. It can be mounted to a steel rod. There are several types of linear bearing are available in market. According to application, linear bearings with flange were selected. LMK25UU linear bearings ware used for the mechanical system. Internal diameter of each bearing is 25mm.

6.2 Mechanical Design

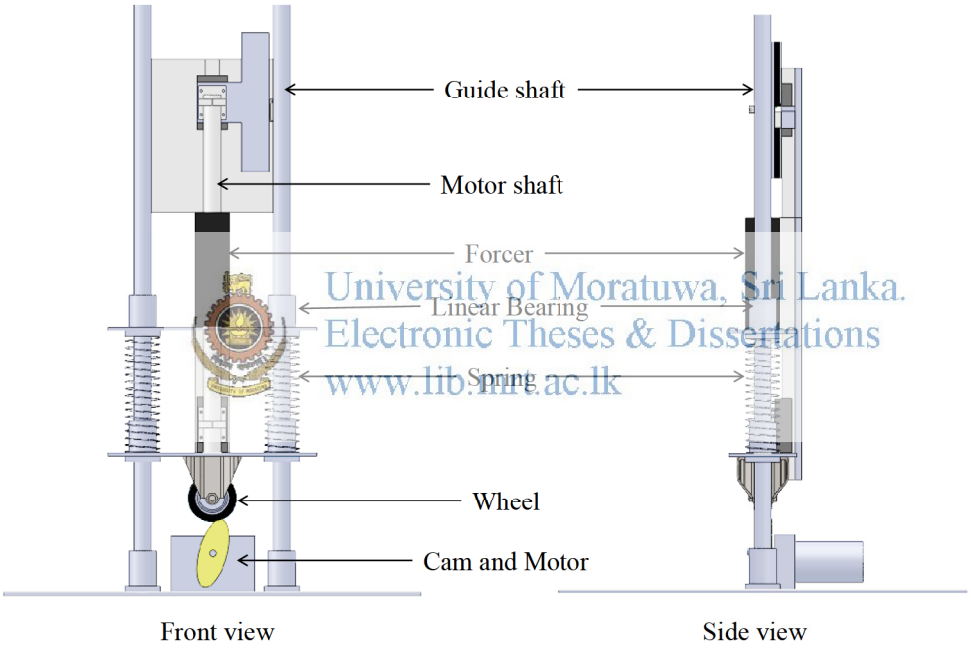

University of Moratuwa, Sri Lanka.
Electronic Theses & Dissertations
www.lib.mrt.ac.lk

Figure 6.4: Mechanical Structure

According to the mathematical model of a suspension system, it is required to separate sprung mass and un-sprung mass by using a physical spring, damper combination. And also it is necessary to add virtual spring, damper combination (Linear motor) between sprung mass and un-sprung mass. By considering above key factors, the mechanical structure was designed as shown in the Figure 6.4.

In this design there are two steel rods are used to keep overall mechanical system vertically. Below two brackets which are tightly fixed with base plate bear the all weight of the structure and stand all system vertically. Below basement plate is a thick steel plate which have higher strength to withstand all mechanical movements including vibrations.

There are two aluminum plates are used to represent sprung and un-sprung masses. Aluminum plates were selected to avoid the interaction between the magnetic shaft of linear motor and the plates. These aluminum platforms provide supporting structure to mount forcer and shaft of linear motor. Forcer of the linear motor is mounted to the sprung mass aluminum plate and forcer of linear motor moves with sprung mass aluminum plate. And also the shaft of the motor is contacted with un-sprung mass aluminum plate. To provide vertical movement of two plates, four linear bearing are connected between aluminum plates and steel rods as shown in figure. A wheel is mounted to bottom of the un-sprung mass to provide smooth contact with cam profile. Two springs are connected between two aluminum plates in order to produce physical spring operation. Rotary motor coupled with cam provide artificial vibration to the mechanical system.

University of Moratuwa, Sri Lanka.
Electronic Theses & Dissertations
www.lib.mrt.ac.lk

6.2.1 Encoder Assembly

Since the linear encoder is a magnetic type one, there can be interfere with magnetic shaft of linear motor. According to the linear encoder specs, linear guide should be mounted in an environment which has the magnetic flux density less than 1mT for the proper operation. The magnetic flux density variation with radial distance to the motor shaft was measured by Maxwell Turn Meter. Distance was 75mm away from the linear motor shaft. Therefore encoder assembly was specially designed for the requirement. Encoder head was mounted 75mm away from the linear motor shaft and magnetic strip also mounted away from that range. It can be shown as below,

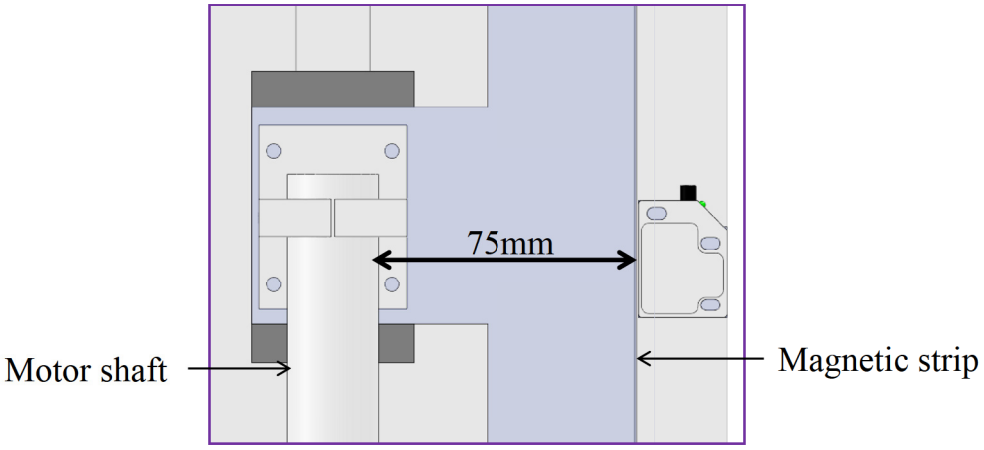

Figure 6.5: (a) Encoder motor shaft assembly

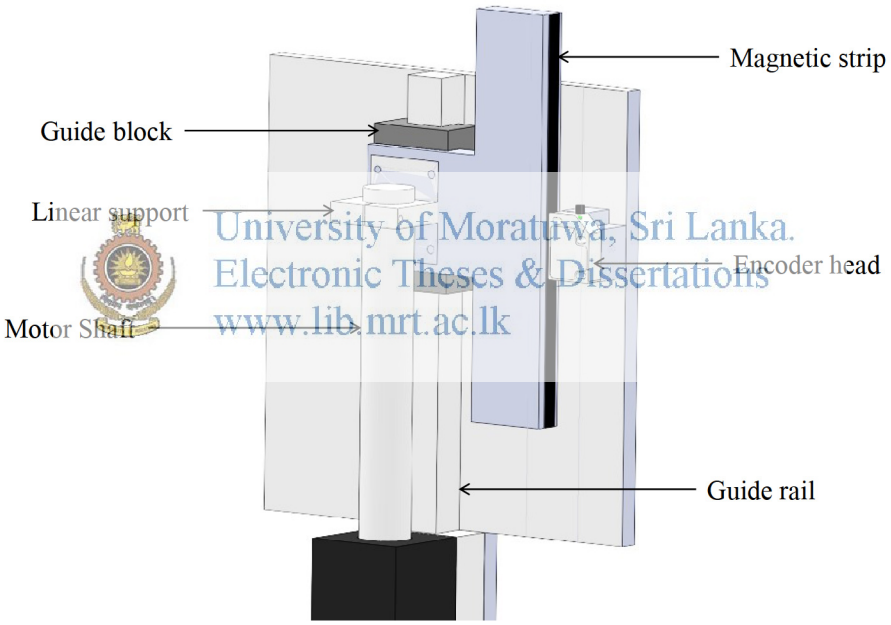

University of Moratuwa, Sri Lanka.
Electronic Theses & Dissertations
www.lib.mrt.ac.lk

Figure 6.6: (b) Encoder motor shaft assembly

6.3 Auxiliary systems

6.3.1 Power Supply

The power supply of the total system needs different voltage levels. The following table shows the rated voltage levels of the different components.

Table 6.1: Rated voltage levels of the different components

Voltage Level	Components
3.3V	FPGA inputs, Mbed digital inputs
5V	FPGA, Mbed, LM Pole sensors, Linear encoder, Rotary encoder
12V	Rotary motor driver
19V	Rotary motor

The 3.3V is needed for the inputs for the FPGA and the Mbed. The input and output logic high level is taken as 3.3V in both FPGA and Mbed. Even though both these controllers are provided with 3.3V power output capability, considering the safety of the equipment it was decided to design a separate power supply for the 3.3V system.

University of Moratuwa, Sri Lanka.
Electronic Theses & Dissertations
www.lib.mrt.ac.lk

The maximum supply voltage of the FPGA is 5.5V. The supply voltage of the Mbed varies from 4.5V to 9V. The input power of the Mbed is about 1W when the peripherals are working. The supply voltage range for the pole sensors of the linear motor is named from 4.5 to 18V. The linear encoder can be operated from 5V to 30V range. The operating range of the rotary encoder is from 5V to 24V. Hence considering all the maximum and minimum voltage levels of the operation of this equipment a 5V DC system was decided to be used. This would also reduce the power loss through resistor dividers which are used for logic level conversion from 5V to 3.3V.

The voltage level of the rotary motor driver was 12V to 18V. The 12V was selected to power up the rotary motor driver due to the low voltage and the availability of the regulators. If a higher voltage level is selected, the power consumption would also be increased which will be a disadvantage in transformer sizing.

The rated voltage of the rotary motor is 19V and the rated current is 2A. Because of that a 19V power supply with high current handling capacity of more than 2A was required for driving the rotary motor. This supply is not needed to be regulated since the motor driving does not require being ripple free.

6.3.2 Pole sensing

The linear motor operates as a brushless DC motor. The permanent magnet poles are located in the shaft and the windings are located in the forcer. This is shown in the Figure 6.7.

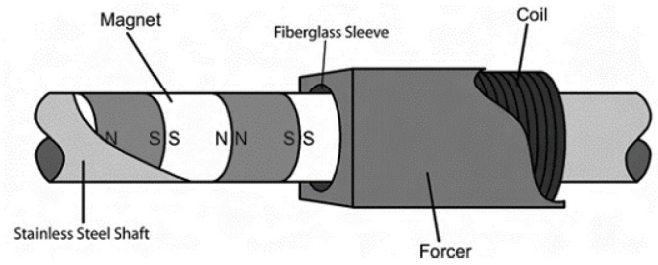

Figure 6.7: Permanent magnet poles and the windings [81]

There are three windings named as U, V, and W inside the forcer. These three windings are needed to be energized to operate the motor. The commutation of the U, V, W windings is required for the continuous run of the motor. The commutation is done from the motor driver based on the pole sensor signals. The following Figure 6.8 shows the pattern of the locations of the pole sensors in the forcer, pole sensor signals and the wiring diagram respectively.

University of Moratuwa, Sri Lanka.
Electronic Theses & Dissertations
www.lib.mrt.ac.lk

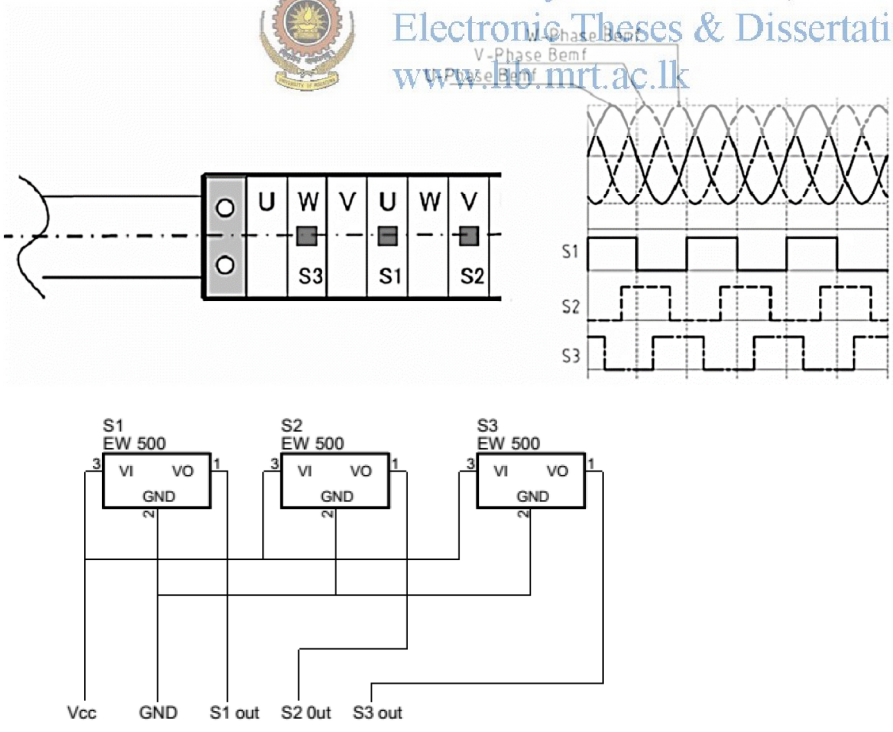

Figure 6.8: Pattern of the locations of the pole sensors, pole sensor signals and the wiring diagram [82]

The pole sensor used is an ultra-high sensitive InSb hall element and a signal processing IC chip. The internal circuit of the hall element is shown in the Figure 6.9. This comprises of an open collector output which acts as a switch. The input voltage Vcc has a range from 4.5V to 18V. The Vcc is designed to be 5V and the output was designed to be 3.3 to connect to the FPGA.

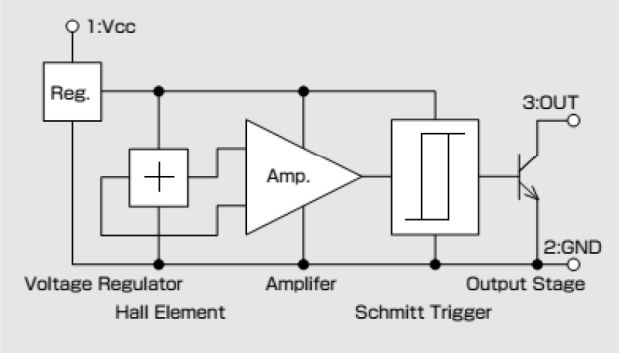

Figure 6.9: Internal circuit of the hall element [83]

6.4 Hardware implementation

6.4.1 Disturbance profile generator

The Disturbance profile for the active suspension system should be artificially generated. A rotary motor and cam assembly is used to generate this Disturbance profile. The main feature of the Disturbance profile generator is it should have the ability to generate different types of Disturbance profiles in order to compare the active suspension ability of the system. The following block diagram shows the basic hardware assembly of the Disturbance profile generator.

University of Moratuwa, Sri Lanka.
Electronic Theses & Dissertations
www.lib.mrt.ac.lk

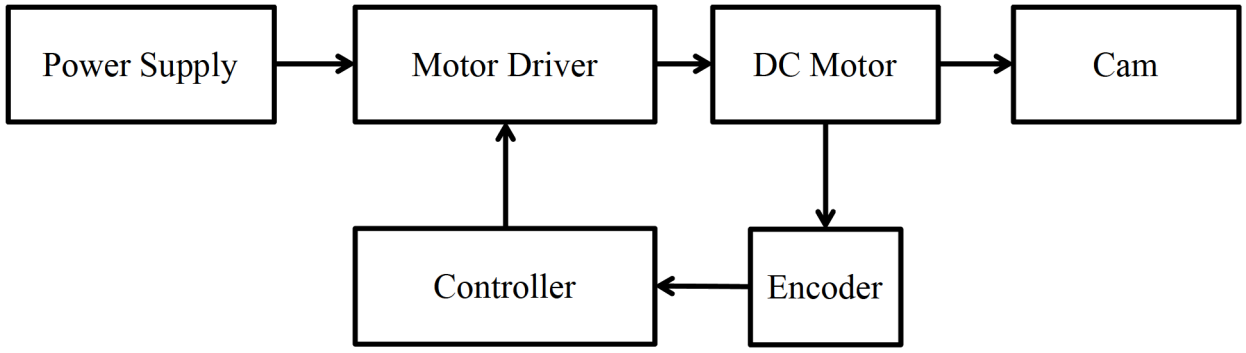

Figure 6.10: Basic hardware assembly of the disturbance profile generator

Mbed micro controller is used as the controller for the system. An incremental rotary encoder with 600 ppr with phase A and phase B output is used for getting the position feedback. A rotary DC motor of 19V with 2A rated current is used to drive the cam. The cam profile and the displacement diagram is indicated in Figure 6.11.

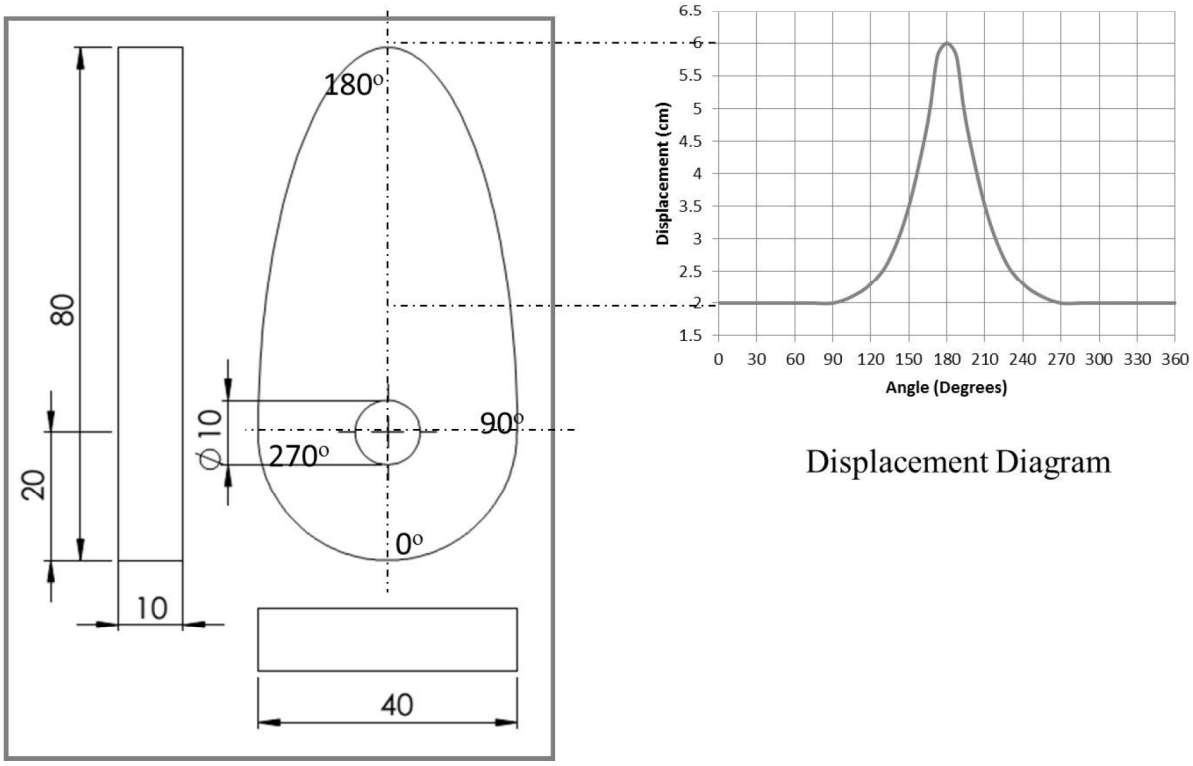

Displacement Diagram

Figure 6.11: The cam profile and the displacement diagram

University of Moratuwa, Sri Lanka.
Electronic Theses & Dissertations
www.lib.mrt.ac.lk

- 150° – 210° oscillatory rotation of cam for continuous disturbance

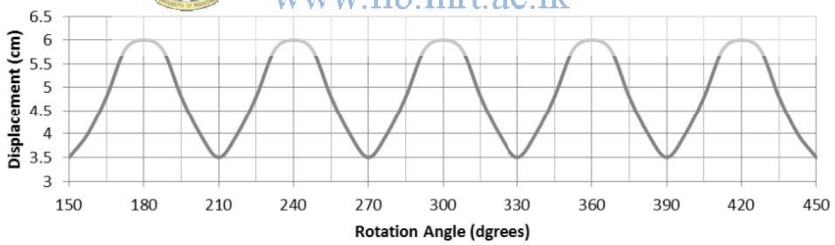

- 0° – 180° rotation of cam for large disturbance

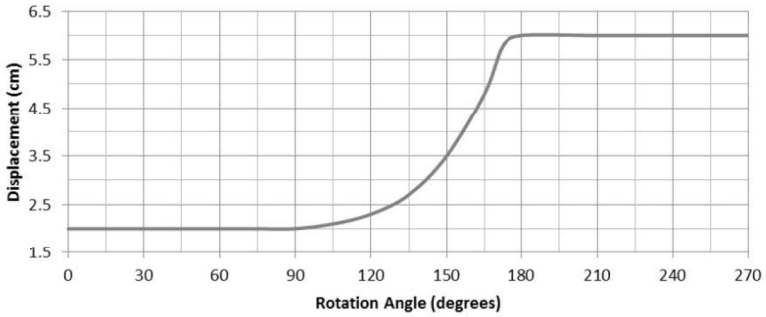

Figure 6.12: Two different Disturbance profiles generated by the cam for different angles of rotation

The displacement diagram of the cam gives the displacement of the follower with the rotation angle of the cam. By using the displacement curve the road profile generated by the cam rotation can be calculated for different angles. The above figure shows two different road profiles generated by the cam for different angles of rotation.

The different Disturbance profiles can be generated by position controlling the rotary motor and hence the cam to rotate in different angles. This could be used to observe the response of the active suspension system for the different disturbances. As shown in the figure by continuous rotation of cam from 150^0 to 210^0, a continuous disturbance can be generated. By rotating cam from 0^0 to 180^0 a discontinuous large disturbance can be generated.

The position control of the cam is done by using the rotary encoder feedback. A PID control is used to generate the desired PWM signals to the motor driver to achieve the desired position as shown in figure 6.13.

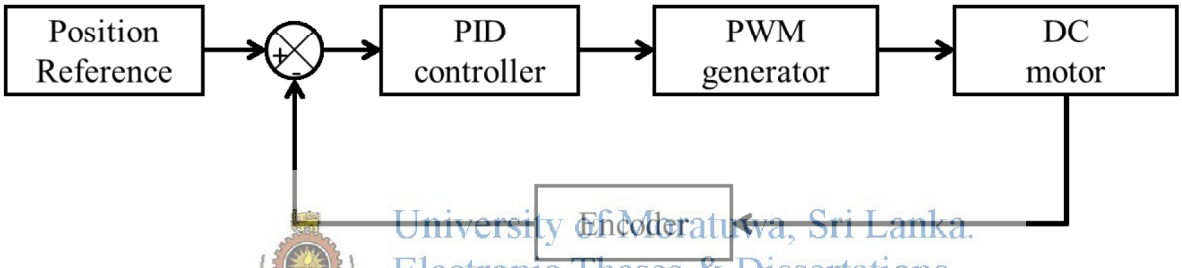

University of Moratuwa, Sri Lanka.
Electronic Theses & Dissertations
www.lib.mrt.ac.lk

Figure 6.13: The position control block diagram

6.4.2 Mechanical assembly

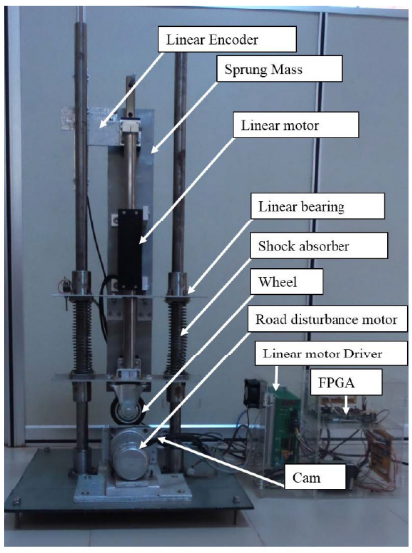

Figure 6.14: Implemented Quarter Car Model

6.4.3 Circuit Implementation

The main electrical systems which needed to be constructed are as follows.

1. Power supply unit.
2. Rotary encoder interface
3. Pole sensor interface
4. Linear encoder interface
5. Mbed microcontroller interface

In order to minimize the cost and time taken for fabrication power supply unit and rotary encoder interface were fabricated in a single PCB. The pole sensor interface and the linear encoder interface were fabricated in a separate PCB in order to enhance the modularity of the system and the ease of trouble shooting. The Mbed microcontroller interface was fabricated in separate PCB. The Easily Applicable Graphical Layout Editor (EAGLE) software was used to design the PCBs.

6.4.3.1 Power supply unit and rotary encoder interface

The schematic diagram of the circuit layout of the power supply unit and the rotary encoder interface is shown in the Figure 6.15.

University of Moratuwa, Sri Lanka.
Electronic Theses & Dissertations
www.lib.mrt.ac.lk

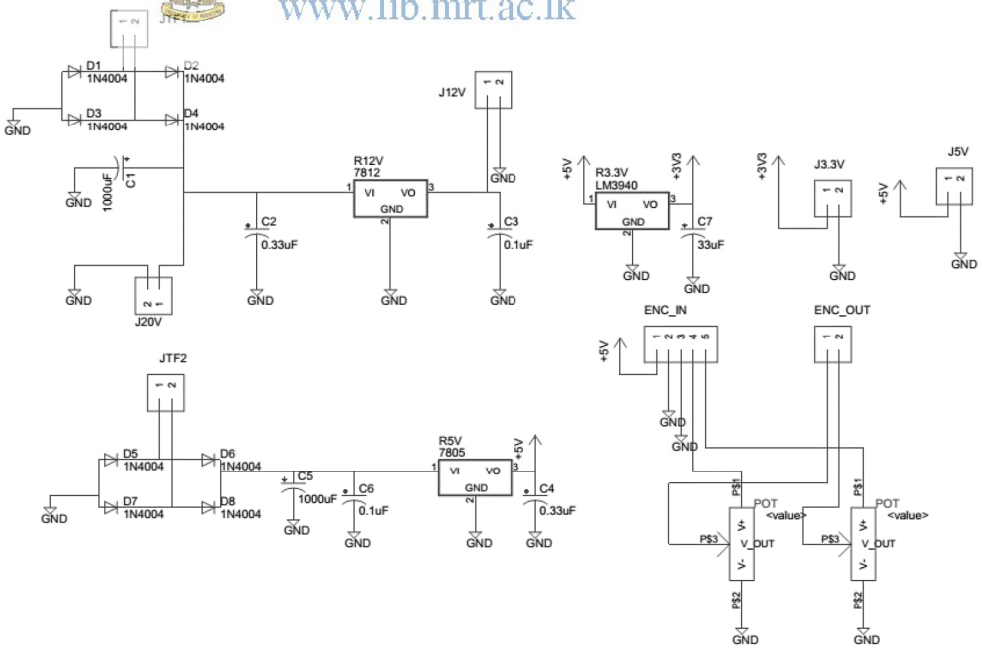

Figure 6.15: Schematic diagram of the circuit layout of the power supply unit and the rotary encoder interface

The connectors are listed below.

- JTF1, JTF2 – Transformer input connectors
- J3.3V, J5V, J12V – Regulated voltage output connectors
- J20V – Unregulated 20V output for rotary motor
- ENC_IN – Rotary encoder input connector
- ENC_OUT – Rotary encoder output to Mbed

A 25VA 230V/20V dual output transformer is used to step down the supply voltage. The TF1 terminal supply power for 20V and 12V outputs. The TF2 terminal supply power for 3.3V and 5V system. The rotary encoder input should be connected to the ENC_IN connector. The two 100kΩ variable resistors reduce the Phase A and Phase B voltages of 5V to 3.3V which is the I/O voltage level of the Mbed. The ENC_OUT connector outputs the 3.3V phase A and phase B signals to the Mbed. 3.3V and 5V regulated outputs are used to power up the 5V and 3.3V systems.

University of Moratuwa, Sri Lanka.
Electronic Theses & Dissertations
www.lib.mrt.ac.lk

6.4.3.2 Pole sensor and linear encoder interface

The pole sensors are working in a voltage range from 4.5V to 18V. Hence 5V is used for the supply voltage of the pole sensors. The output of the pole sensors is open collector type. Since the output of the pole sensors is interfaced with FPGA the 3.3V was used for switching the output of the pole sensors. The 10kΩ resistors are used to pull up the open collector output. When the motor was operating there was about 15 MHz noise added to the output signal of the pole sensors. 10uF capacitors are used in order to filter out the noise.

The linear encoder supply voltage range is 4.7V to 5V. Hence 5V is used to power the linear encoder. The output of the linear encoder is a digital output with RS 422 connector. The high level is 5V and the low level is 0V. In order to interface this with the FPGA, the output is reduced to 3.3V through 100kΩ variable resistors. The schematic diagram is in figure 6.16.

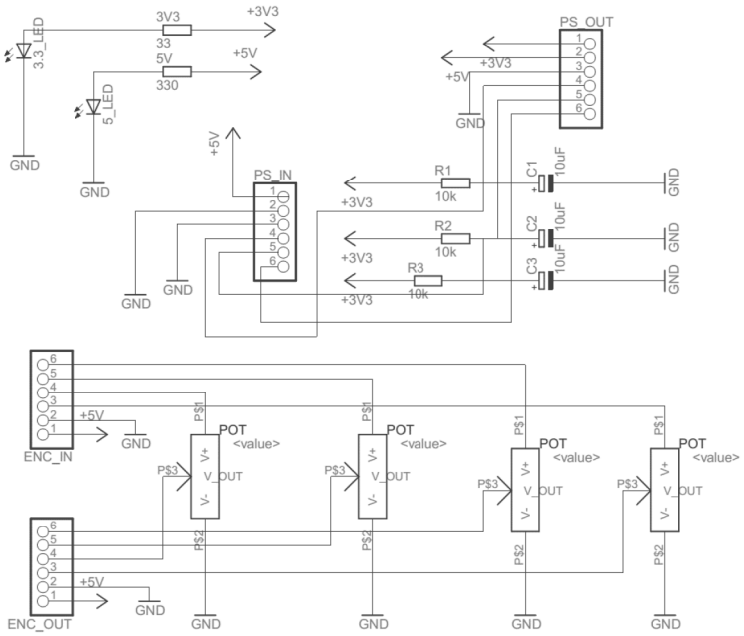

Figure 6.16: Schematic diagram of pole sensor and the linear encoder interface

University of Moratuwa, Sri Lanka.
Electronic Theses & Dissertations
www.lib.mrt.ac.lk

The connectors are listed below.

- PS_IN – Pole sensor input
- PS_OUT – Pole sensor output to FPGA
- ENC_IN – Linear encoder input
- ENC_OUT – Linear Encoder output to FPGA

The power supply to the circuit is connected through PS_OUT connector. Following pins are used to supply the board power.

- Pin 1 – 3.3V supply
- Pin 2 – 5V supply
- Pin 3 – Ground

The following pins are used to send input signals to the FPGA.

- PS_OUT: 4 - pole sensor 1 , 5 – pole sensor 2, 6 – pole sensor 3
- ENC_OUT: 3 – Phase A , 6 – Phase B

6.4.3.3 Mbed microcontroller interface

The Mbed micro controller is used for data acquisition and rotary motor control. The data acquisition system is made of following components.

1. ADXL 345 accelerometer
2. SD card reader

The Mbed communicates with the accelerometer by I^2C communication protocol. These accelerometer readings are recorded in the SD card via SD card reader. SPI communication protocol is used to communicate between the SD card reader and the Mbed.

The rotary motor control system is made of the following components.

1. Rotary encoder
2. Rotary motor driver

The SPI communication port from the FPGA is used to get the data from the FPGA. The USB and Ethernet connection ports are used for future expansions.

University of Moratuwa, Sri Lanka.
Electronic Theses & Dissertations
www.lib.mrt.ac.lk

The Mbed is powered up with a 5V supply. The supply voltage range of the Mbed is from 4.5V to 14V. The 3.3V supply is used for the accelerometer.

The connectors are listed as bellow.

- 3.3V_CON , 5V_CON – power supply connectors
- SPI_FPGA – SPI port to FPGA
- SD_CARD – SD card reader output
- ROT_EN – Rotary encoder input from rotary encoder interface board
- PB – push button switch
- MTR_DRV – Rotary motor driver output
- ACC_I2C – Accelerometer input
- USB, ETHERNET - Communication ports

The plan view of the Mbed interface circuit layout is in Figure 6.17.

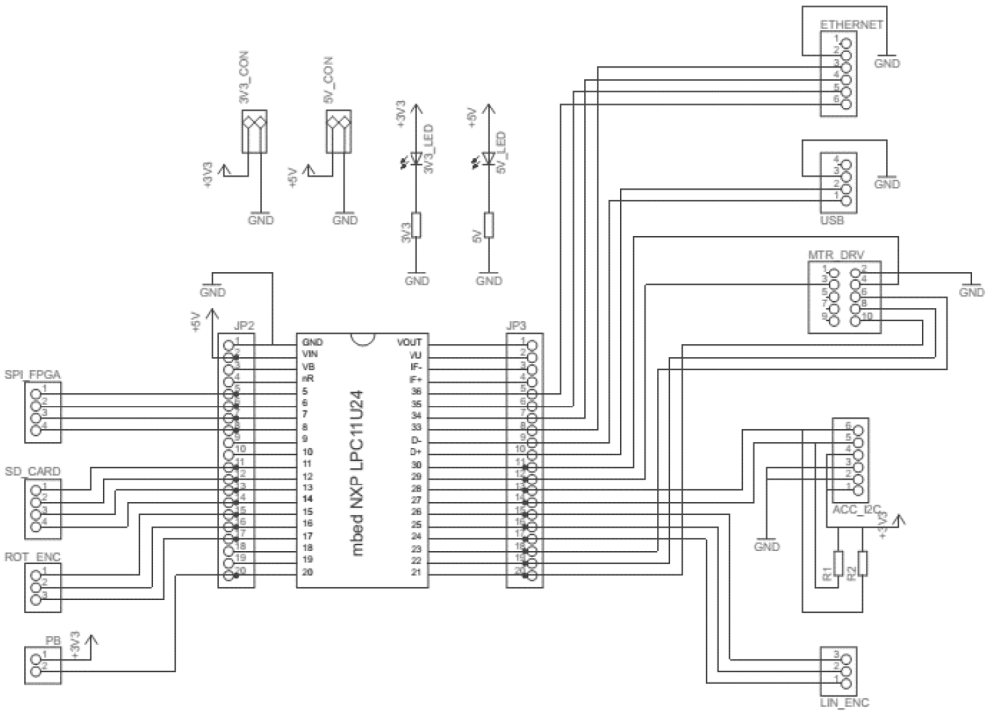

Figure 6.17: Mbed interface circuit layout

University of Moratuwa, Sri Lanka.
Electronic Theses & Dissertations
www.lib.mrt.ac.lk

6.5 Software implementation

6.5.1 Software and hardware description language (HDL) coding

6.5.1.1 HDL and field programmable gate arrays (FPGAs)

FPGA is an integrated circuit containing programmable logic components (i.e. logic blocks) and optional block RAM elements. Designer can program these integrated circuits in FPGA using hardware description languages (HDL) thereby giving it the description “field programmable”. In FPGA design FPGAs provide large number of logic gates and RAM blocks that can be allocated in the digital design to do complex tasks or computations. In addition FPGA design contains very fast input output ports and buses and in designing it is required to measure perfect timing of these ports and inside circuit design to achieve desired output. This should be done with the use of HDL and further analysis provided by FPGA producer software such as Quartus II 14.1 tools which used in this project. Other method to implement such designs is to develop an application specific integrated circuit (ASIC) which do not have dynamic capabilities such as in FPGAs and ability to change its circuit according to changing requirements similar to FPGAs ability to redesign itself with the change of HDL synthesis code.. FPGA advantages include

ability to update the functionality after shipping, partial re-configuration of a portion of the design and the low non-recurring engineering costs relative to an ASIC design offer advantages for many applications.

In FPGA design all hardware circuitry should be developed by the programmer using HDL circuit synthesis with the knowledge of digital electronics logic blocks. And a TerasicDE1 SOC development board was for the project. This FPGA is from an optimized FPGA provided by Altera manufacturers. Altera development board provides following input output ports in their development board. These ports should be programmed by designer inside FPGA using HDL for proper use. Otherwise they can be used as input output pins to FPGA logic arrays.

HDL is a specialized computer language used to program the structure, design and operation of electronic circuits, and most commonly, digital logic circuits. A hardware description language enables a precise, formal description of an electronic circuit that allows for the automated analysis, simulation, and simulated testing of an electronic circuit. It also allows for the compilation of an HDL program into a lower level specification of physical electronic components, such as the set of masks used to create an integrated circuit. Using the proper subset of hardware description language, a program called a synthesizer (i.e Quartus ISE) can infer hardware logic operations from the language statements and produce an equivalent net list of generic hardware primitives to implement the specified behavior. Synthesizers generally ignore the expression of any timing constructs in the text. Digital logic synthesizers, for example, generally use clock edges as the way to time the circuit, ignoring any timing constructs. The ability to have a synthesizable subset of the language does not itself make a hardware description language.

University of Moratuwa, Sri Lanka.
Electronic Theses & Dissertations
www.lib.mrt.ac.lk

Verilog is the HDL language we use in this project to synthesis and simulate FPGA design. Verilog HDL is a hardware description language used to design and document electronic systems. Verilog HDL allows designers to design at various levels of abstraction. It is the most widely used HDL with a user community of more than 50,000 active designers.

6.5.1.2 Verilog HDL synthesis modules

6.5.1.2.1 Slow Clock generator module

The FPGA work using the 100MHz crystal provided by development board. Therefore total design works using 100MHz clock positive edge. And some of our functions such as speed

calculation does not need to done every 10ns which will not provide a good speed resolution and slow speed detection due to fast calculation speeds. To avoid those circumstances we use out 100MHz clock to generate a slow positive edge using slow clock generator module. This module allow us to change some of those register values in slower period than compared to others 10ns 100MHz speed. This block can generate 25Hz and below frequencies depending upon design requirements. And these signals only route through FPGAs clock IO block therefore external port usage to direct positive edge triggering is not allowed in design.

6.5.1.2.2 Encoder interface module

Encoder interface provide a gateway to measure encoder position and speed of the system. Encoder input is connected to block C of the FPGA and routed to encoder interface module that change pulse count register every 10ns and a pulse changing speed every register 10ms. These registers are 64bit in length. Input of phase A and phase B of encoder used to check direction of movement and provide outputs in μm and $0.1ms^{-1}$. This module still doesn't use A not and B not interfaces to check errors in signals. One slow clock generator module is connected to this module allow the low speed variation identification in the system.

University of Moratuwa, Sri Lanka.
Electronic Theses & Dissertations
www.lib.mrt.ac.lk

6.5.1.2.3 MOVO interface module

MOVO communication interface take a 16 bit parallel current value and generate a MOVO clock, DATA A, DATA B, latch bus signals to communicate with the motor drive. This module work in 8.33MHz frequency and send motor phase U and phase V currents continuously. This module send single bit of data to motor drive every positive edge of movo driver clock. Motor driver work as slave device and take input to its shift register according to FPGA MOVO interface latch bus value.

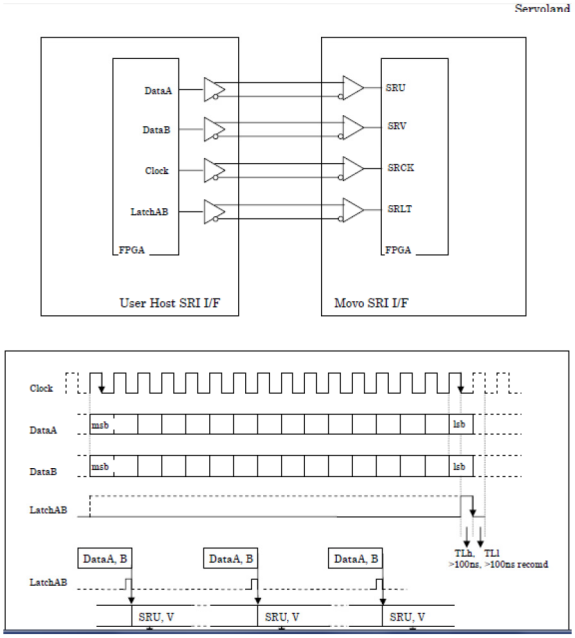

Figure 6.18: MOVO SRI current command wave form and connection

6.5.1.2.4 SPI slave interface module

FPGA doesn't contain any preprogrammed hardware to send it's inside register values to outside systems. Therefore similar to MOVO interface spi slave interface is designed to send FPGA 32bit register values such as encoder pulse reading, pulse speed, spring constant etc. this interface get connected to a Mbed SPI master pins and can communicate any master Mbed frequency without a problem.

University of Moratuwa, Sri Lanka.
Electronic Theses & Dissertations
www.lib.mrt.ac.lk

6.5.1.2.5 Trapezoidal brushless DC current generation module

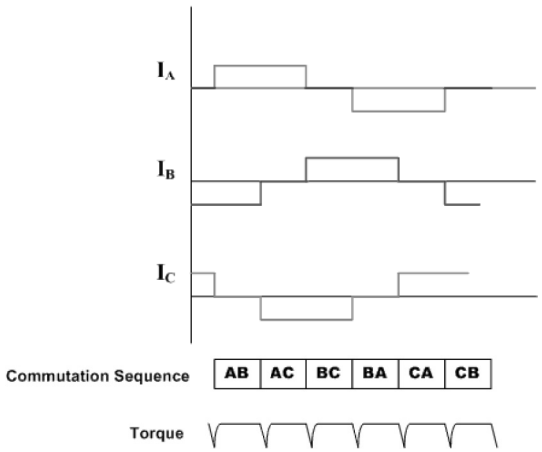

Figure 6.19: Trapezoidal BLDC current command and torque output

Trapezoidal brushless DC current generation module takes hall sensor H1, H2, H3 inputs to generate phase A phase B current sign value that should be send to current control inverter driver(ie. MOVO motor driver). The current pattern and motor control pattern decided upon required torque and hall sensor position. For positive torque one pattern and for negative torque another pattern was found for this module by experiment. But due to problems in trapezoidal brushless DC method, small torque pulsations were observed at hall sensor changing (ie. Current sign changing) positions as shown in the diagram.

6.5.1.2.6 Main module

Main module is designed to connect all other module to generate a complete system. This connector have inputs of circuit clock, push buttons, switches, encoder inputs, hall sensor inputs and SPI slave connector to Mbed. The outputs can be named as MOVO current command output and SPI slave master in slave out port that connected through a mail box. And inside the module these external input out pins are connected to respected modules to generate a complete system circuit.

University of Moratuwa, Sri Lanka.
Electronic Theses & Dissertations
www.lib.mrt.ac.lk

Encoder inputs connected to encoder interface module and speed and pulse count taken out from it. This pulse count and pulse speed then used to calculate motor spring force and damping force to get total force required. Then that torque is converted to a current value. This current value then converted to MOVO current command by sending it throughout BLDC trapezoidal current reference generation module. This module consider hall sensor positions and change current command phase A phase B values considering that and torque sign of system.

Push buttons are used for tuning purposes where spring and damping constant change using up and down push buttons. SPI slave is there to check 32 bit register values of pulse, pulse speed, spring damper forces and spring damper constants by changing switch arrangements in the development board.

6.5.1.2.7 Verilog simulation modules

Verilog is used in simulation of HDL components to check proper performance before hardware implementation. Here FPGA or any HDL hardware description is tested using a Verilog script

that programmed by user give required input outputs to module input and check outputs and inside register value changes in the module.

6.5.1.2.7.1 Encoder interface simulator

Encoder interface module is check using this simulator by giving phase A, phase B inputs according to both direction requirements and observe the output register pulse and pulse speed readings to measure proper outputs in the module.

6.5.1.2.7.2 MOVO interface simulator

This simulator script used to simulate MOVO current command waveform generation by giving clock pulse and 16bit register A and B to MOVO interface module. So that we can observe outputs variations and MSB first output generation according to values in input registers. And parallel to serial bus conversion.

6.5.2 Design stages

Logic design -»

Designed logic to system according to developed model

University of Moratuwa, Sri Lanka.
Electronic Theses & Dissertations
www.lib.mrt.ac.lk

Module Synthesis -»

Generated required modules considering system requirements.

Module simulation -»

Check proper working of those modules using simulations in ModelSim.

Module interconnection -»

Connect those modules to create a complete system from external inputs to external outputs.

Hardware test deign -»

Modify main module to test inside partial modules and register values sign SPI slave interface.

Synthesis -»

Synthesis a new complete module after inside module testing.

Testing -»

Tested new complete module using linear motor and encoder and hall sensor inputs.

Final tunable design -»

Add spring damper constant tuning using push buttons to main module.

Testing -»

Testing force variations in linear motor by changing spring constant values using push buttons.

Tuning -»

Tuning of whole system started after all equipment are connected to mechanical design.

6.5.3 Mbed microprocessor software

Mbed C++ program include functionalities of

- PID Motor position controller
- Accelerometer reading and data saving
- Giving instructions to FPGA in parameter estimation.
- Communicate with FPGA and record FPGA data

University of Moratuwa, Sri Lanka.
Electronic Theses & Dissertations
www.lib.mrt.ac.lk

Chapter 7

7 CONCLUSION AND RESULTS

7.1 Experimental Results of DOB based disturbance estimation

The hardware system has been developed according to the hardware system described in chapter 6. The system sprung mass acceleration for different frequency disturbances are shown in Figure 7.1, 7.2, 7.3 and 7.4. The nominal spring damper based system provides better performance throughout the measured frequency range. The disturbance suppression capabilities of the system reduces in the low frequency range and both passive and active suspension responses improve with the increased frequency as expected from the simulation results. The passive suspension system response shows a 0.2182 standard deviation in sprung mass acceleration for 1.5Hz disturbance and the standard deviation of the acceleration significantly reduces to 0.0988 after the operation of the active vibration suppression controller as shown in Figure 4.6. The active system shows significant reduction in vibrations for frequencies of 3Hz, 4Hz, and 6Hz with a Standard deviation of acceleration of 0.1244, 0.1264 and 0.1342 respectively which is a considerable level of performance improvement compared to passive suspension sprung mass vibration levels of 0.2294, 0.1830 and 0.1960 respectively. The passive and active suspension system performance further improves with the increase of frequency and the proposed system provides good vibration suppression levels even for the low frequency ranges. The system simulation results suggest the natural vibration suppression occurs in higher frequencies in addition due to the limitations of the disturbance motor and system simulations were limited to lower frequencies.

University of Moratuwa, Sri Lanka.
Electronic Theses & Dissertations
www.lib.mrt.ac.lk

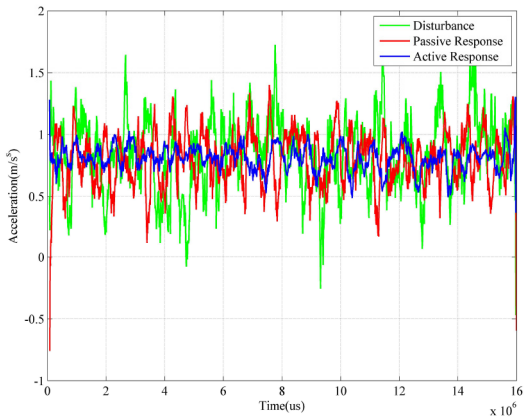

Figure 7.1: System response for 1.5Hz Vibration

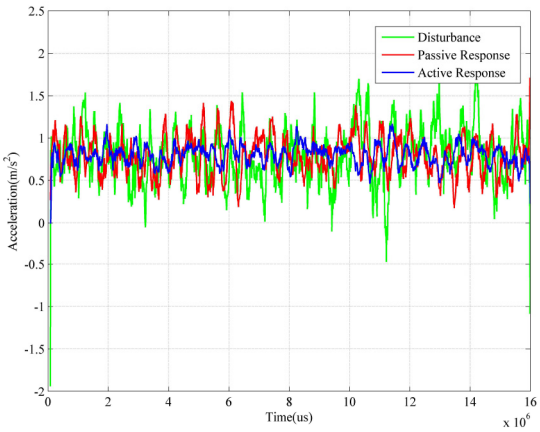

Figure 7.2: System response for 3Hz Vibration

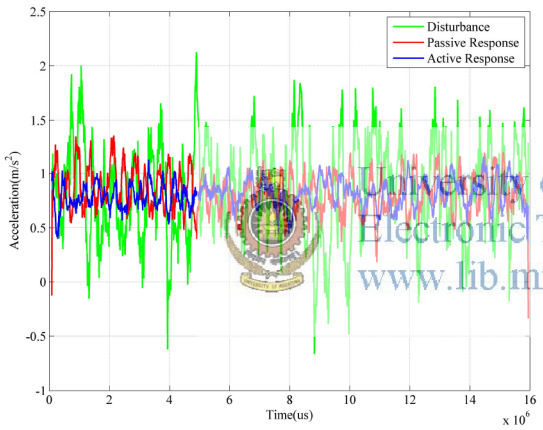

University of Moratuwa, Sri Lanka
Electronic Theses & Dissertations
www.lib.mrt.ac.lk

Figure 7.3: System response for 4Hz Vibration

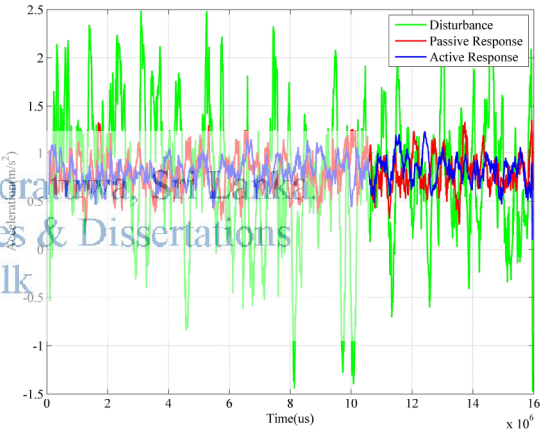

Figure 7.4: System Response for 6Hz Vibration

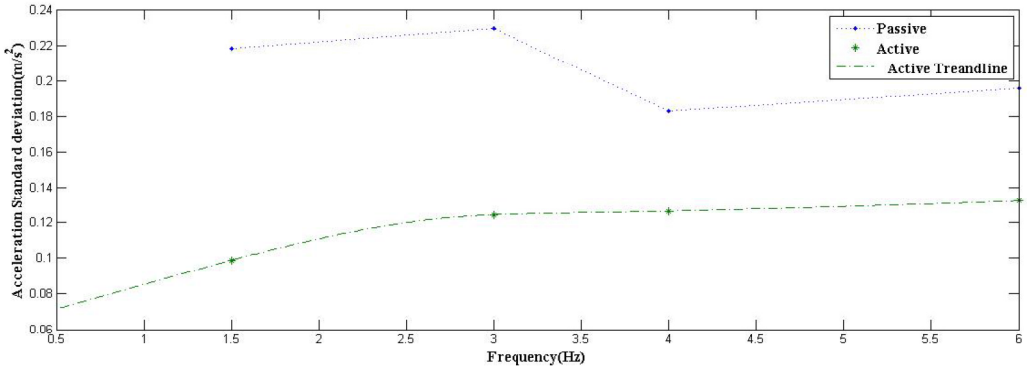

Figure 7.5: Passive and Active Experimental Results

7.2 Experimental Results of spring damper based disturbance estimation

Hardware system expressed in chapter 6 has been used to measure the performance of the proposed controller in chapter 4. The system is subjected to sinusoidal vibration from a frequency of 1-10Hz to generate the system performance results. The ultra-low frequency vibration suppression capability was measured considering the natural high frequency vibration suppression occur in the system. The system response for an increasing vibration is shown in Figure 7.6. According to the results the proposed controller provide superior vibration suppression compared to the passive system. The controller performance is then measured for different frequency levels and sprung mass deflection levels are shown in Figure 7.7 and 7.8. According to the results the system agrees with the simulation performance for low frequency vibrations. This suggests that the virtual spring damper based controller provide superior quality vibration suppression.

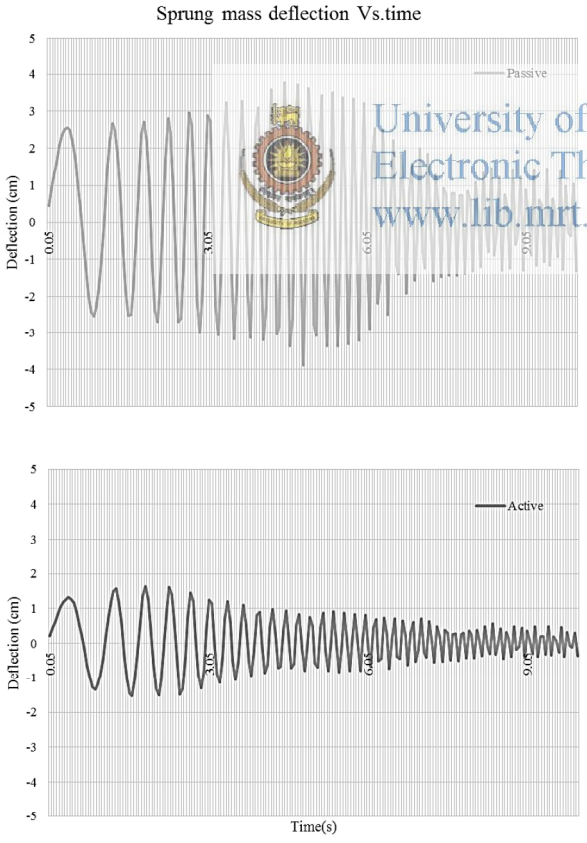

University of Moratuwa, Sri Lanka.
Electronic Theses & Dissertations
www.lib.mrt.ac.lk

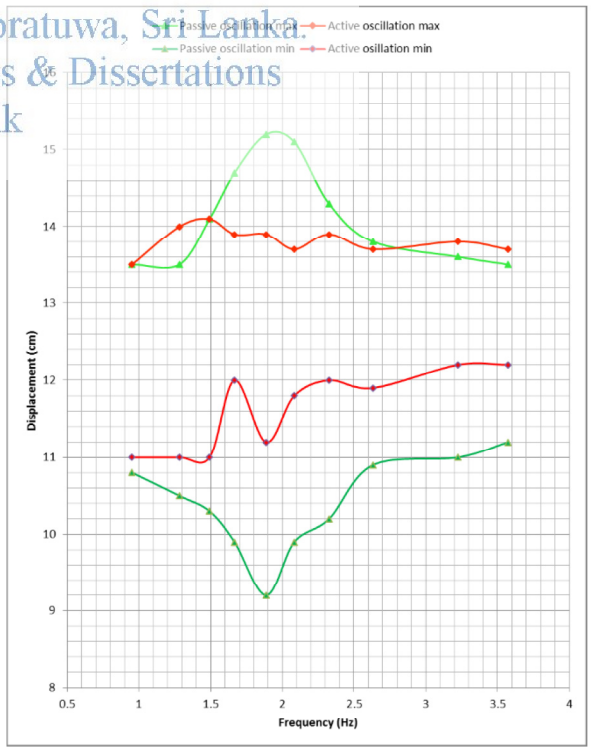

Figure 7.6: Sprung mass deflection for increasing vibration

Figure 7.7: Sprung mass Deflection with frequency

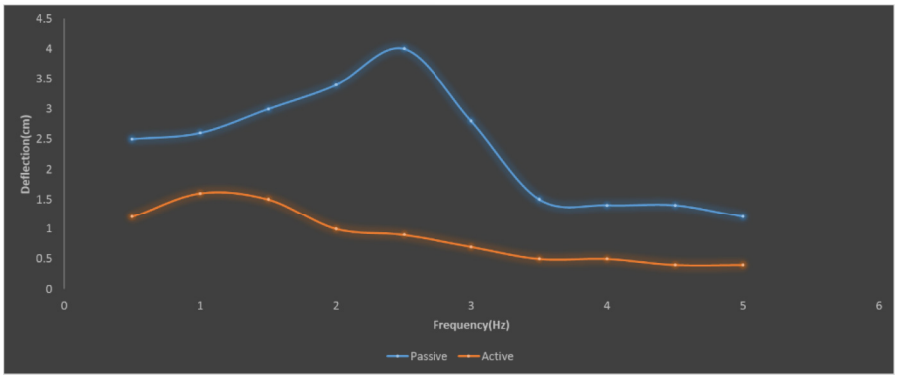

Figure 7.8: Average deflection of the active controller for 3.5cm Deflection level at different frequencies

7.3 Conclusion

A novel active vibration suppression scheme has been developed with disturbance estimation only using the acceleration or suspension deflection measurement. The accelerometer based disturbance observer was experimented and experimental results suggest the applicability of the system for lower frequency vibrations. But the system suffered from the effects of sensor noises. Therefore in sensor selection and position a high quality vibration measurement accelerometers are necessary to improve the controller bandwidth. The controller then implemented using the motor deflection measurement which improves the vibration suppression system performance compared to the conventional system. The system was simulated and compared with the available literature to suggest the applicability of the system. The proposed system was experimented with a quarter car model and results suggest the applicability of the proposed system and the superior performance only with the internal sensors. Finally the parameter estimation method and effects was simulated and tested to provide evidence of the system performance under different conditions. And the results suggest that passive suspension element linear properties greatly improve the suspension system measurement and performances. The system can be further developed for vehicular systems by creating virtual spring damper effects with the use of force reference in the controller. The disturbance estimation controller will virtually nullify the forces in between the sprung mass and the unsprung mass and the external force reference can be used to create a desired virtual effect.

University of Moratuwa, Sri Lanka.
Electronic Theses & Dissertations
www.lib.mrt.ac.lk

8 REFERENCES

[1]. "Ace Controls," Ace Controls, 2014. [Online]. Available: http://www.acecontrols.co.uk/news/understanding-shock-absorbers/. [Accessed 2014].

[2]. D. B. Howad and Geoffrey, in *Car Suspention and Handling 3rd edition*, Ed. London, Pentech Press, 1993.

[3]. A. A. Aly, F. A. Salem, "Vehicle Suspension Systems Control: A Review," *International journal of control, automation and systems*, vol. Vol.2, no. No.2, pp. 2165-8277, 2013.

[4]. K. Yuki, T. Murakami, K. Ohnishi, "Vibration Control of 2 Mass Resonant System by Resonance Ratio Control," *IEEE Int. Con/. Industrial ElectroniCS*, Vo1.3, pp.2009-2014, 1993.

[5]. Y. Ohba, M. Sazawa, K. Ohishi, T. Asai, K. Majima, Y. Yoshizawa, and K. Kageyama, "Sensorless Force Control for Injection Molding Machine Using Reaction Torque Observer Considering Torsion Phenomenon," *IEEE Transactions on Industrial Electronics*, vol. 56, no. 8, pp. 2955– 2960, Aug. 2009.

[6]. K. Ohishi, "Realization of fine motion control based on disturbance observer," *in 10th IEEE International Workshop on Advanced Motion Control*, 2008. AMC '08, Mar. 2008, pp. 1–8.

[7]. K.-s. Kim, K.-H. Rew, and S. Kim, "Disturbance Observer for Estimating Higher Order Disturbances in Time Series Expansion," *IEEE Transactions on Automatic Control*, vol. 55, no. 8, pp. 1905–1911, Aug. 2010.

[8]. Y. Tsukamoto and C. Ishii, "Estimation of the grasping torque of robotic forceps using the robust reaction torque observer," in *2014 IEEE International Conference on Robotics and Biomimetics (ROBIO)*, Dec. 2014, pp. 1650–1655.

[9]. Y. Ohba, K. Ohishi, S. Katsura, Y. Yoshizawa, K. Kageyama, and K. Majima, "Sensor-less force control for injection molding machine using reaction torque observer," in IEEE International Conference on Industrial Technology, 2008. ICIT 2008, Apr. 2008, pp. 1–6.

[10]. Y. Ohba, S. Katsura, and K. Ohishi, "Sensor-less Force Control for Machine Tool Using Reaction Torque Observer," in *IEEE International Conference on Industrial Technology, 2006. ICIT 2006*, Dec. 2006, pp. 860–865.

[11]. E. Saito and S. Katsura, "A filter design method in disturbance observer for improvement of robustness against disturbance in time delay system," in *2012 IEEE International Symposium on Industrial Electronics (ISIE)*, May 2012, pp. 1650–1655.

[12]. J. Lei and G.-Y. Tang, "Optimal vibration control for active suspension sampled-data systems with actuator and sensor delays," in *10th International Conference on Control, Automation, Robotics and Vision, 2008. ICARCV 2008*, Dec. 2008, pp. 988–993.

[13]. K. Boo, J. Park, D. Lee, B. Cho, and S. Son, "Development of a vehicle height sensor for active suspension," in *International Conference on Control, Automation and Systems, 2007. ICCAS '07,* Oct. 2007, pp. 278– 282

[14]. M. van de Wal and B. de Jager, "Selection of sensors and actuators for an active suspension control problem," in , *Proceedings of the 1996 IEEE International Conference on Control Applications*, 1996, Sep. 1996, pp. 55–60.

[15]. W. Sun, Y. Zhao, J. Li, L. Zhang, and H. Gao, "Active Suspension Control With Frequency Band Constraints and Actuator Input Delay," *IEEE Transactions on Industrial Electronics*, vol. 59, no. 1, pp. 530–537, Jan. 2012.

[16]. A. Chamseddine, H. Noura, and M. Ouladsine, "Sensor location for actuator fault diagnosis in vehicle active suspension," in *IEEE International Conference on Control Applications*, *2008. CCA 2008*, Sep. 2008, pp. 456–461.

[17]. Tongue, Benson, *Principles of Vibration*, Oxford University Press, 2001,Inman.

[18]. Daniel J., *Engineering Vibration*, Prentice Hall, 2001.

[19]. H. Li, Z. Gong, W. Lin, and T. Lippa, "A New Motion Control Approach for Jerk and Transient Vibration Suppression," in *2006 IEEE International Conference on Industrial Informatics*, Aug. 2006, pp. 676–681.

[20]. B. Chandekar and H. D. Lagdive, "Design of Electro-Hydraulic Active Suspension System for Four Wheel Vehicles," *International Journal of Emerging Technology and Advanced Engineering*, vol. 4, no. 4, pp. 885-889, 2014.

[21]. W. Evers, A. Teerhuis, A. van der Knaap, I. Besselink and H. Nijmeijer, " The electromechanical low-power active suspension: Modeling, control, and prototype testing," *Journal of Dynamic Systems, Measurement, and Control* , vol. 133, no. 4, p. 041008, 2011.

University of Moratuwa, Sri Lanka.
Electronic Theses & Dissertations
www.lib.mrt.ac.lk

[22]. M. J. Thoresson, P. E. Uys, P. S. Els and J. A. Snyman, "Efficient optimisation of a vehicle suspension system, using a gradient-based approximation method, Part 1: Mathematical modelling," *Mathematical and Computer Modelling*, vol. 50, no. 9–10, p. 1421–1436, 2009.
[23]. Fischer D., and Isermann R., "Mechatronic Semi-Active and Active Vehicle Suspensions," *Control Engineering Practice*, vol. 12, no. 11, p. 1353–1367, 2004.
[24]. J. H. E. A. Muijderman, "Flexible Objective Controllers for Semi-Active Suspensions with Preview," Eindhoven University of Technology, Eindhoven, The Netherlands, 1997.
[25]. A. Conway and R. Stanway, "The Influence of Magneto-Rheological Fluid Time Response on the Performance of Semi-Active Automotive Suspensions," in *ASME 2006 International Mechanical Engineering Congress and Exposition*, Chicago, Illinois, USA, 2006.
[26]. J. Martins, I., Esteves, J., Marques, G. and Pina da Silva, F., "Permanent-Magnets Linear Actuators Applicability in Automobile Active Suspensions," *IEEE Transactions on Vehicular Technology*, vol. 55, no. 1, pp. 86-94, 2006.
[27]. Gysen, B., van der Sande, T., Paulides, J. and Lomonova, E., "Efficiency of a Regenerative Direct-Drive Electromagnetic Active Suspension.," *IEEE Transactions on Vehicular Technology*, vol. 60, no. 4, pp. 1384-1393, 2011.
[28]. Boo K., Park, J., Lee D., Cho B. and Son S., "Development of a vehicle height sensor for active suspension," in I*CCAS '07*, Seoul, 2007.
[29]. P. Intani, P. Boonwong, and C. Mitsantisuk, "Study on sensorless force control based on disturbance observer with friction force compensation," in *2013 13th International Conference on Control, Automation and Systems (ICCAS),* Oct. 2013, pp. 593–598.
[30]. S. Katsura, Y. Matsumoto, and K. Ohnishi, "Modeling of Force Sensing and Validation of Disturbance Observer for force Control," *IEEE Transactions on Industrial Electronics*, vol. 54, no. 1, pp. 530–538, Feb. 2007.
[31]. K. Iwazaki, K. Ohishi, Y. Yokokura, K. Kageyama, M. Takatsu, and S. Urushihara, "Robust pressure control of electric injection molding machine using automatic parameter switching reaction force observer," in *IECON 2013 - 39th Annual Conference of the IEEE Industrial Electronics Society*, Nov. 2013, pp. 6557–6562.
[32]. E. Sariyildiz and K. Ohnishi, "An Adaptive Reaction Force Observer Design," *IEEE/ASME Transactions on Mechatronics*, vol. 20, no. 2, pp. 750–760, Apr. 2015.
[33]. N.-V. Truong, "Mechanical parameter estimation of motion control systems," in 2012 4th International Conference on Intelligent and Advanced Systems (ICIAS), vol. 1, Jun. 2012, pp. 100–104.
[34]. E. Wood, "Prevention of the pathophysiologic effects of acceleration in humans: fundamentals and historic perspectives," *IEEE Engineering in Medicine and Biology Magazine*, vol. 10, no. 1, pp. 26–36, Mar. 1991.
[35]. R. Burton, L. Meeker, and J. Raddin, J.H., "Centrifuges for studying the effects of sustained acceleration on human physiology," *IEEE Engineering in Medicine and Biology Magazine*, vol. 10, no. 1, pp. 56–65, Mar. 1991.
[36]. G. Kjell and J. Lang, "Comparing different vibration tests proposed for li-ion batteries with vibration measurement in an electric vehicle," in *2013 World Electric Vehicle Symposium and Exhibition (EVS27),* Nov. 2013, pp. 1–11.
[37]. Y.-D. Yoon, E. Jung, and S.-K. Sul, "Application of a disturbance observer for a relative position control system," in *twenty-Third Annual IEEE Applied Power Electronics Conference and Exposition, 2008. APEC 2008*,Feb. 2008, pp. 377–382.
[38]. M. J. Griffin, *Handbook of Human Vibration*. Academic Press, Dec. 2012.
[39]. S. John, J. Pedro, and C. Pozna, "Enhanced slip control performance using nonlinear passive suspension system," in 2011 *IEEE/ASME International Conference on Advanced Intelligent Mechatronics (AIM)*, Jul. 2011, pp. 277–282.
[40]. "Solid-Axle Suspension - History & Technical Specs - Rod and Custom Magazine." [Online]. Available: http://www.hotrod.com/how-to/additional-how-to/135-0312-solid-axle-front-suspension-details/
[41]. P. Christensen, "Division of Mechanics." [Online]. Available: http://www.mechanics.iei.liu.se/edu ug/tmme11/
[42]. "Front Suspensions." [Online]. Available: http://auto.howstuffworks.com/car-suspension.htm
[43]. "Suncore - Coil Spring Conversion Kit." [Online]. Available: http://www.carid.com/1990-toyota-celica-suspension-systems/suncore-air-spring-to-coil-spring-conversion-kit-14253862.html

University of Moratuwa, Sri Lanka.
Electronic Theses & Dissertations
www.lib.mrt.ac.lk

[44]. "Audiophile hard drive." [Online]. Available: http://www.diyaudio.com/forums/pc-based/194098-audiophile-hard-drive.html

[45]. C. Liao, K. Wang, M. Yu, and W. Chen, "Modeling of Magnetorheological Fluid Damper Employing Recurrent Neural Networks," in *International Conference on Neural Networks and Brain, 2005*. ICNN B '05, vol. 2, Oct. 2005, pp. 616–620.

[46]. A. Ashfak, K. Abdul Rasheed, and J. Abdul Jaleel, "Modeling, simulation and experimental validation of Magneto-Rheological damper," in *2013 International Conference on Advanced Nanomaterials and Emerging Engineering Technologies (ICANMEET)*, Jul. 2013, pp. 267–274.

[47]. S. Choi, M. Gandhi, and B. Thompson, "An Active Vibration Tuning Methodology for Smart Flexible Structures Incorporating Electro- Rheological Fluids: A Proof-of-Concept Investigation," in *American Control Conference, 1989*, Jun. 1989, pp. 694–703.

[48]. G. Long-ming, S. Wen-ku, and L. Wei, "A semi-active suspension design for off-road vehicle base on Magneto-rheological technology," in *2012 9th International Conference on Fuzzy Systems and Knowledge Discovery (FSKD)*, May 2012, pp. 2565–2568.

[49]. L. H. Nguyen, S. Park, A. Turnip, and K.-S. Hong, "Modified skyhook control of a suspension system with hydraulic strut mount," in *ICCASSICE, 2009*, Aug. 2009, pp. 1347–1352.

[50]. L. Felix-Herran, R. Soto, J. Rodriguez-Ortiz, and R. Ramirez-Mendoza, "Fuzzy control for a semi-active vehicle suspension with a magnetorheological damper," in *Control Conference (ECC), 2009 European*, Aug. 2009, pp. 4398–4403.

[51]. L. H. Nguyen, S. Park, A. Turnip, and K.-S. Hong, "Application of LQR control theory to the design of modified skyhook control gains for semiactive suspension systems," in *ICCAS-SICE, 2009*, Aug. 2009, pp. 4698– 4703.

[52]. A. Ashari, "Sliding-mode control of active suspension systems: unit vector approach," in Proceedings of the *2004 IEEE International Conference on Control Applications*, 2004, vol. 1, Sep. 2004, pp. 370–375 Vol.1.

[53]. C.-P. Cheng, C.-H. Chao, and T. Li, "Design of observer-based fuzzy sliding-mode control for an active suspension system with full-car model," in *2010 IEEE International Conference on Systems Man and Cybernetics (SMC)*, Oct. 2010, pp. 1939–1944.

[54]. F. Kou and Z. Fang, "An Experimental Investigation into the Design of Vehicle Fuzzy Active Suspension," in *2007 IEEE International Conference on Automation and Logistics*, Aug. 2007, pp. 959–963.

[55]. c. andy, "Ride Analysis and Suspension Control," Nov. 2014. [Online]. Available: http://www.ni.com/white-paper/13019/en/

[56]. Chen Yi, Wang Zhong-Lai and Huang Hong-Zhong, "Hybrid Fuzzy Skyhook Surface Control Using Multi-Objective Microgenetic Algorithm for Semi-Active Vehicle Suspension System Ride Comfort Stability Analysis", *"Journal of Dynamic Systems, Measurement, and Control"*, June. 2012, issue 4, pp. 0022-0434

[57]. Chenghao Han and Dingxuan Zhao, "Multi-objective Static Output Feedback Control for Vehicle Active Suspension", *Proceedings of 2014 IEEE International Conference on Mechatronics and Automation* , Aug. 2014, pp.1526-1532.

[58]. Balazs Nemeth and Peter Gaspar, "Variable-Geometry Suspension Design in Driver Assistance Systems", *2013 European Control Conference (ECC)* , Jul. 2013, pp.1481-1486.

[59]. N. Berg, R. Holm, and P. Rasmussen, "A novel magnetic lead screw active suspension system for vehicles," in *2014 IEEE Energy Conversion Congress and Exposition (ECCE),* Sep. 2014, pp. 3139–3146.

[60]. B. Gysen, J. Paulides, J. Janssen, and E. Lomonova, "Active electromagnetic suspension system for improved vehicle dynamics," in *IEEE Vehicle Power and Propulsion Conference, 2008. VPPC '08*, Sep. 2008, pp. 1–6.

[61]. A. K. S. Ehsan Sarshari, "Selection of Sensors for Hydro-Active Suspension System of Passenger Car With InputOutput Pairing Considerations," *Journal of Dynamic Systems, Measurement, and Control*, vol. 135, no. 1, p. 011004, 2012.

[62]. Bruel and Kjaer, *Measuring Vibration*. Bruel and Kjaer. [Online].Available: https://books.google.lk/books?id=HPoOrgEACAAJ

[63]. J. Lei and G.-Y. Tang, "Optimal vibration control for active suspension sampled-data systems with actuator and sensor delays," in *10th International Conference on Control, Automation, Robotics and Vision, 2008. ICARCV 2008*, Dec. 2008, pp. 988–993.

[64]. ——, "Optimal vibration control for active suspension systems with actuator and sensor delays," in *IEEE International Conference on Systems, Man and Cybernetics, 2008*. SMC 2008, Oct. 2008, pp. 2828–2833.

University of Moratuwa, Sri Lanka.
Electronic Theses & Dissertations
www.lib.mrt.ac.lk

[65]. Katsuhiko Ogata (2006) Modern Control Engineering. Prentice Hall of India Private Limited, India, (Fourth Edition).
[66]. Sabri Cetinkunt (2007) *Mechatronics*. John Wiley and sons; Inc., USA, (First Edition).
[67]. Wahyudi, (2003) "Friction Identification and Compensation for High Precision Motion Control Sysyem – Part 1: Friction Identification", *Processing of industrial Electronics Seminar (IES).*
[68]. D.P Castle, J.P Bobis (1992). "Velocity model reference adaptive control of the conventional permanent magnet and variable flux DC motors". *Proceeding of the IEEE International Conference on Industrial Electronics, Control, Instrumentation, and Automation*, November, 1992, Australia, 1303-1308.
[69]. C. Jeram, "Cylindrical-shaft linear motors." [Online]. Available: http://machinedesign.com/technologies/cylindrical-shaft-linear-motors
[70]. "Linear Shaft Motor Catalog." [Online]. Available: http://nipponpulse. com/catalog/document/4e1f2c0a01a0f lsm.pdf
[71]. "Nippon Pulse America Technical Notes -," Apr. 2011. [Online]. Available: http://www.electromate.com/news/?c=featurearticles&article id=10180
[72]. "Nippon pulse s250t datasheet." [Online]. Available: http://nipponpulse. com/catalog/document/554d17e86e0a4 S250.pdf
[73]. "Terasic Altera DE1-SOC." [Online]. Available: http://www.terasic.com.tw/cgi-bin/page/archive.pl?Language=English& CategoryNo=165&No=836&PartNo=1
[74]. "mbed NXP LPC1768 Getting Started." [Online]. Available: https: //developer.mbed.org/handbook/mbed-NXP-LPC1768-Getting-Started
[75]. "About Servoland." [Online]. Available: http://www.servoland.co.jp/en/
[76]. "Servoland SVF Series (Release version C or later)." [Online]. Available: http://www.servoland.co.jp/reference/SV51-11-en.pdf
[77]. "LM10 LINEAR MAGNETIC ENCODER." [Online]. Available: http://www.rls.si/lm10-linear-magnetic-encoder-system
[78]. "ADXL345 Digital Accelerometer." [Online]. Available: http://www.analog.com/media/en/technical-documentation/data-sheets/ADXL345.pdf
[79]. "linear guide - All number - SKF FAG NSK NTN ZWZ LYC TIMKENand so on (China Manufacturer) - Industrial Supplies Stocks – Industrial Supplies." [Online]. Available: http%3A%2F%2Fwww.diytrade.com%2Fchina%2Fpd%2F7588965%2Flinear guide.html
[80]. "Flanged Linear Motion Ball Bearing(LMH Series)." [Online]. Available: http://www.seekpart.com/product/Flanged-Linear-Motion-Ball-Bearing-LMH-Series-1594180.html
[81]. J. Chamberlain, "The difference between linear motors and linear mechanical devices." [Online]. Available: http://www.seekpart.com/product/Flanged-Linear-Motion-Ball-Bearing-LMII-Series-1594180.html
[82]. "Nippon Pulse S250 Linear Shaft Motor." [Online]. Available:http://nipponpulse.com/catalog/document/554d17e86e0a4 S250.pdf
[83]. "Hybrid Hall Effect ICs EW-series." [Online]. Available: http: //www.akm.com/akm/en/file/datasheet/EW-500.pdf
[84]. "Motor Control Algorithms." [Online]. Available: http://in.renesas.com/applications/key technology/motor control/motor algorithms/child/bldc.jsp

University of Moratuwa, Sri Lanka.
Electronic Theses & Dissertations
www.lib.mrt.ac.lk

9 APPENDIX

9.1 Equipment Details

9.1.1 Linear motor

Motor specifications

Continuous Force	60N (13.5lbs)
Continuous Current	1.3Arms
Acceleration Force	240N (54.0lbs)
Acceleration Current	5.1Arms
Force Constant (Kf)	47N/Arms (10.67lbs/amp)
Back EMF (Ke)	16V/m/s
Resistance 25°C	12Ω
Inductance	15mH
Electric Time Constant	1.25ms
Rated Voltage (AC)	240V
Fundamental Motor Constant (Km)	11.19N√W
Magnetic Pitch (North-North)	90mm (3.54lbs)
Usable stroke length	250mm
Shaft length	515mm
Shaft mass	1.6kg

Linear Motor [72]

University of Moratuwa, Sri Lanka.
Electronic Theses & Dissertations
www.lib.mrt.ac.lk

Dimensions of selected motor as shown in the figure 6.5,

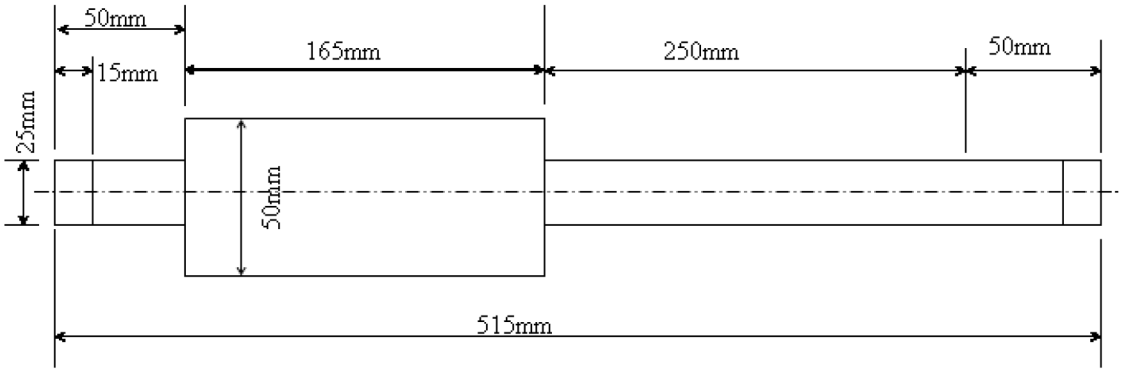

Figure 9.2: Motor Dimensions

9.1.2 FPGA

Altera Terasic DE1 Soc field programmable gate array is used as the controller to provid high speed processing with following specifications.

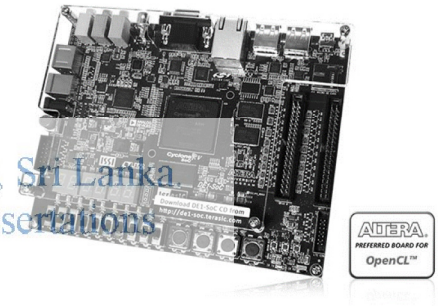

Terasic Altera DE1-SOC [73]

University of Moratuwa, Sri Lanka.
Electronic Theses & Dissertations
www.lib.mrt.ac.lk

Cyclone V SoC 5CSEMA5F31C6 Device

85K Programmable Logic Elements

4,450 Kbits embedded memory

6 Fractional PLLs

This controller provides 100MHz sampling and processing with a minimum amount of latency. Controller desing is included in the appendix.

9.1.3 Mbed Microcontroller

Mbed NXP LPC1768 microcontroller is used as secondary controller to control cam assembly. Mbed microcontroller is taking input signals mainly from accelerometer and rotary encoder and giving output PWM signals to rotary motor driver.

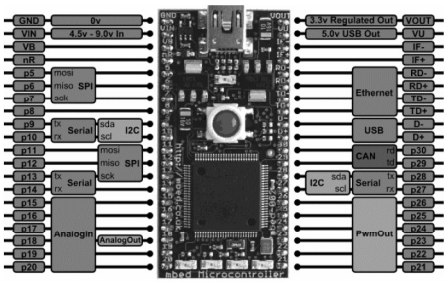

Mbed Microcontroller[74]

Mbed 32-bit ARM Cortex-M3 core is running at 96MHz. It includes 512KB FLASH, 32KB RAM and lots of interfaces including built-in Ethernet, USB Host and Device, CAN, SPI, I2C, ADC, DAC, PWM and other I/O interfaces.
NXP LPC1768 MCU

- High performance ARM® Cortex™-M3 Core
- 96MHz, 32KB RAM, 512KB FLAS
- Ethernet, USB Host/Device, 2xSPI, 2xI2C, 3xUART, CAN, 6xPWM, 6xADC, GPIO

Prototyping form-factor

- 40-pin 0.1" pitch DIP package, 54x26mm
- 5V USB or 4.5-9V supply
- Built-in USB drag 'n' drop FLASH programmer

Mbed.org Developer Website

- Lightweight Online Compiler
- High level C/C++ SDK
- Cookbook of published libraries and projects

9.1.3.1.1 Linear Motor Driver

Linear Motor Driver is one of the key components of the system. It communicates with host controller (FPGA) and control linear motor according to signals. SVFH3-H3-DSP*SRI Servo land linear motor driver is selected as linear motor driver. It is capable to control motor current of the linear motor. Serial 2 phase current command type was added for the driver for that purpose.

University of Moratuwa, Sri Lanka.
Electronic Theses & Dissertations
www.lib.mrt.ac.lk

Principal specifications

- Motion mode - SRI Serial 2 phase current command mode
- Analog input port - 2 channels, Differential / Single end
- Input command data - 16 bit
- Control type - DQ Vector control
- A/D Resolution of current detection - 16 bit fast sigma-delta type
- PWM frequency - 15 to 40 kHz
- PWM Resolution - 7 ns
- Current control cycle - Synchronized with PWM frequency
- Current response - 3 kHz (DSP model), 1.5 kHz (Base model)
- Output - 436W

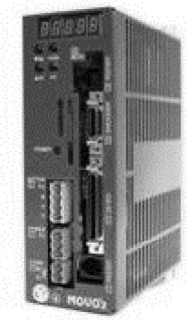

Linear Motor Driver [75]

Internal block diagram of the motor driver is as shown in the figure 6.9,

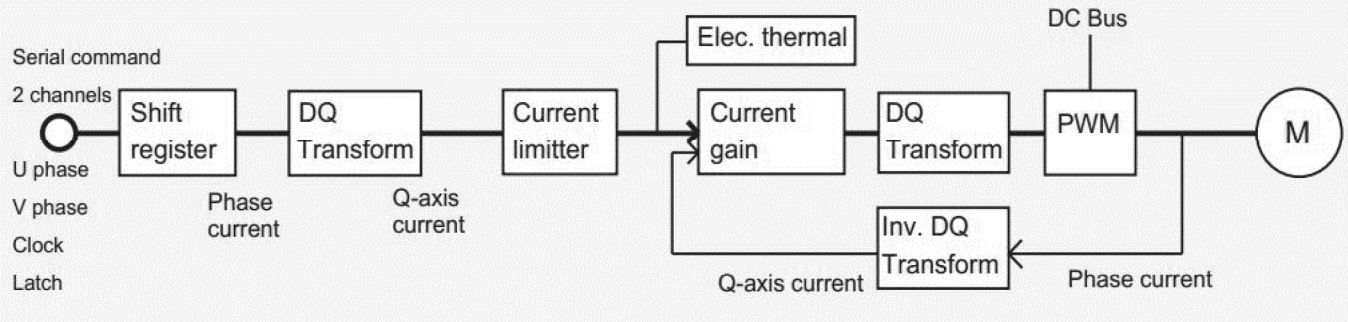

Internal Block Diagram of Linear Motor [76]

9.1.3.1.2 Linear Encoder

Linear encoder is the main and the only sensor which take measurements for controlling the system. Linear encoder signals are directly connected with FPGA. From the linear Encoder, relative displacement between sprung mass and un-sprung mass is measured. LM10 magnetic type linear encoder is selected from Renishaw Company for the application. System data

University of Moratuwa, Sri Lanka.
Electronic Theses & Dissertations
www.lib.mrt.ac.lk

- Maximum length for MS scale 50 m (100 m special order)
- Pole length 2 mm
- Available resolutions 1 µm, 2 µm, 5 µm, 10 µm, 20 µm and 50 µm
- Sinusoidal period length 2 mm
- Maximum speed For a Precision class for MS scales ±20 µm/m and ±40 µm/m
- Linear expansion coefficient for MS scale ~ 17 × 10-6/K
- Repeatability Better than unit of resolution for movement in the same direction
- Hysteresis < 3 µm up to 0.5 mm ride height
- Sub divisional error ±3.5 µm for < 0.7 mm ride height ±7.5 µm for 1 mm ride height

Linear Encoder [77]

9.1.3.1.3 Accelerometer

Accelerometer is used for data collection purposes. Accelerometer is connected to Mbed microcontroller. For that ADXL345 3-Axis digital accelerometer is used. The ADXL345 is a small, thin, ultralow power, 3-axis accelerometer with high resolution (13-bit) measurement at up to ±16 g. Digital output data is formatted as 16-bit twos complement and is accessible through either a SPI (3- or 4-wire) or I^2C digital interface.

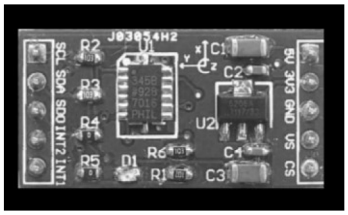

Accelerometer [78]

9.1.4 Mechanical equipment

University of Moratuwa, Sri Lanka.
Electronic Theses & Dissertations
www.lib.mrt.ac.lk

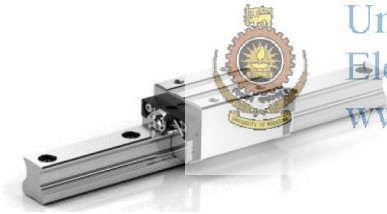

Linear Guide [79]

Linear Bearings [80]

9.2 Main module code

This only includes the main module code of one version of implementation due to limitations of pages.

```
module ACTIVE_MODULE(

        //////////// CLOCK //////////
        input                       CLOCK_50,
        input                       CLOCK2_50,
        input                       CLOCK3_50,
        input                       CLOCK4_50,
        output          [6:0]       HEX5,


        //////////// KEY //////////
```

```
        input           [3:0]       KEY,
        ////////// LED //////////
        output          [9:0]       LEDR,
        ////////// SW //////////
        input           [9:0]       SW,
        ////////// GPIO_0, GPIO_0 connect to GPIO Default //////////
        inout           [35:0]      GPIO_0,
        ////////// GPIO_1, GPIO_1 connect to GPIO Default //////////
        inout           [35:0]      GPIO_1
); //=======================================================
// REG/WIRE declarations
//=======================================================
wire res;   //async reset
reg reset = 0;                  //sync reset
wire enable;            //enable
//pll pins
reg pll_reset = 0;              //oustside clock sync pll_reset
wire [4:0] pll_cascade;
wire pll_lock;
wire pll_lock_2;
wire CLOCK_1000;
wire CLOCK_500;
wire CLOCK_200;
wire CLOCK_100;
wire CLOCK_50_PLL;
wire CLOCK_40;
wire CLOCK_4;


//reg input Key edge detection
reg [3:0] KEY_prev = 0;
wire [3:0] KEY_edge;
//led register for sync led out
reg [9:0] LED_OUT = 9'b000000000;
//input switch logics
wire SW_12_logic_00;
```

University of Moratuwa, Sri Lanka.
Electronic Theses & Dissertations
www.lib.mrt.ac.lk

```
wire SW_12_logic_01;
wire SW_12_logic_11;
wire SW_12_logic_10;
wire SW_345_logic_000 ;
wire SW_345_logic_001;
wire SW_345_logic_010;
wire SW_345_logic_011 ;
wire SW_345_logic_100;
wire SW_345_logic_101 ;
wire SW_345_logic_110 ;
wire SW_345_logic_111;
wire SW_6_logic_0;
wire SW_6_logic_1;
//register read SPIO logic
wire GPIO1_1357_logic_0000;
wire GPIO1_1357_logic_0001;
wire GPIO1_1357_logic_0010;
wire GPIO1_1357_logic_0011;
wire GPIO1_1357_logic_0100;
wire GPIO1_1357_logic_0101;
wire GPIO1_1357_logic_0110;
wire GPIO1_1357_logic_0111;
wire GPIO1_1357_logic_1000;
wire GPIO1_1357_logic_1001;
wire GPIO1_1357_logic_1010;
wire GPIO1_1357_logic_1011;
wire GPIO1_1357_logic_1100;
wire GPIO1_1357_logic_1101;
wire GPIO1_1357_logic_1110;
wire GPIO1_1357_logic_1111;
//wires for mbed spi slave GPIO connections
wire MBED_SCLK;
wire MBED_CS;
wire MBED_MOSI;
wire MBED_MISO;
```

University of Moratuwa, Sri Lanka.
Electronic Theses & Dissertations
www.lib.mrt.ac.lk

```
wire MBED_READY;
wire MBED_FINISH;
wire MBED_BUSY;
reg [15:0]  MBED_DATAOUT = 16'b0;
wire [15:0] MBED_DATAIN;
reg [15:0] MBED_READ_REG = 16'b0;
reg [15:0] MBED_READ_REG_HIGH = 16'b0;
//adc read values
reg [15:0] ADC_DIN_VALUE = 16'b10_00_00_110_000_0000;
wire [15:0] ADC_DOUT_VALUE;
//input wires for movo drive GPIOs
wire movo_data_A;
wire movo_data_B;
wire movo_clk;
wire movo_latch;
wire movo_data_A_not;
wire movo_data_B_not;
wire movo_clk_not;
wire movo_latch_not;
wire data_status ;
//BLDC commutation
wire hall_1;
wire hall_2;
wire hall_3;
wire [15:0] current_U;
wire [15:0] current_V;
wire hall_error;
//quadrature encoder interface
wire encoder_phaseA;
wire encoder_phaseB;
wire [31:0] pulse_position;
wire pulse;
//force output to send to the drivers
reg [31:0] forceOutFloat = 0;
//calculated float values
```

University of Moratuwa, Sri Lanka.
Electronic Theses & Dissertations
www.lib.mrt.ac.lk

```
wire [31:0] position;
wire [31:0] acceleration;
wire [31:0] velocity;
wire[31:0] Kspring;
wire[31:0] Cdamper;
wire[31:0] Kp;
wire[31:0] Ki;
wire[31:0] Kd;
wire[31:0] mass;
wire[31:0] forceCurrentSense;
wire[31:0] forceRef;
wire[15:0] currentOutDAC;
wire[15:0] currentOutMOVO;
reg [31:0] forceRef_in = 0;
wire[31:0] forceRFOB;
wire[31:0] forceOutRFOB_act;
wire[31:0] forceOutSpring;
//raw integers of values
reg [15:0] forceRefRaw = 0;
reg [15:0] KpRaw = 950;
reg [15:0] KiRaw = 0;
reg [15:0] KdRaw = 0;
reg [15:0] massRaw = 110;
reg [15:0] KspringRaw = 1200;
reg [15:0] CdamperRaw = 0;
assign res = ~KEY[0];
assign enable = SW[0] & pll_lock;
// LED indicator assignmene
assign LEDR = LED_OUT;
//mbed spi slave conncector ---check input pin filters
assign GPIO_1[2] = MBED_MISO;          //output
//movo communication pins
assign GPIO_0[0] = movo_data_A;
assign GPIO_0[2] = movo_data_B;
assign GPIO_0[4] = movo_clk;
```

University of Moratuwa, Sri Lanka.
Electronic Theses & Dissertations
www.lib.mrt.ac.lk

```
assign GPIO_0[6] = movo_latch;
assign GPIO_0[1] = movo_data_A_not;
assign GPIO_0[3] = movo_data_B_not;
assign GPIO_0[5] = movo_clk_not;
assign GPIO_0[7] = movo_latch_not;
assign GPIO_0[8] = 1'b0;
assign GPIO_0[9] = 1'b0;
//check input filters
//DAC 712 ouput pins
assign GPIO_1[25:10] = currentOutDAC[15:0];
// positive edge detection of the input keys
assign KEY_edge[0] = ~KEY_prev[0] & KEY[0];
assign KEY_edge[1] = ~KEY_prev[1] & KEY[1];
assign KEY_edge[2] = ~KEY_prev[2] & KEY[2];
assign KEY_edge[3] = ~KEY_prev[3] & KEY[3];
//SW 0-9 logic connectors
assign SW_12_logic_00 = ~SW[1] & ~SW[2];
assign SW_12_logic_01 = ~SW[1] & SW[2];
assign SW_12_logic_11 = SW[1] & SW[2];
assign SW_12_logic_10 = SW[1] & ~SW[2];
assign SW_345_logic_000 = ~SW[3] & ~SW[4] & ~SW[5];
assign SW_345_logic_001 = ~SW[3] & ~SW[4] & SW[5];
assign SW_345_logic_010 = ~SW[3] & SW[4] & ~SW[5];
assign SW_345_logic_011 = ~SW[3] & SW[4] & SW[5];
assign SW_345_logic_100 = SW[3] & ~SW[4] & ~SW[5];
assign SW_345_logic_101 = SW[3] & ~SW[4] & SW[5];
assign SW_345_logic_110 = SW[3] & SW[4] & ~SW[5];
assign SW_345_logic_111 = SW[3] & SW[4] & SW[5];
assign SW_6_logic_0 = ~SW[6];
assign SW_6_logic_1 = SW[6];
//GPIO_1 [1-7] Mbed register read connection
assign GPIO1_1357_logic_0000 = ~GPIO_1[1] & ~GPIO_1[3] & ~GPIO_1[5] & ~GPIO_1[7];
assign GPIO1_1357_logic_0001 = ~GPIO_1[1] & ~GPIO_1[3] & ~GPIO_1[5] & GPIO_1[7];
assign GPIO1_1357_logic_0010 = ~GPIO_1[1] & ~GPIO_1[3] & GPIO_1[5] & ~GPIO_1[7];
assign GPIO1_1357_logic_0011 = ~GPIO_1[1] & ~GPIO_1[3] & GPIO_1[5] & GPIO_1[7];
```

University of Moratuwa, Sri Lanka.
Electronic Theses & Dissertations
www.lib.mrt.ac.lk

```
assign GPIO1_1357_logic_0100 = ~GPIO_1[1] & GPIO_1[3] & ~GPIO_1[5] & ~GPIO_1[7];
assign GPIO1_1357_logic_0101 = ~GPIO_1[1] & GPIO_1[3] & ~GPIO_1[5] & GPIO_1[7];
assign GPIO1_1357_logic_0110 = ~GPIO_1[1] & GPIO_1[3] & GPIO_1[5] & ~GPIO_1[7];
assign GPIO1_1357_logic_0111 = ~GPIO_1[1] & GPIO_1[3] & GPIO_1[5] & GPIO_1[7];
assign GPIO1_1357_logic_1000 = GPIO_1[1] & ~GPIO_1[3] & ~GPIO_1[5] & ~GPIO_1[7];
assign GPIO1_1357_logic_1001 = GPIO_1[1] & ~GPIO_1[3] & ~GPIO_1[5] & GPIO_1[7];
assign GPIO1_1357_logic_1010 = GPIO_1[1] & ~GPIO_1[3] & GPIO_1[5] & ~GPIO_1[7];
assign GPIO1_1357_logic_1011 = GPIO_1[1] & ~GPIO_1[3] & GPIO_1[5] & GPIO_1[7];
assign GPIO1_1357_logic_1100 = GPIO_1[1] & GPIO_1[3] & ~GPIO_1[5] & ~GPIO_1[7];
assign GPIO1_1357_logic_1101 = GPIO_1[1] & GPIO_1[3] & ~GPIO_1[5] & GPIO_1[7];
assign GPIO1_1357_logic_1110 = GPIO_1[1] & GPIO_1[3] & GPIO_1[5] & ~GPIO_1[7];
assign GPIO1_1357_logic_1111 = GPIO_1[1] & GPIO_1[3] & GPIO_1[5] & GPIO_1[7];
//external clock sync reset
always @(posedge CLOCK_50) begin
        pll_reset <= ~KEY[0] & ~KEY[3];
end
//logic
always @(posedge CLOCK_200) begin
        reset <= res;
        KEY_prev[3:0] <= KEY[3:0];
        LED_OUT[0] <= enable;
        LED_OUT[1] <= reset;
        LED_OUT[6:2] <= SW[5:1];
        LED_OUT[7] <= hall_error;
        LED_OUT[8] <= pulse;
        LED_OUT[9] <= data_status;

        //LED_OUT = MBED_DATAIN[9:0];
        if(reset) begin
                forceRef_in <= 0;
                forceOutFloat <= 0;
                forceRefRaw <= 0;
                KpRaw <= 995;
                KiRaw <= 0;
                KdRaw <= 0;
```

University of Moratuwa, Sri Lanka.
Electronic Theses & Dissertations
www.lib.mrt.ac.lk

```
                KspringRaw <= 1200;
                CdamperRaw <= 1;
                forceOutFloat <= 0;
        end
end
// observations of values using mbed SPI
always @ (posedge CLOCK_200)        begin
        if (reset)begin
                MBED_DATAOUT <= 16'b0;
                MBED_READ_REG <= 16'b0;
                MBED_READ_REG_IIIGII <= 16'b0;
        end
        else begin
                if (enable)begin
                        if(MBED_CS) begin
                                MBED_DATAOUT <= MBED_READ_REG;
                                if ( GPIO1_1357_logic_0000 ) begin
                                        MBED_DATAOUT <= pulse_position[15:0];
                                        MBED_READ_REG_HIGH <= pulse_position[31:16];
                                end
                                if ( GPIO1_1357_logic_0001 ) begin
                                        MBED_DATAOUT <= velocity[15:0];
                                        MBED_READ_REG_HIGH <= velocity[31:16];
                                end
                                if ( GPIO1_1357_logic_0010 ) begin
                                        MBED_DATAOUT <= forceRFOB[15:0];
                                        MBED_READ_REG_HIGH <= forceRFOB[31:16];
                                end
                                if ( GPIO1_1357_logic_0011 ) begin
                                        MBED_DATAOUT <= forceOutRFOB_act[15:0];
                                        MBED_READ_REG_HIGH <= forceOutRFOB_act[31:16];
                                end
                                if ( GPIO1_1357_logic_0100 ) begin
                                        MBED_DATAOUT <= forceOutSpring[15:0];
                                        MBED_READ_REG_HIGH <= forceOutSpring[31:16];
```

University of Moratuwa, Sri Lanka.
Electronic Theses & Dissertations
www.lib.mrt.ac.lk

```
end
if ( GPIO1_1357_logic_0101 ) begin
        MBED_DATAOUT <= Kspring[15:0];
        MBED_READ_REG_HIGH <= Kspring[31:16];
end
if ( GPIO1_1357_logic_0110 ) begin
        MBED_DATAOUT <= Kp[15:0];
        MBED_READ_REG_HIGH <= Kp[31:16];
end
if ( GPIO1_1357_logic_0111 ) begin
        MBED_DATAOUT <= MBED_READ_REG_IIIGII;
end
if ( GPIO1_1357_logic_1000 ) begin
        MBED_DATAOUT <= currentOutDAC;
        MBED_READ_REG_HIGH <= 16'b0;
end
if ( GPIO1_1357_logic_1001 ) begin
        MBED_DATAOUT <= ADC_DOUT_VALUE;
        MBED_READ_REG_HIGH <= 16'b0;
end
if ( GPIO1_1357_logic_1010 ) begin
        MBED_DATAOUT <= KpRaw;
        MBED_READ_REG_HIGH <= 16'b0;
end
if ( GPIO1_1357_logic_1011 ) begin
        MBED_DATAOUT <= KdRaw;
        MBED_READ_REG_HIGH <= 16'b0;
end
if ( GPIO1_1357_logic_1100 ) begin
        MBED_DATAOUT <= KiRaw;
        MBED_READ_REG_HIGH <= 16'b0;
end
if ( GPIO1_1357_logic_1101 ) begin
        MBED_DATAOUT <= KspringRaw;
        MBED_READ_REG_HIGH <= 16'b0;
```

University of Moratuwa, Sri Lanka.
Electronic Theses & Dissertations
www.lib.mrt.ac.lk

```
                                        end
                                        if ( GPIO1_1357_logic_1110 ) begin
                                                MBED_READ_REG <= CdamperRaw;
                                                MBED_READ_REG_HIGH <= 16'b0;
                                        end
                                        if ( GPIO1_1357_logic_1111 ) begin
                                                MBED_READ_REG <= forceRefRaw;
                                                //MBED_DATAOUT <= MBED_DATAIN;
                                                MBED_READ_REG_HIGH <= 16'b0;
                                        end
                                end
                        end
                        else begin
                        end
                end
end
//input pin filters
/*
assign MBED_SCLK =      GPIO_0[24]; //input
assign MBED_CS     =    GPIO_0[26];         //input
assign MBED_MOSI =      GPIO_0[20];         //input
*/
filter_1_bit filter_1_bitMBED_SCLK(
                CLOCK_500,
                GPIO_1[4],
                MBED_SCLK
   );
filter_1_bit filter_1_bitMBED_CS(
                CLOCK_500,
                GPIO_1[6],
                MBED_CS
   );
filter_1_bit filter_1_bitMBED_MOSI(
                CLOCK_500,
                GPIO_1[0],
```

University of Moratuwa, Sri Lanka.
Electronic Theses & Dissertations
www.lib.mrt.ac.lk

```
            MBED_MOSI
    );
/*
assign hall_1 = GPIO_0[10];
assign hall_2 = GPIO_0[12];
assign hall_3 = GPIO_0[14];
*/
filter_1_bit filter_1_bithall_1(
            CLOCK_200,
            GPIO_0[30],
            hall_1
    );
filter_1_bit filter_1_bithall_2(
            CLOCK_200,
            GPIO_0[32],
            hall_2
    );
filter_1_bit filter_1_bithall_3(
            CLOCK_200,
            GPIO_0[34],
            hall_3
    );
/*assign encoder_phaseA = GPIO_0[17];
assign encoder_phaseB = GPIO_0[19];
*/
filter_1_bit filter_1_bitencoder_phaseA(
            CLOCK_200,
            GPIO_0[27],
            encoder_phaseA
    );
filter_1_bit filter_1_bitencoder_phaseB(
            CLOCK_200,
            GPIO_0[29],
            encoder_phaseB
    );
```

University of Moratuwa, Sri Lanka.
Electronic Theses & Dissertations
www.lib.mrt.ac.lk

```
//PLL connection
//module pll_main (    refclk,   rst, 50,40,4, locked );
pll_main pll_main_inst(
                        CLOCK_50,
                        pll_reset,
                        CLOCK_50_PLL,
                        CLOCK_200,
                        CLOCK_500,
                        pll_lock
);
//spi 16bit slave to tranfer data to mbed
spi_slave mbed_spi(
            CLOCK_500,
            reset,
            enable,
            MBED_SCLK,
            MBED_CS,
            MBED_MOSI,
            MBED_DATAOUT,
            MBED_MISO,
            MBED_DATAIN,
            MBED_READY,
            MBED_FINISH,
            MBED_BUSY
);
//encoder interface
quadrature_encoder quadrature_encoder_inst(
            .clk(CLOCK_200),
            .rst(reset),
            .A(encoder_phaseA),
            .B(encoder_phaseB),
            .up(),
            .down(),
            .pulse(pulse),
            .direction(),
```

University of Moratuwa, Sri Lanka.
Electronic Theses & Dissertations
www.lib.mrt.ac.lk

```
        .pulse_count(pulse_position)
    );
//data converter module
data_converter data_converter_inst(
        .clk(CLOCK_200),
        .rst(reset),
        .enable(enable),

        .positionRaw(pulse_position),
        .accelerationRaw(MBED_DATAIN),
        .KspringRaw(KspringRaw),
        .CdamperRaw(CdamperRaw),
        .KpRaw(KpRaw),
        .KiRaw(KiRaw),
        .KdRaw(KdRaw),
        .massRaw(massRaw),
        .senseCurrentRaw(ADC_DOUT_VALUE),
        .forceRefRaw(forceRefRaw),
        .forceFloat(forceOutFloat),
        .position(position),
        .velocity(velocity),
        .acceleration(acceleration),
        .Kspring(Kspring),
        .Cdamper(Cdamper),
        .Kp(Kp),
        .Ki(Ki),
        .Kd(Kd),
        .mass(mass),
        .forceCurrentSense(forceCurrentSense),
        .forceRef(forceRef),
        .currentOutDAC(currentOutDAC),
        .currentOutMOVO(currentOutMOVO)
    );
//active RFOB connection
activeRFOB activeRTOB_inst(
```

University of Moratuwa, Sri Lanka.
Electronic Theses & Dissertations
www.lib.mrt.ac.lk

```
        .clk(CLOCK_200),
        .rst(reset),
        .enable(enable),
        .acceleration(acceleration),
        .position(position),
        .velocity(velocity),
        .senseForce(forceCurrentSense),
        .Kp(Kp),
        .Ki(Ki),
        .Kd(Kd),
        .mass(mass),
        .forceRef(forceRef_in),
        .forceRFOB(forceRFOB),
        .forceOutFloat(forceOutRFOB_act)
    );
//active spring damper connection
activeVirtualSpring activeVirtualSpring_inst(
        .clk(CLOCK_200),
        .rst(reset),
        .enable(enable),
        .position(position),
        .velocity(velocity),
        .K(Kspring),
        .C(Cdamper),
        .forceOutFloat(forceOutSpring)
    );
//BLDC commutation
BLDC_commutation BLDC_commutation_inst(
        .clk(CLOCK_200),
        .rst(reset),
        .enable(enable),
        .hall_1(hall_1),
        .hall_2(hall_2),
        .hall_3(hall_3),
        .current_in(currentOutMOVO),
```

University of Moratuwa, Sri Lanka.
Electronic Theses & Dissertations
www.lib.mrt.ac.lk

```
            .current_out_U(current_U),
            .current_out_V(current_V),
            .hall_error(hall_error)
    );

//Movo interface
movo_interface movo_interface_inst(
            .clk(CLOCK_50_PLL),
            .rst(reset),
            .enable(enable),
            .value_A(current_U),
            .value_B(current_V),
            .clk_movo(movo_clk),
            .clk_movo_not(movo_clk_not),
            .data_A(movo_data_A),
            .data_A_not(movo_data_A_not),
            .data_B(movo_data_B),
            .data_B_not(movo_data_B_not),
            .latch(movo_latch),
            .latch_not(movo_latch_not),
            .status(),
            .data_status(data_status)
            );
endmodule
```

University of Moratuwa, Sri Lanka.
Electronic Theses & Dissertations
www.lib.mrt.ac.lk